CIVIL ENGINEERING STUDIES

STRUCTURAL RESEARCH SERIES NO. 300

FATIGUE OF PLATES AND WELDMENTS IN HY-100 AND HY-130/150 STEELS

By

W. H. MUNSE
W. H. BRUCKNER
J. B. RADZIMINSKI
R. W. HINTON
J. W. LEIBOLD

A Report of an Investigation Conducted
by
THE CIVIL ENGINEERING DEPARTMENT
UNIVERSITY OF ILLINOIS
in cooperation with
The Bureau of Ships, U. S. Navy
Contract NObs 92226
Project Series No. SR-007-01-01, Task 855

UNIVERSITY OF ILLINOIS
URBANA, ILLINOIS
NOVEMBER, 1965

FATIGUE OF PLATES AND WELDMENTS IN HY-100 AND HY-130/150 STEELS

by

W. H. Munse

W. H. Bruckner

J. B. Radziminski

R. W. Hinton

J. W. Leibold

A Report of an Investigation Conducted

by

THE CIVIL ENGINEERING DEPARTMENT
UNIVERSITY OF ILLINOIS

In Cooperation With
The Bureau of Ships, U. S. Navy
Contract NObs 92226
Project Series No. SR-007-01-01, Task 855

UNIVERSITY OF ILLINOIS

URBANA, ILLINOIS

NOVEMBER 1965

ABSTRACT

An evaluation of the axial fatigue behavior of plain plates and full penetration weldments in HY-100 steel is presented. Transverse butt-welded specimens welded with the MIL-11018 electrodes were found to contain minute internal weld flaws which often serve as critical locations for fatigue crack initiation. The weld flaws, although not detected by usual radiographic inspection, were successfully located with the use of ultrasonic detection equipment. The ultrasonic equipment was used also to study the initiation and propagation of fatigue cracks in several test weldments. A preliminary investigation of the axial fatigue behavior of HY-130/150 steel plain plates is reported.

TABLE OF CONTENTS

TABLE OF CONTENTS (CONTD)

LIST OF TABLES

LIST OF FIGURES

LIST OF FIGURES (CONTD)

LIST OF FIGURES (CONTD)

1. INTRODUCTION

1.1 Object of Study

The principal purpose of the investigation reported herein was to evaluate the fatigue behavior of plain plates and welded joints of 3/4 in. thick HY-100 steel. The tests were conducted using axially-loaded fatigue specimens. In addition, both radiographic and ultrasonic examinations were made on several transverse butt-welded specimens to obtain an indication of the relative sensitivity of the two techniques in determining weld quality. The ultrasonic detection equipment was also used to study the initiation of fatigue cracks at internal weld flaws.

The fatigue cracks in a number of the transverse butt-welded joints welded with the MIL-11018 electrode were found to initiate at small internal flaws rather than at changes in external geometry. As a result, several modifications were made in the welding procedures and specimens prepared by these modified procedures were subjected to metallographic examination to determine their suitability for use with the HY-100 base metal. Members prepared with two of the experimental procedures were subsequently subjected to cyclic loadings and the results compared with the fatigue behavior of specimens welded using the standard procedure.

A preliminary investigation of the fatigue behavior of HY-130/150 plate has been included also. Results are reported for fatigue tests of 1/2 in. thick plain plate specimens.

1.2 Scope of Investigation

The studies reported herein were conducted on 3/4 in. thick HY-100 plain plates and transverse welded joints using stress cycles of zero-to-tension and complete-reversal. The preliminary study of the HY-130/150 material consisted of

fatigue tests performed using a zero-to-tension stress cycle. The report covers tests conducted during the period from August 1964 to September 1965.

Several types of welded joints using the HY-100 base metal have been tested. These include transverse butt-welded specimens (as-welded and with reinforcement removed), specimens with full penetration transverse attachments (attachment on one and two sides of main member), and full penetration tee joints. A total of four welding procedures were used in the fatigue evaluation of the transverse butt-welded specimens. In addition, specimens were fabricated with intentional weld porosity to further examine the effect of internal defects on fatigue life.

1.3 Acknowledgments

The tests reported in this study are the result of an investigation conducted in the Civil Engineering Department of the University of Illinois. The program was carried out with funds provided by the Bureau of Ships, U. S. Navy, under Contract 92226, Project Serial No. SR-007-01-01, Task 855.

The investigation constitutes a part of the structural research program of the Department of Civil Engineering, of which Dr. N. M. Newmark is the Head. The program is under the general direction of W. H. Munse, Professor of Civil Engineering; the fatigue research was conducted by J. B. Radziminski and J. W. Leibold, Research Assistants in Civil Engineering, and the metallurgical studies were conducted by R. W. Hinton, Research Assistant in Metallurgical Engineering, under the direction of W. H. Bruckner, Professor of Metallurgical Engineering.

The authors wish to express their appreciation to the many people on the staff of the University who so ably assisted in the investigation.

II. DESCRIPTION OF TEST PROGRAM

2.1 Materials

The main emphasis of the program was on the fatigue behavior of welded joints fabricated from HY-100 steel of 3/4 in. thickness. A limited number of preliminary fatigue tests were also conducted on 1/2 in. thick HY-130/150 plain plates. The physical and chemical properties of the two materials are presented in Tables 2.1 and 2.2, respectively.

The majority of the HY-100 welded joints were fabricated using electrodes of MIL-11018 grade. The electrodes were conditioned in accordance with requirements of the current Navy Specifications;[5]* the procedure is fully defined in Ref. (2). Exploratory tests were also initiated using MIL-12018 grade electrodes with the HY-100 base metal.

2.2 Fabrication of Specimens

Details of the test specimens are presented in Figs. 2.1 and 2.2. In general, the fabrication process was similar for all specimens except for the differences in welding procedure. Specimen blanks, 9 in. by 48 in. were flame cut from larger plates of 3/4 in. thick HY-100 and 1/2 in. thick HY-130/150 steel.

For the transverse butt-welded specimens, the blanks were saw cut in half (9 in. x 24 in.) and the edges beveled to provide a double "V" groove with a 60° included angle for welding. All welding was performed in the flat position with the specimens clamped in a special jig which could be rotated about a horizontal axis (the longitudinal axis of the weld). The standard welding procedure for the butt joints in HY-100 steel is presented in Fig. 2.3. A stringer bead technique was employed which insures that the deposition of successive passes causes a tempering of the preceding passes. A series of butt-welded fatigue specimens was also prepared using the modified procedures illustrated in Figs. 2.4

* Numbers in parentheses refer to corresponding entries in bibliography.

and 2.5 (MIL-11018 electrode), and Fig. 2.9 (MIL-12018 electrode). The base plate preparation for these special weldments was the same as that described above for the standard welding procedure.

Details for the specimens with transverse attachments on one and two sides are shown in Figs. 2.2a and b; the corresponding welding procedures are presented in Figs. 2.6 and 2.7, respectively. No special preparation of the main member was necessary for welding other than grinding the surface clean.

The fabrication of specimens with full penetration tee joints was similar to that of specimens with attachments. The specimen geometry is illustrated in Fig. 2.2c and the welding procedure is presented in Fig. 2.8.

After the welding was completed, holes were drilled in the ends of the specimens as shown in Figs. 2.1 and 2.2. The test section was then saw cut and milled down to a 5 in. long straight section in the center. No material in the region of the test section was removed by flame-cutting. The width of this test section was governed by the test load range and the capacity of the fatigue machine; the width being made as large as possible within the machine capacity.

As a final stage in fabrication, the edges of the specimens in the test section were filed and ground smooth. For those butt joints which had the reinforcement removed, the specimen face was given a final polish with a belt sander in a direction parallel to the direction of subsequent loading.

2.3 Test Equipment

All fatigue tests were conducted using the University of Illinois' 250,000 lb. lever-type fatigue machines. The speeds of the machines used were 100 and 160 cpm.

The essential features of the fatigue machines are shown schematically in Fig. 2.10. The lever system provides a force multiplication ratio of approximately 15 to 1. The load range is adjusted through the throw of the eccentric, while the

maximum load is controlled by the adjustable turnbuckle mounted just below the dynamometer.

2.4 Testing Procedure

The testing procedure was similar for all specimens. After the load had been set and the machine started, an automatic microswitch was set so that the machine would shut off when a crack had propagated partially through the specimen. The load was maintained within limits of ±0.5 ksi by periodic checks and adjustments when necessary. Fatigue failure was assumed to have occurred when the microswitch shut off the machine; the crack had normally propagated through about 3/4 of the specimen at this stage. Cycling was then continued until complete fracture occurred so that the fracture surface could be examined and photographed.

2.5 Radiographic and Ultrasonic Studies

All transverse butt-welded specimens were subjected to radiographic examination prior to testing. Except for those with intentional defects, all specimens were classified as "sound" welds with no internal flaws visible on the radiographs (1 to 2 percent sensitivity).

A number of the transverse butt-welded specimens (with weld reinforcement removed) were also examined ultrasonically. The ultrasonic equipment detected numerous minute flaws, a number of which were verified when the fatigue fractures initiated at or passed through the flaws.

In addition, ultrasonic readings were taken at various stages in the lives of a limited number of specimens to study crack initiation and propagation.

2.6 Metallurgical Studies

Metallurgical studies were undertaken in an attempt to develop welding procedures for butt joints of HY-100 steel that would provide improved fatigue resistance. In addition, a number of butt-welded specimens were sectioned and

examined metallographically to verify the location of flaws predicted in the ultrasonic studies.

A preliminary study was made also to relate fatigue crack initiation and propagation to the associated microstructure observed in the HY-100 weldments.

III. FATIGUE TESTS OF 3/4 INCH HY-100 MATERIAL

3.1 Introductory Remarks

Several series of tests were conducted on a variety of specimens fabricated from 3/4 in. HY-100 steel to evaluate the fatigue behavior of different HY-100 weldments. Specimens were tested using both complete-reversal and zero-to-tension stress cycles. The fatigue strength of the plain plate specimens was determined and later used as a base of reference for computing the reduction in fatigue strength resulting from the various welded joints. The S-N relationship for the particular tests corresponding to each type of weldment was plotted where feasible and the fatigue resistance then compared to that of similar specimens fabricated using HY-80 steel (reported in previous studies).

3.2 Tests of Plain Plate Specimens

The fatigue test results for plain plate specimens on a zero-to-tension stress cycle are tabulated in Table 3.1 and plotted in Fig. 3.1. The S-N curve for these data, and for the other fatigue data presented in the report, were calculated using the procedure detailed in Ref. (2). For comparison the S-N relationship for 3/4 in. HY-80 plain plates is also presented in the figure.[3] As observed previously,[4] the S-N curve for the HY-100 steel exhibits a somewhat steeper slope than the curve for the HY-80 material. For the range of lives examined, however, both materials had similar fatigue strengths.

Five plain plate specimens were tested on a complete-reversal stress cycle. Test results are summarized in Table 3.2 and are plotted in Fig. 3.2. Two of the specimens, HY-21 and HY-22, initially failed in the pull-head as a result of fretting. New pull-heads were welded on and testing was continued with both specimens eventually failing in the radius of the test section. All other specimens failed either at the radius of the test section or near the radius. Also

shown in the figure is the S-N curve for similar tests of HY-80 material.[3] Comparing the curves, it is apparent that the HY-100 material has a slightly higher fatigue strength than the HY-80 base material for the complete-reversal stress levels studied.

A photograph of a typical fracture surface for a specimen which failed near the radius (initiation on the mill scale surface) of the test section is shown in Fig. 3.3.

3.3 Tests of As-Welded Butt Joints

A total of 14 transverse butt-welded specimens were tested in the as-welded condition. The specimen details and welding procedure (P100-11018-J) are presented in Figs. 2.1b and 2.3, respectively. Further information concerning the welding procedure is presented in Sect. 3.4. A typical microstructure of the heat affected zone (HAZ) of these weldments is compared to that of the HY-100 base metal in Fig. 3.4. The microstructure of the base metal shows the effect of the hot rolling and then the quenching and tempering treatment provided by the mill. The prior austenite grain size of this structure was small and the grains were elongated in the rolling direction. In the heat affected zone of the weld, where the maximum temperature was near the melting point for a short time, the prior austenite grain size was larger and the martensite platelets were larger than those in the microstructure of the original base metal. The martensitic structure in the austenitized part of the heat affected zone may have been only partially tempered and, therefore, of a higher hardness than the base metal. The fully tempered heat affected zone results when a successive weld bead is placed next to the deposited bead and provides a tempering heat treatment.

Six specimens were tested using a complete-reversal stress cycle. The fatigue data are summarized in Table 3.3 and the corresponding S-N curve is plotted in Fig. 3.5. Also presented in the figure is the S-N relationship for similar

joints of HY-80 steel, which were tested in a previous study.[3] Comparison of the S-N curves for the two materials shows that the fatigue resistance of the HY-100 butt-welded joints is lower than that of the HY-80 material at the complete-reversal stress levels studied. All of the HY-100 specimens failed at the stress concentrations at the edge of the weld reinforcement. However, one specimen, HY-26, also exhibited a small fatigue crack in the weld which initiated at a minute internal weld flaw not detected by radiography.

The fatigue data for the as-welded HY-100 butt joints tested on a zero-to-tension stress cycle are tabulated in Table 3.4 and plotted in Fig. 3.6. These tests were reported previously in Ref. (4). In a number of cases, specimens tested at the zero-to-tension stress cycle failed within the weld at small defects. These defects were not visible on the radiographs taken prior to testing. Photographs of the fracture surface of a specimen which failed at the toe of the weld reinforcement and of one in which failure initiated internally are presented in Fig. 3.7. It is apparent that, for the butt joints of HY-100 steel tested on a zero-to-tension stress cycle, the internal weld flaws had a greater effect on fatigue resistance than did the external weld geometry, especially at the higher nominal stress levels. The tendency for fatigue failures to initiate at small flaws within the weld metal becomes even more pronounced in specimens where the weld reinforcement has been removed (see Sect. 3.4). Possible reasons for this behavior are discussed in the following section.

The percentage reduction in fatigue strength of a plain plate due to the inclusion of a transverse butt weld in the as-welded condition is presented in Fig. 3.8 for both the zero-to-tension and complete-reversal stress cycles. Here it may be seen that the percentage reduction increases as the life increases and that the rate of change in this reduction is greater for the tests in complete-reversal than for those under a zero-to-tension cycle. Furthermore, complete-

reversal produces a more severe fatigue condition than zero-to-tension cycles at the longer lives.

3.4 Tests of Butt Joints with Reinforcement Removed

3.4.1 Standard Welding Procedure

The standard welding procedure used for most transverse butt welds in HY-100 consisted of a six pass weld using a MIL-11018 electrode with a maximum heat input of 40,000 joules per inch. This procedure, P100-11018-J, is presented in Fig. 2.3. Microhardness traces for a weld prepared with this procedure are shown in Fig. 3.12. The "near-surface" trace is 1.25 mm from the rolled surface and the "mid-thickness" trace is through the center transverse section of the weldment. In the HAZ near the surface the hardness is as high as 410 DPH; however at mid-thickness the corresponding values are only about 325 DPH. Thus, the tempering effect of the weld passes is readily evident as the peak hardnesses are significantly reduced in the mid-thickness HAZ.

Six transverse butt joints welded with the standard procedure and with the reinforcement removed were tested on a zero-to-tension stress cycle. Specimen details are shown in Fig. 2.1b; the fatigue data are presented in Table 3.5 and plotted in Fig. 3.9. The dashed line S-N relationship in Fig. 3.9 is for similar specimens of 3/4 in. thick HY-80 steel.[3] Although six out of seven of the HY-80 specimens failed away from the weld region, fatigue cracks in all but one of the HY-100 specimens initiated at a minute pore(s) in the weld metal. Photographs of the fracture surface of two typical specimens are shown in Fig. 3.10.

It is significant that no defects were visible in the radiographs of any of the HY-100 weldments. However, the fatigue initiating flaws, as well as others, were usually detected by ultrasonic inspection in those specimens which were subjected to that detection technique (see Sect. IV). The wide scatter in fatigue lives of the HY-100 specimens (i.e. from 57,900 to 1,108,600 cycles at 0 to

+50.0 ksi), together with the fact that all but one specimen failed at internal weld flaws, precluded the construction of a meaningful S-N curve that could be compared effectively with the curve for the joints of HY-80 steel.

In an attempt to decrease the porosity in the HY-100 weldments, one of the six butt joints fabricated with the standard welding procedure was prepared with an extra effort made to keep all surfaces clean between passes. The double "V" groove was machined in the standard manner, the preheat was applied with an oxy-acetylene torch, and a chipping hammer was used to remove the slag following each weld pass. In addition, an abrasive wheel was used to grind the "V" groove after each pass in order to remove spattered weld metal which had adhered to the exposed edges of the beveled base plates. Compressed air was then used to clean the weld area of loose particles.

This specially cleaned specimen, HY-60, was tested at a 0 to +50.0 ksi stress cycle. It had a life of only 57,900 cycles, the shortest of those tested at 0 to +50.0 ksi. A photograph of the fracture surface is presented in Fig. 3.10. Fatigue cracking is seen to have initiated at three separate pores, indicating that the special weld preparation techniques were not sufficient to eliminate porosity in the HY-100 joint when welded with the MIL-11018 electrode.

Six butt-welded specimens with reinforcement removed were tested using a cyclic loading of complete-reversal. The results of the tests are presented in Table 3.6 and are plotted in Fig. 3.11 together with the S-N curve of similar specimens of HY-80 material.[3] Although all of the HY-100 specimens were judged as "sound" weldments on the basis of radiographic examination, they all failed in the weld at small flaws. The wide scatter in the fatigue lives and the location of the fatigue fractures again prevents the construction of a suitable S-N relationship.

Overall examination of the series of fatigue tests of butt joints with reinforcement removed leads to the following observations. First, welding the HY-100 steel with the standard welding procedure used in this program (Fig. 2.3)

and the MIL-11018 electrode will produce welds with minute flaws within the weld. Although these defects may be of such a size as to escape radiographic detection, they are nevertheless points at which the initiation of fatigue cracking can take place. In view of the large amount of scatter obtained in the fatigue tests, improvements in the fatigue resistance of the members should be possible through improved weld quality and a better understanding of how the fractures initiate.

A second observation is that the use of an undermatching electrode, MIL-11018, with the HY-100 base metal appears to force the critical location for crack initiation into the weld at internal flaws rather than at the geometrical stress raiser at the radius of the test section. Especially at the higher stress levels, it appears that the combination of high stress concentration at internal weld defects and the close match of weld strength to base metal strength may be the cause of the very low fatigue lives obtained in some instances. It also may be recalled that, even in those HY-100 specimens tested in the as-welded condition, failure initiated internally in tests conducted at a 0 to +80.0 ksi stress cycle.

3.4.2 Experimental Welding Procedures

In an attempt to improve the fatigue resistance of HY-100 butt-welded joints, three modifications in the standard welding procedure were examined and compared. Each of the experimental procedures used the MIL-11018 electrode; the altered parameter was the energy input per unit length of weld metal. The first sample (1) was welded with the standard welding procedure of the current program. Higher and lower values of energy input, as compared to the standard procedure, were used to make samples 2 and 3. Sample 2 was fabricated with a higher energy 6 pass weld and sample 3 with a lower energy 12 pass weld. Sample 4 was identical to sample 1 except that a higher interpass and a higher preheat temperature was used for the weldment. Details of the welding procedures for the four samples are listed in Table 3.7.

Each of the four weldments was initially evaluated on the basis of micro-hardness traces located in the "near surface" and "mid-thickness" positions described previously (Sect. 3.4.1). These two traces provide the micro-hardness of the tempered weld metal and heat affected zone ("mid-thickness" trace), and the single bead (untempered) weld metal and heat affected zone ("near-surface" trace). The microhardness traces of the four samples are presented in Figs. 3.12 to 3.15. The microhardness survey from sample 1 (normal energy input) shows weld metal and base metal hardnesses that are approximately equal. The "near-surface" trace shows a high hardness (relative to that of the base metal) in part of the heat affected zone, and in the over-tempered region of the HAZ a hardness that was no lower than the minimum base metal hardness. However, at the "mid-thickness" the tempered HAZ shows some indication of an over-tempering and a hardness lower than that of the base metal. In sample 2 (high energy input) a microhardness trace similar to that of sample 1 was obtained as shown in Figs. 3.13 and 3.12, respectively, except that the maximum hardness in the HAZ of the single bead or "near-surface" trace was greater in sample 2. The lower energy weldment shown in Fig. 3.14 (sample 3) has a HAZ similar to that of the standard weldment, but the weld metal appears slightly harder in the "near-surface" trace. Use of a normal energy input with a higher preheat and interpass temperature (sample 4) resulted in a weldment with the hardness variation shown in Fig. 3.15. The hardness of the HAZ was lowered slightly in the untempered region of the "near-surface" trace; the weld metal hardness was also low in comparison to the other welding procedures used. Frequently, a softer region of hardness was observed in the weld metal adjacent to the fusion line, but this hardness value was not below the minimum hardness of the base metal.

A center-line hardness trace was then taken for each of the four samples through the thickness of the weldment to provide a representative average weld metal hardness and an indication of hardness variation. Average values of the hardness data for all weld sample traces are presented in Table 3.7. The hardness

values in the HAZ for each of the weldments listed in Table 3.7 represent average hardnesses for the untempered region of the HAZ. The standard deviation for a number of readings of the same indentation, made by three experienced investigators, was ±6 Diamond Pyramid Hardness. The heterogeneity of the microstructure is indicated by the large standard deviation of a number of hardness indentations in a region of similar microstructure. In samples 2 and 3 the untempered bead or "near-surface" trace had a slightly higher average weld metal hardness than the "mid-thickness" or tempered bead trace; the reverse was observed in samples 1 and 4. The hardnesses shown by the mid-thickness traces were dependent upon the exact location of the trace. When the tempered root pass was located in the path of the trace, which was taken at the geometrical mid-thickness of the joint, the lower hardness values were obtained (samples 2 and 3). However, when the untempered part of the second pass was located in the path of the trace, a higher hardness value was obtained (samples 1 and 4).

The center-line hardness trace through the weld metal, for which readings were taken at one millimeter intervals, gives a measure of the weld metal hardness in a variety of conditions; the average weld metal hardness is shown in Table 3.7. Note that the standard deviation for a center-line trace is greater than that of the other traces because the hardness of the tempered and untempered beads are averaged. The results of this center-line trace show that on the average the weld metal hardness is not appreciably changed by the energy input or the preheat used in this investigation.

Macrographs of the weldments of samples 1, 2 and 3 are shown in Fig. 3.16. The macrographs show the increased size and penetration of the higher energy and lower energy weldments compared to that of the standard weldment. The additional amount of weld metal used in the weldments having a higher or lower energy

input, is in part, a function of the welding procedure and in part a function of the root opening employed.

It should be noted also that each of the four weld samples described above were found to be radiographically sound.

In order to study the fatigue resistance of the experimental welds, four transverse butt-welded specimens with the reinforcement removed were fabricated using the procedures employed for samples 2 and 3 (Figs. 2.5 and 2.4). The procedure used for sample 4 was eliminated from this phase of the program since it produced weld metal hardnesses which were low in comparison to the other samples, Table 3.7, and would be expected to give a lower fatigue strength. Two of the fatigue specimens, HY-56 and HY-57, were tested on a stress cycle of 0 to +50.0 ksi. The other two specimens, HY-52 and HY-53, were tested on a stress cycle of +10.0 ksi to +60.0 ksi. The purpose of testing at a minimum stress level of +10.0 ksi was to protect the fracture surface from pounding during the latter stages of crack propagation.

Three of the experimental weld specimens failed within the weld. The flaws which initiated the fatigue fractures were again small flaws which were not detected by radiographic examination. The fatigue fracture of the other specimen initiated at a small weld undercut which remained after the reinforcement had been removed. The test results are presented in Table 3.8 and are plotted in Fig. 3.17. Also plotted in the figure are the test results of similar specimens welded with the standard welding procedure.

As with the previous studies of butt-welded specimens with the reinforcement removed, the modified weld procedure specimens exhibited a wide scatter in fatigue lives. The results appear to indicate that the modifications in the welding procedure provide no improvement over the standard procedure which has been used to date.

As a result of a study made at the Naval Applied Science Laboratory[6] on the use of higher strength electrodes for welding HY-100 material, a MIL-12018 electrode was selected for further evaluation of the axial fatigue resistance of transverse butt-welded joints. A sample weldment using the MIL-12018 electrode was prepared following the standard welding procedure. This procedure includes an 800°F bake-out of the electrodes for one hour and then the use of a 250°F holding temperature until the electrodes are used for welding. As shown in Table 3.7, the hardness of this weldment was increased considerably except at the center of the weld. A comparison of the microstructures of deposited weld metal using the MIL-11018 and MIL-12018 electrodes is presented in Figs. 3.18a and 3.18b, respectively. The grain structures are quite similar in both weld metals.

To obtain an indication of the comparative fatigue resistance of weldments made with the MIL-12018 electrode, one transverse butt-welded specimen with the reinforcement removed was tested on a 0 to +50.0 ksi stress cycle. The welding procedure (P100-12018-A) is shown in Fig. 2.9; it varies from the standard procedure only in the electrode used. The specimen, HY-61, had a fatigue life of 607,600 cycles and fracture initiated at a small single flaw within the weld which was not detected by radiography. The fatigue life is plotted in Fig. 3.17 along with the results of similar HY-100 specimens (MIL-11018 electrodes) tested at the same stress range. Although the life of specimen HY-61 is above the average of the other specimens in the figure, these are not sufficient data to draw any sound conclusions. The greatest life of any specimen welded with the standard procedure was 1,108,600 cycles and the shortest life was 57,900 cycles for the same stress cycle as that used for HY-61. Nonetheless, it is anticipated that the use of the MIL-12018 electrode will improve the fatigue resistance of weldments in HY-100 steel. Further fatigue studies in this area are planned to validate these preliminary predictions.

It should be noted also that the use of inert gas welding of HY-100 steel was investigated; however, the weldments contained porosity and the study has been discontinued for the present.

3.5 Tests of Butt Joints Fabricated with Intentional Weld Porosity

Two transverse butt-welded specimens containing intentional weld porosity were tested at a stress cycle of 0 to +50.0 ksi. The standard welding procedure (Fig. 2.3) was used. The porosity was produced by removing a 3/8 in. length of electrode coating so that subsequent welding with this defective electrode produced the desired porosity cluster in the center of the 6 in. length of weld. The porosity was placed in the third weld pass. On the basis of radiographic examination, the amount of porosity, i.e., flaw area relative to total cross-sectional area, was approximately 0.1 percent for both specimens. Although this percentage area reduction is within the allowable limits of present Navy Specifications,[5] the welds would nevertheless be classified as unacceptable as a result of an excessive number of fine pores (>8) in the cluster.

Both specimens were tested with the weld reinforcement removed. The test data are presented in Table 3.9. It should be noted that the fatigue failures of both specimens initiated at small single flaws which were not part of the intentional porosity and were not visible on the radiographs. Evidently the shape, location and orientation of these flaws forced the critical location for crack initiation to develop away from the larger intentionally placed porosity cluster. The results of these tests of defect specimens are plotted in Fig. 3.19 and are compared to the results of tests of radiographically sound specimens reported in Sect. 3.4.1. The wide spread in fatigue lives of both the "sound" and the porosity specimens, and the fact that the cracks in both porosity specimens initiated at defects not associated with the porosity cluster preclude a sound evaluation of the relative effect of such porosity clusters on fatigue resistance.

3.6 Tests of Plates with Transverse Attachments

3.6.1 Full Penetration Transverse Attachments on One Side

The welding procedure developed for joints with a full penetration transverse attachment on one side is shown in Fig. 2.6 and the fatigue specimen details are presented in Fig. 2.2b. Four welded joints of this type were tested in fatigue at a complete-reversal stress cycle. The two specimens tested at a stress level of ±20.0 ksi had similar fractures that initiated at the toe of the weld on the main member. This is the usual location of fatigue crack initiation for specimens with attachments. However, the fractures of both specimens tested at ±40.0 ksi appeared to have initiated on the mill scale surface of the plate behind the attachment and to have then propagated toward the weld. Photographs showing both types of fracture are presented in Fig. 3.20.

The test data for this series of tests are presented in Table 3.10. The S-N curve for the data is plotted in Fig. 3.21 along with the S-N relationship for similar tests of 1-1/2 in. thick HY-80 steel.[1] The HY-100 joints exhibited slightly higher fatigue lives at both stress levels studied.

3.6.2 Full Penetration Transverse Attachments on Two Sides

Four specimens with full penetration transverse attachments on two sides of the main member were tested at a stress cycle of complete-reversal. The specimen details and welding procedure are shown in Figs. 2.2a and 2.7, respectively. The failures of all the specimens were similar and initiated at the toe of the weld on the main member. A photograph of a typical fracture surface is shown in Fig. 3.22.

The fatigue test results are presented in Table 3.11; the slope of the log-log S-N curve is computed as $K = 0.405$. The S-N relationship for the member with attachments on two sides is plotted in Fig. 3.23 and is compared to similar members of 1-1/2 in. thick HY-80 material.[1] The S-N curves for the two materials have the same slope, although the HY-100 joints show slightly better fatigue behavior.

The HY-100 plates with attachments on two sides had lower fatigue lives than the plates with attachments on one side when tested at the higher stress level. However, both specimen types had similar lives at the lower stress level (longer lives). Thus, the effect of the different attachments upon the fatigue resistance of the member appears to depend upon the loading conditions to which the member is subjected. It should be noted, however, that these observations are based on a very limited amount of test data.

3.6.3 Full Penetration Tee Joints

The specimen details and welding procedure for full penetration tee joints are presented in Figs. 2.2c and 2.8, respectively. Four such specimens were tested using a cyclic loading of complete-reversal. The test results are presented in Table 3.12. The fractures of all specimens initiated at the toe of the weld on the main member. A typical fracture surface is presented in the photograph in Fig. 3.24. The fatigue lives of these joints were comparable to the lives of the HY-100 specimens with attachments on two sides (Sect. 3.6.2). The S-N relationship for the tee joints is plotted in Fig. 3.25 ($K = 0.383$) and is compared to the curve for similar joints of 1-1/2 in. thick HY-80 material.[1] The HY-100 joints exhibited better fatigue behavior at the higher stress level but were inferior to the HY-80 joints at the lower stress level studied (longer lives).

The percent reduction in fatigue strength of the plain plate specimens due to each of the three types of transverse attachments studied is presented in Fig. 3.26. The plots for specimens with tee joints and attachments on two sides are very similar, in fact, almost identical. The specimens with attachments on one side showed a much lower reduction in strength than did the other joints at the higher stress levels (short lives); the reverse was true for fatigue lives beyond approximately 200,000 cycles. Thus, it appears that several factors must affect the behavior of these members. The stress concentration at the toe of the weld provides a local effect for all three types of members. However, in the

case of the members with attachments on one side only, other factors, such as the bending resulting from eccentricity in the specimen, probably causes a further change in the stress condition in the member. This is borne out in part by the fact that two of the members with attachments on one side had failures which initiated on the side of the member away from the attachment.

IV. ULTRASONIC FLAW DETECTION STUDIES

4.1 Introductory Remarks

With the advent of high strength steel weldments and their greater notch sensitivity, increasing importance must be placed upon the detection and elimination of small internal flaws. Radiographic examination has often failed to detect these small flaws because of the flaw size, geometry, orientation and density. Fortunately, however, ultrasonic equipment, with its high sensitivity, often permits rapid location and evaluation of such small defects.

Ultrasonic examinations were first employed in the program to study the initiation and propagation of fatigue cracks in specimens containing large intentional defects in HY-80 steel.[4] The initial attempts to employ ultrasonics were partially successful, although some difficulties were encountered with the relatively new techniques used in the testing. During the current program progress has been made in improving the testing apparatus and detection procedures. With these improvements the ultrasonic studies have been continued on the detection of internal weld flaws and of the initiation and propagation of fatigue cracks.

Ultrasonic readings were recorded for a number of transverse butt-welded specimens both before and during cyclic testing, and the results of the predicted flaw locations compared with the flaw locations observed on the fracture surfaces. These comparisons are shown in Figs. 4.3 through 4.8.

A description of the ultrasonic equipment and testing procedure used in the flaw detection study is presented in the following paragraphs. In addition, a critical evaluation of the detection technique is given at the end of this section.

4.2 Test Equipment and Testing Procedure

The major equipment employed consisted of a Krautkramer Ultrasonic Flaw Detector Type USIP 10 and auxiliary accessories as shown in Fig. 4.1a. The probe used was a 5 megacycle/sec. miniature 45^{o} angle probe. A special unit was

constructed to hold and manipulate the probe across a fatigue specimen surface in a consistent and highly reproducible manner. The probe support consists of a movable table which supports the probe in a special housing, and permits mechanically controlled horizontal and vertical movement across the face of a specimen. The probe itself is held against the specimen from behind by a spring which presses it flush against the specimen with a constant pressure and thus insures reproducibility in readings. Linear transducers are attached to the traveling table of the probe support; the transducers are connected in turn to an X-Y recorder. The detector screen is suitably scaled so that the position of a flaw echo indicates directly the depth of the flaw within the weld. Once a flaw echo is located on the oscilloscope screen, the position of the echo together with the output of the transducers enable the operator to record on the X-Y plotter the horizontal and vertical location of the flaw in a plane parallel to the specimen surface.

Figure 4.1b shows the ultrasonic equipment in position for testing with the probe support secured to the lower pullhead of the fatigue machine and the probe bearing against the test surface. The support device can be clamped to the pullhead on either side of the specimen.

The ultrasonic examinations were performed in the fatigue machine with the test specimen under full static tension. All specimens examined contained transverse butt welds with the reinforcement removed. The specimen face was polished smooth to prevent excessive wear on the probe and to improve the sensitivity of the test. Light machine oil was used as an acoustic couplant between the probe and the specimen surface. As shown in Fig. 4.2, the weld area (including the heat affected zone) was scanned by traversing horizontally across the specimen face below the weld in 1/8 in. vertical increments until one-half of the weld area had been scanned. The probe was then placed on the opposite side of the specimen to scan the other half of the weld. An appropriate test range scale was selected and the detector screen adjusted so that the echo trace between the first reflection

from the rear surface and the second reflection from the front surface was visible (see Fig. 4.2).

Oscilloscope readings which exceeded a preselected minimum response level were assumed to indicate defects. Once a flaw (usually a small, isolated pore) was detected, its location was pinpointed by moving the probe both horizontally and vertically until the maximum echo height was seen on the detector screen. The projected position of the flaw on a plane parallel to the face of the specimen was then automatically plotted on the X-Y recorder. The depth of the flaw beneath the surface was determined from the position of the flaw echo on the oscilloscope screen and was manually recorded together with the height of the echo. Once the position of the peak response had been located, the probe was again moved horizontally and vertically until the height of the echo fell beneath the selected minimum response rejection level. These limits were indicated on the X-Y plots by crosses extending from the peak response in directions parallel and transverse to the long axis of the test specimen.

4.3 Flaw Detection Results

A number of transverse butt-welded specimens with the reinforcement removed were examined ultrasonically using the procedure outlined above. All specimens (except the intentional weld defect specimens) had been previously radiographed with no evidence of internal flaws. Ultrasonic readings were taken before cyclic loading was begun. After the specimen had failed, those flaws visible on the fracture surface were compared with the location and magnitude of the ultrasonic responses. The results of these comparisons are presented in Figs. 4.3 to 4.8 inclusive. These plots represent the projection of all the ultrasonic responses onto a cross-sectional plane through the weld perpendicular to the longitudinal axis of the fatigue specimen. The crosses indicate the projected limits of probe scan for which the echo amplitude remained above a selected minimum

rejection level. Since all of the flaws which were detected did not lie in the same plane, a letter designation is used to indicate the vertical position of the flaw with respect to the longitudinal axis of the specimen. The sketches of the fracture surfaces, shown in Figs. 4.3 through 4.8, represent a projection of the flaws visible on the fracture surface onto a similar plane perpendicular to the longitudinal axis of the specimen. The approximate sizes of those flaws which initiated the fatigue failures are presented with the corresponding specimen lives in Tables 3.5, 3.6, 3.8, and 3.9.

In general, the ultrasonic equipment did prove capable of detecting very small defects which had escaped radiographic detection. Furthermore, the plots show that most flaws seen on the fracture surface were picked up by the ultrasonic equipment. The predicted locations of the flaws as projected onto the face of the specimen were sometimes somewhat in error due to slight misalignments inherent in the design of the mechanical traversing equipment. The magnitude of the flaw echo on the detector screen was in itself not always a good indication of the actual flaw size, since a response will depend on the distance from probe to flaw, flaw geometry, test frequency, size and penetration power of probe, etc. However, when successive readings were taken during the life of a specimen, the initiation of fatigue cracking at a defect was indicated by a rise in the peak of the ultrasonic response corresponding to that particular defect. This is clearly shown in Fig. 4.8 for specimen HY-35, which was tested at ±30.0 ksi. The responses from the regions of the weld in which fatigue fracture initiated continued to increase in magnitude with the number of cycles while the other responses remained fairly constant. It can also be seen that there are several ultrasonic responses which do not correspond to defects visible on the fracture surface, indicating that there may be similar flaws in other planes beneath the surface.

Another transverse butt-welded specimen, HY-34, tested at a stress cycle of +10.0 to +60.0 ksi, was similarly subjected to periodic ultrasonic examination.

Readings were taken at zero cycles, 116,000 cycles, 209,000 cycles, and finally at 263,000 cycles. At 263,000 cycles the ultrasonic data indicated that the magnitude of one response had grown considerably since the previous reading, while the other responses remained at about the same level as the initial (zero cycles) reading. Initiation of a fatigue crack was suspected and the specimen was removed from the testing machine. At this time no cracks were visible on the surface.

In an attempt to find the suspected crack and verify the other ultrasonic responses, metallographic sections of specimen HY-34 were prepared at the positions shown in Fig. 4.9. Radiographs were taken of each of the eight sections. Only three of the sections showed flaws as indicated in Fig. 4.9. An example of the observed porosity is shown in the photomicrograph of Fig. 4.10; the pore is located in a region of coarse grain size. However, in the other porous areas, a normal grain size was observed around the flaws.

Section 5 (Fig. 4.9) produced the ultrasonic indication which was interpreted as a fatigue crack since it did not appear until after the 116,000 cycle reading. When subjected to radiography, however, this section did not reveal the presence of the suspected fatigue crack. At this point, a microsaw with a 0.020 in. thick blade was used to cut 0.015 in. thick slices from the section in the positions shown in Fig. 4.11. When the slices were polished and etched the fatigue crack was found; it had been progressing inward from the surface at the HAZ as shown in Fig. 4.11. This was an unexpected position for the fatigue crack in view of the fact that most weldments tested with the reinforcement removed had cracks which initiated at internal weld defects.

The ultrasonically located fatigue crack was still quite small, even though at least 50,000 cycles of stress were applied to the specimen after the crack was first observed on the detector screen. The crack had extended into the HAZ in a roughly semicircular manner. The length of the crack along the longitudinal axis of the weld varied from 0.09 in. to 0.12 in., with the greatest length being

found a short distance beneath the specimen surface. The maximum observed depth of the crack was approximately 0.04 in.

As a final note it should be mentioned that the ultrasonic equipment had accurately located the position of the crack in the vicinity of the polished surface of specimen HY-34. However, the predicted crack position in the longitudinal direction of the weld, as plotted on the X-Y recorder, was in error by approximately 1/4 in. This positioning error was a result of the inaccuracies of the traveling probe support and not of the ultrasonic detector itself. It is anticipated that such errors will be eliminated by the use of a new probe support device currently under development.

4.4 Evaluation of Equipment and Detection Technique

The use of the ultrasonic equipment is still relatively new as a means of detecting the initiation of fatigue cracking in welded joints. However, based on the results obtained thus far, it is apparent that the ultrasonic equipment is capable of accurately detecting minute internal weld flaws. In this respect the ultrasonic equipment was found superior to radiography. Furthermore, by comparing successive ultrasonic readings taken at different intervals during the cyclic loading of a specimen, the equipment has shown the ability of detecting the initiation and early growth of fatigue cracks.

As noted earlier, the traveling probe support has been a source of mechanical error in pinpointing and permanently recording the exact three dimensional location of the detected small internal weld flaws. A number of improvements in the design of this equipment are currently under way to minimize the mechanical positioning errors in future tests.

The interpretation of the ultrasonic responses with regard to the size and type of small flaws encountered to date provides a more difficult problem. A series of experimental weldments are being prepared which are to contain various

shapes and sizes of intentional internal flaws. It is hoped that the ultrasonic examination of these flaws with known dimensions will result in the development of suitable calibration standards that can be used in subsequent studies, at least where the same test material and specimen thicknesses are concerned.

Should these procedures prove feasible, it is anticipated that the ultrasonic equipment will prove a valuable mechanism in detecting, locating, and evaluating minute weld flaws, and in the identification and evaluation of fatigue crack initiation and propagation.

V. CRACK INITIATION AND PROPAGATION

5.1 Introductory Remarks

The HY-100 weldments were tested in fatigue in two conditions with respect to weld geometry, either in the as-welded condition or with the weld reinforcement removed. When the reinforcement was left on, the fatigue cracks often initiated at the edge of the reinforcement, propagated through the heat affected zone (HAZ) in a direction perpendicular to the direction of stress, and then progressed through the base metal. With the reinforcement removed the fatigue cracks were found to initiate in the weld metal at internal flaws (with two exceptions, specimens HY-34 and HY-57, where the crack originated at or near the polished specimen surface).

Internal fatigue crack initiation is important because failure in the weld metal apparently can occur at any weak point in the structure of the weld, and a fatigue crack so formed may remain undetected until fairly late in the course of propagation. Few of the internal defects that initiated fatigue cracks were large enough to be detected by radiographing the 3/4 in. thick weldment with its reinforcement removed. However, the diameter of the flaws visible in the plane of the specimen fracture surface was usually larger than the radiographic sensitivity (2 percent of specimen thickness) indicated by the penetrameter. The disagreement between actual flaw size and radiographic sensitivity suggests that the flaw shape in the failures was irregular rather than spherical. Metallographic examinations of the flaws verified this supposition; the results of these examinations are detailed in the following section.

5.2 Test Results

A typical example of the location and appearance of a flaw that caused the nucleation of a fatigue crack is shown on the fractured surface in Fig. 5.1. This fracture surface is from specimen HY-43, which was tested at a stress cycle of 0 to +50.0 ksi. Immediately after failure the fracture surfaces of the specimen

were preserved with a C_aCl_2 dessicant, thus preventing corrosion of the exposed surfaces. The pore shown in Fig. 5.1 was located in the weld metal near the fusion line. The fatigue crack propagated through the weld metal and then through the HAZ; the fracture surface resulting from this stage of propagation is observed in the figure as the smooth circular region around the crack initiating pore. When the radially propagating crack intersected the surface of the test specimen, the smooth fracture was replaced by a more rapidly propagating, coarser crack as the remaining net section was reduced and the stresses increased. The final stage in the failure sequence was evidenced by a "shear-type" crack which extended at approximately 45^{o} to the direction of loading (right half of fracture surface, Fig. 5.1).

As frequently observed in other fractures, a weld metal finger protruded into the critical pore of specimen HY-43, resulting in a doughnut-shaped flaw when viewed in profile. This flaw, at the center of the circular fracture surface in Fig. 5.1, is shown at a higher magnification in Fig. 5.2. Dark field illumination of this pore on the fracture surface reveals a bright "as-cast" appearance. No noticeable difference in fracture texture was observed between the fracture surface at the edge of this flaw and the fatigue fracture surface at a distance from it. Attempts at replication of the pore's edge for observation with an electron microscope to obtain better resolution have failed to date.

The surface condition of the fatigue fracture in the weld metal adjacent to the flaw is shown in Fig. 5.3 to 6,400X magnification. Transgranular fracture surfaces are evident with hard spherical particles on these surfaces. Between grains large steps that appear to follow grain boundaries are observed. Although the two stage replication technique used made it difficult to maintain the orientation of crack propagation, the direction of shadowing was used as a guide and the direction of fatigue crack propagation is roughly from the upper left to the lower right corner of the print. A single stage replication technique will be

attempted in the future in order to maintain a known orientation with respect to the microstructure and to the direction of crack propagation.

Another fatigue specimen, HY-25, was tested at a stress cycle from 0 to +50.0 ksi and the test was stopped soon after the fatigue crack reached the surface of the specimen. The end of the fatigue crack was exposed by sectioning the specimen. The fracture was next coated with an electroless nickel deposit and the section metallographically polished in the area of interest. A sketch of the fatigue crack near its origin is shown in Fig. 5.4. The tendency for the fatigue crack to follow the fusion line is shown in the sketch which can be used to orient the micrographs of Figs. 5.5a and 5.5b. Small particles which result from numerous crack paths in the region of lower hardness and smaller prior austenite grain size in the HAZ were observed in a branch of the fatigue crack located in the heat affected zone. Such particles are normally lost when complete separation takes place upon fracture. Prior austenite grain boundaries appear to provide the preferred paths of crack propagation in the higher hardness region of the HAZ as shown in Fig. 5.5a. The fatigue crack shown in Fig. 5.5b propagated through the weld metal. The precise origin of the fatigue crack is unknown, but it is believed to have initiated below the surface of the weldment.

The initiation and propagation of a fatigue crack in a third test specimen, HY-34, was observed by ultrasonic inspection as described in Sect. 4.3. This specimen was tested at a stress cycle of +10.0 to +60.0 ksi, the minimum stress of +10.0 ksi being maintained to prevent deformation of the fatigue cracked surface during the course of propagation. The ultrasonic response indicated that a crack began to grow between a life of 116,000 cycles and 209,000 cycles. The approximate position of the suspected crack was in section (5) illustrated in Fig. 4.9. The precise position of the crack, determined by thin sectioning of section 5 and by subsequent metallographic observation, is sketched in Fig. 4.11. The metallographic samples were prepared as described earlier by polishing and etching eight transverse

slices cut from the region containing the suspected fatigue crack. The surface of slice 6 west, Fig. 4.11, which contained the crack at its maximum observed depth, is shown in Figs. 5.6 (100X magnification) and 5.7 (200X magnification).

The right hand side of the fatigue crack shown in Fig. 5.6 is observed to have propagated around prior austenite grain boundaries. This is in the region of maximum hardness of the HAZ where sulfide wetting of austenite grain boundaries frequently occurs. The region of lower hardness and lower maximum temperature in the HAZ contains the end of the fatigue crack, shown in Fig. 5.7 at a point where the crack branched out and propagated along martensite boundaries rather than prior austenite boundaries. The other slices cut from section 5 of the specimen have cracks that are only 0.02 in. deep or less compared to the 0.04 in. maximum depth. The less penetrating branches of the crack are almost entirely in the part of the HAZ with the highest hardness. These branches propagated around prior austenite grain boundaries, and in some cases stopped before reaching the specimen surface when the edge of the weld metal was in their path. It appears, then, that the fatigue crack at the stage in which the fatigue test was stopped was confined to the HAZ, even though the reinforcement was removed. The reason for nucleation of this crack in the HAZ is not certain, but, it is probably not related to a geometrical surface stress raiser of any size. In the absence of such a stress raiser, it is most likely that the nucleation is associated with the metallurgical structure of the HAZ. Once initiated, the crack prefers to propagate around prior austenite boundaries; it is also possible that these grain boundaries could be the site of nucleation.

VI. INITIAL FATIGUE TESTS OF 1/2 INCH HY-130/150 MATERIAL

6.1 Introductory Remarks

Preliminary studies were conducted to evaluate the fatigue behavior of HY-130/150 steel. All specimens were 1/2 in. thick plain plates which were tested on a zero-to-tension stress cycle. The specimen details are presented in Fig. 2.1.

6.2 Tests of Plain Plate Specimens

A photomicrograph of the HY-130/150 base metal is presented in Fig. 6.1a. It was noted also that the HY-130/150 plates had a thin exterior mill scale surface which easily flaked off, as shown in Fig. 6.1b. Beneath this thin layer was a rough, oxidized surface. The thin, outer mill scale layer (that was observed to flake off during fatigue testing of the HY-130/150 metal) was not present on the HY-80 and HY-100 plates which were tested previously.

The HY-130/150 plain plates were tested at three stress levels. The fatigue data are presented in Table 6.1. The data are plotted in Fig. 6.2 together with the results of similar tests for 3/4 in. HY-100 plain plates. All specimens tested at the two higher stress levels failed either in the test section or at the radius. Photographs showing a typical fracture surface of a specimen which failed at the mill scale surface and one which failed at the test radius are presented in Fig. 6.3.

Five specimens were tested at the lower stress level of 0 to +50.0 ksi. Two of the specimens had fretting failures in the pullheads at the ends of the specimens. Another specimen, NA-4, fractured in the test section, but the fatigue life is uncertain due to a mechanical malfunction of the cycle counter on the fatigue machine. Fatigue failure is known to have occurred, however, between 484,000 and 627,000 cycles; an average value of 555,000 cycles has been reported as the fatigue life. The remaining two specimens fractured in the test section but had fatigue lives which were low in comparison to the other three. The results

of all five of these specimens were used in computing the S-N relationship for the plain plates. Since the fatigue lives of two of the specimens, NA-6 and NA-10, represent minimum values, the computed slope, K, is a maximum value.

The results shown in Fig. 6.1 indicate that the HY-130/150 plain plates exhibit slightly better fatigue resistance than the HY-100 plates at the lower stress level studied; however, the fatigue lives for the two materials are approximately equal at higher stress levels. A summary of all the fatigue tests of both the HY-130/150 and HY-100 materials which were conducted during the course of this study is presented in Table 6.2.

VII. SUMMARY AND CONCLUSIONS

The following is a summary of the results of the tests conducted in this study. It should be recognized that many of the reported evaluations are based on a minimal amount of data, and must be viewed accordingly. However, there are a number of basic observations which are considered significant; these are briefly summarized in the following paragraphs.

7.1 Fatigue Behavior of HY-100 Steel

Fatigue tests of 3/4 in. plain plates and transverse, full penetration weldments of HY-100 steel have indicated that:

1. The axial fatigue strength of the HY-100 steel base plate was similar to that of the HY-80 base material when evaluated on the basis of both zero-to-tension and complete-reversal stress cycles.

2. Transverse butt-welded joints of HY-100 in the as-welded condition had somewhat lower fatigue strengths than comparable joints of HY-80 steel at both the zero-to-tension and complete-reversal stress cycles. With the weld reinforcement removed, fatigue failure in the HY-100 material almost invariably occurred at small internal weld flaws. The resultant fatigue lives of the HY-100 specimens with reinforcement removed were usually lower than corresponding lives for similar HY-80 specimens and exhibited so wide a scatter at both stress cycles examined that appropriate S-N relationships could not be constructed.

3. A number of modifications in the welding procedures using the MIL-11018 electrodes were found to be unsuccessful in eliminating the small internal defects which proved critical in fatigue crack initiation for specimens tested with the reinforcement removed. A single HY-100 test weldment, using the MIL-12018 electrode, exhibited a fatigue life greater than all but one of the MIL-11018 electrode welded joints tested at the same stress level. Although failure in this weldment also initiated at an internal flaw, it is believed that use of the

MIL-12018 electrode may improve the fatigue behavior and reduce the scatter in test data of HY-100 steel weldments, especially in tests conducted with the weld reinforcement removed. Further studies in this direction are scheduled.

4. The fatigue strengths of HY-100 plates with attachments welded on either one or two sides were slightly higher than comparable joints of HY-80 steel tested at the same complete-reversal stress cycle. HY-100 welded tee joints showed slightly greater fatigue resistance than tee joints of HY-80 at the higher stress level studied; the reverse was true at the lower stress level. These tests were also conducted on a complete-reversal stress cycle. Failure in most of the specimens with attachments and in the tee weldments initiated at the toe of the weld on the stressed member.

7.2 Ultrasonic Flaw Detection Studies

Ultrasonic equipment provides a highly sensitive non-destructive testing technique for the detection of undesirable irregularities in the base materials and welded connections. An ultrasonic detector and auxiliary equipment was used in the present study: (1) to detect and geometrically locate the position of small flaws invariably found to exist in the HY-100 weldments tested; and (2) to determine the location and time to initiation of internal fatigue cracks in specimens subjected to cyclic loading. As a result of these investigations, it has been determined that:

1. The ultrasonic equipment was quite successful in detecting the presence of very small weld defects which, due to size, shape, and/or orientation, were not found with the use of standard radiographic inspection techniques. The existence of many of the flaws indicated by the ultrasonic detector was verified by examination of fracture surfaces of fatigue tested specimens, or by metallographic examination of thin sections cut from welded joints which contained the suspected flaws. It is anticipated that ultrasonic detection techniques of this

type will gain further widespread acceptance in the future as a replacement for or supplement to radiography for inspection of field connections. The most restrictive drawback at present to ultrasonic testing however, is the relative difficulty of correlating the magnitude and appearance of response to actual flaw shape, size, and type (i.e., porosity, slag, single voids, etc.). It is desirable that investigations be continued in this area to obtain, if possible, a reliable quantitative relationship between ultrasonic response and defect severity.

2. Ultrasonic weld inspection, when performed at various intervals during the cyclic testing of welded specimens, was capable of determining the approximate time to initiation of an internal fatigue crack. Two fatigue specimens (HY-34 and HY-35) were subjected to this type of continuous inspection, which indicated that cracking had begun at approximately one-half of the total test lifetime in each case.

7.3 Crack Initiation and Propagation

Based on the observations of crack initiation and propagation in the weldments of 3/4 in. thick HY-100 steel the following remarks and conclusions may be made:

1. Most fatigue cracks nucleated at a pore in the weld metal in specimens tested with the weld reinforcement removed. Small flaws, undetected by radiographic procedures, may provide serious internal stress raisers when the geometry of the flaws is such as to form disc-like cavities. The most severe internal stress raising condition occurs when the plane of the disc-like cavity is perpendicular to the direction of principal stress. Furthermore, these flaws appear to become increasingly more critical as points of fatigue crack initiation as the strength of the welded materials increases.

2. Following nucleation, a transgranular fatigue crack usually propagated in the weld metal (specimens welded with MIL-11018 electrodes and weld reinforcement removed).

3. Fatigue crack propagation in the heat affected zone of higher hardness was found to take place along prior austenitic grain boundaries; some parallel cracks were found in the heat affected zone of lower hardness.

7.4 Initial Fatigue Study of HY-130/150 Steel

Fatigue tests conducted on 1/2 in. HY-130/150 plain plates indicate that there may be some improvement in fatigue strength relative to comparable specimens of both HY-80 and HY-100 steels. The fatigue strengths obtained from tests at a zero-to-tension stress cycle are compared for the three materials in the table below.

Steel	Thickness (in.)	Fatigue Strength, ksi (Zero-to-Tension)			
		$F_{50,000}$	$F_{100,000}$	$F_{200,000}$	$F_{500,000}$
HY-80*	3/4	75.6	65.6	57.1	47.4
HY-80**	1-1/2	78.5	67.9	60.9	54.5
HY-100	3/4	84.5	68.6	55.7	42.9
HY-130/150	1/2	83.8	70.8	60.3	51.4

* Results reported in Ref. 3.

** Results reported in Ref. 2.

BIBLIOGRAPHY

1. Sahgal, R. K. and Munse, W. H., "Fatigue Behavior of Axially Loaded Weldments in HY-80 Steel," University of Illinois, Department of Civil Engineering, Structural Research Series 204, September 1960.

2. Hartmann, A. J. and Munse, W. H., "Fatigue Behavior of Welded Joints and Weldments in HY-80 Steel Subjected to Axial Loadings," University of Illinois, Department of Civil Engineering, Structural Research Series 250, July 1962.

3. Hartmann, A. J., Bruckner, W. H., Mooney, J. and Munse, W. H., "Effect of Weld Flaws on the Fatigue Behavior of Butt-Welded Joints in HY-80 Steel," University of Illinois, Department of Civil Engineering, Structural Research Series 275, December 1963.

4. Munse, W. H., Bruckner, W. H., Hartmann, A. J., Radziminski, J. B., Hinton, R. W. and Mooney, J. L., "Studies of the Fatigue Behavior of Butt-Welded Joints in HY-80 and HY-100 Steel," University of Illinois, Department of Civil Engineering, Structural Research Series 285, November 1964.

5. Bureau of Ships, U. S. Navy, "Fabrication, Welding and Inspection of HY-80 Submarine Hulls," NAVSHIPS 250-637-3, January 1962.

6. Private communication from I. L. Stern, U. S. Naval Applied Science Laboratory, Brooklyn, New York.

TABLE 2.1

PHYSICAL PROPERTIES OF BASE METAL
(Data Supplied by Manufacturer)

Heat Number	Designation	Thickness (inches)	Properties in the Longitudinal Direction				
			Yield Strength* (ksi)	Tensile Strength (ksi)	Elong. in 2 inches (percent)	Reduction in area (percent)	Charpy V-Notch ft-lbs**
N15423	HY(HY-100)	3/4	110.0	127.5	23.0	71.1	83 (a)
3P0074	NA(HY-130/150)	1/2	138.0	144.0	20.0	69.8	102 (b)

* 0.2 percent offset

** (a) @ -120°F
(b) @ 0°F

TABLE 2.2

CHEMICAL COMPOSITION OF BASE METAL
(Data Supplied by Manufacturer)

Chemical Composition (percent)	Heat Number	
	N15423	3P0074
Base Metal Designation	HY-100	HY-130/150
C	0.20	0.110
Mn	0.30	0.78
P	0.010	0.008
S	0.014	0.006
Si	0.21	0.29
Ni	3.00	5.03
Cr	1.67	0.56
Mo	0.50	0.42
Cu	0.11	----
V	----	0.05
Al*	----	0.008
Al**	----	0.015
N	----	0.011
O	----	0.0029

* acid soluble

** total

TABLE 3.1

RESULTS OF FATIGUE TESTS OF HY-100 PLAIN PLATE SPECIMENS*
(Zero-to-Tension)

Specimen Number	Stress Cycle (ksi)	Life (cycles)	Location of Fracture***	Computed Fatigue Strength, ksi**			
				$F_{50,000}$	$F_{100,000}$	$F_{200,000}$	$F_{500,000}$
HY-7	0 to +76.5	81,200	f	88.4	71.7	58.4	----
HY-6	0 to +80.0	57,100	f	83.1	67.6	54.8	----
HY-4	0 to +80.0	46,400	a	78.3	63.5	51.7	----
HY-5	0 to +50.0	546,300	a	102.5	83.2	67.5	51.3
HY-2	0 to +50.0	253,100	a	81.1	66.1	53.6	40.7
HY-3	0 to +50.0	180,100	f	73.5	59.7	48.4	36.8
			Average	84.5	68.6	55.7	42.9

* Results initially reported in Ref. 4

** K = 0.301

*** a: failure initiated at radius of test section
b: failure initiated at mill scale surface near radius of test section

TABLE 3.2

RESULTS OF FATIGUE TESTS OF HY-100 PLAIN PLATE SPECIMENS
(Complete Reversal)

Specimen Number	Stress Cycle (ksi)	Life (cycles)	Location of Fracture**	Computed Fatigue Strength, ksi*				
				$F_{50,000}$	$F_{100,000}$	$F_{200,000}$	$F_{500,000}$	$F_{2,000,000}$
HY-20	±49.5	118,000	a	58.2	51.1	44.9	37.8	----
HY-23	±50.0	106,100	f	57.6	50.6	44.4	37.4	----
HY-24	±50.0	67,100	a	52.8	46.4	40.8	----	----
HY-21	±30.0	1,837,700	a	----	----	----	38.2	29.5
HY-22	±30.0	1,077,200	f	----	----	----	34.7	26.7
			Average	56.2	49.4	43.4	37.0	28.1

* K = 0.187

** a: failure initiated at radius of test section
f: failure initiated at mill scale surface near radius of test section

TABLE 3.3

RESULTS OF FATIGUE TESTS OF HY-100 TRANSVERSE BUTT WELDS IN THE AS-WELDED CONDITION

(Complete Reversal)

Specimen Number	Stress Cycle (ksi)	Life (cycles)	Location of Fracture**	Computed Fatigue Strength, ksi*			
				$F_{20,000}$	$F_{50,000}$	$F_{100,000}$	$F_{200,000}$
HY-27	±50.0	30,300	b	57.8	42.1	33.1	----
HY-26	±50.0	30,100	b,c	57.6	42.0	33.0	----
HY-19	±50.0	24,300	b	53.5	38.9	30.6	----
HY-18	±30.0	123,500	b	----	41.0	32.3	25.4
HY-17	±30.0	122,800	b	----	40.9	32.2	25.3
HY-16	±30.0	114,200	b	----	39.9	31.4	24.7
			Average	56.3	40.8	32.1	25.1

* K = 0.346

** b: at edge of weld reinforcement
c: initiation in weld at small defect(s) not detected by radiography

TABLE 3.4

RESULTS OF FATIGUE TESTS OF HY-100 TRANSVERSE BUTT WELDS IN THE AS-WELDED CONDITION*

(Zero-to-Tension)

Specimen Number	Stress Cycle (ksi)	Life (cycles)	Location of Fracture****	Computed Fatigue Strength, ksi**			
				$F_{20,000}$	$F_{50,000}$	$F_{100,000}$	$F_{200,000}$
HY-10	0 to +80.0	8,200	c	(56.3) ***	----	----	----
HY-8	0 to +80.0	5,400	c	(47.7) ***	----	----	----
HY-9	0 to +80.0	4,700	c	(45.1) ***	----	----	----
HY-12	0 to +50.0	61,800	b	77.9	54.4	41.4	31.5
HY-11	0 to +50.0	61,500	b	77.7	54.3	41.3	31.4
HY-13	0 to +50.0	24,100	c	(53.8) ***	----	----	----
HY-15	0 to +30.0	240,600	b	----	55.2	42.4	32.2
HY-14	0 to +30.0	212,500	b	----	53.1	40.4	30.8
			Average	77.8	54.2	41.4	31.5

* Results initially reported in Ref. 4

** K = 0.394

*** Not included in average; strengths calculated only for sound welds

**** b: at edge of weld reinforcement
c: initiation in weld at small defect(s) not detected by radiography

TABLE 3.5

RESULTS OF FATIGUE TESTS OF HY-100 TRANSVERSE BUTT WELDS WITH WELD REINFORCEMENT REMOVED*

(Zero-to-Tension)

Specimen Number	Welding Procedure (see Fig. 2.3)	Stress Cycle (ksi)	Life (cycles)	Location of Fracture**
HY-41	P100-11018-J	0 to +80.0	14,800	in weld-initiation at single flaw, < 0.01" dia.
HY-42	P100-11018-J	0 to +80.0	13,700	in weld-initiation at single flaw, 0.03" dia.
HY-25	P100-11018-J	0 to +50.0	1,108,600	in weld
HY-43	P100-11018-J	0 to +50.0	198,100	in weld-initiation at single flaw, 0.04" dia.
HY-39	P100-11018-J	0 to +50.0	88,100	in weld-initiation at single flaw, 0.04" dia.
HY-60	P100-11018-J	0 to +50.0	57,900	in weld-initiation at 3 separate flaws, 2 @ 0.02" dia. 1 @ 0.04" dia.
HY-34	P100-11018-J	+10.0 to +60.0	263,400***	initiation at or beneath polished specimen surface in HAZ

* S-N curves not constructed since all specimens failed at internal weld flaws

** Weld flaws not detected by radiography

*** Specimen not tested to failure-removed for metallurgical examination following ultrasonic indication of crack initiation

TABLE 3.6

RESULTS OF FATIGUE TESTS OF HY-100 TRANSVERSE BUTT WELDS WITH WELD REINFORCEMENT REMOVED*

(Complete Reversal)

Specimen Number	Welding Procedure (see Fig. 2.3)	Stress Cycle (ksi)	Life (cycles)	Location of Fracture**
HY-29	P100-11018-J	± 50.0	70,900	in weld-initiation at single flaw, 0.03" dia.
HY-30	P100-11018-J	± 50.0	53,500	in weld-initiation at single flaw, 0.04" dia.
HY-31	P100-11018-J	± 50.0	28,800	in weld-initiation at single flaw, < 0.01" dia.
HY-35	P100-11018-J	± 30.0	403,100	in weld-initiation at 2 separate flaws, 0.03" dia.
HY-28	P100-11018-J	± 30.0	220,700	in weld-initiation at single flaw, 0.05" dia.
HY-33	P100-11018-J	± 30.0	43,900	in weld-initiation at single flaw, 0.05" dia.

* S-N curves not constructed since all specimens failed at internal weld flaws

** Weld flaws not detected by radiography

TABLE 3.7

MICROHARDNESS SURVEY OF THE WELD METAL FOR HY-100 SPECIMENS PREPARED WITH VARIOUS WELDING PROCEDURES*

Sample	Welding Procedure	Number of Passes	Avg. Energy Input During Each Pass (joules/in.)	Avg. HAZ Hardness, DPH**	Average Weld Hardness, DPH**		
					Parallel to plate thickness		Center-line of weld through thickness
					M.T.***	N.S.***	
1	P100-11018-J	6	40,000	409±7(a)	286±11(a)	274±8(a)	283±12(b)
2	P100-11018-J50	6	50,000	463±12	276±11	300±12	280±12
3	P100-11018-J30	12	30,000	416±15	276±10	285±11	278±15
4	P100-11018-JH	6	40,000	390±11	270±7	259±10	274±12
5	P100-12018-A	6	40,000	------	284±10	314±7	302±17

* Minimum preheat and interpass temperatures for all samples except No. 4 were 150°F and 200°F, respectively. Temperatures for sample 4 were 300°F preheat and 400°F interpass.
The average base metal hardness obtained from a large number of determinations was 270DPH.

** The Diamond Pyramid Hardness values were obtained with a 1 kg. load.

*** M.T. refers to "mid-thickness"; N.S. refers to "near-surface" (1.25 mm beneath rolled surface)

(a) Standard deviation for a minimum of six hardness indentations

(b) Standard deviation for a minimum of sixteen hardness indentations

TABLE 3.8

RESULTS OF FATIGUE TESTS OF EXPERIMENTAL HY-100
TRANSVERSE BUTT WELDS WITH WELD REINFORCEMENT REMOVED

Specimen Number	Welding Procedure (see Figs. 2.4, 2.5, 2.9)	Stress Cycle (ksi)	Life (cycles)	Location of Fracture*
HY-57	P100-11018-J30	0 to +50.0	412,300	at weld undercut
HY-52	P100-11018-J30	+10.0 to +60.0	85,400	in weld-initiation at single flaw, .03" dia.
HY-53	P100-11018-J50	+10.0 to +60.0	318,600	in weld-initiation at single flaw, .03" dia.
HY-56	P100-11018-J50	0 to +50.0	137,900	in weld-initiation at single flaw, 0.04" dia.
HY-61	P100-12018-A	0 to +50.0	607,600	in weld-initiation at single flaw, 0.02" dia.

* Weld flaws not detected by radiography

TABLE 3.9

RESULTS OF FATIGUE TESTS OF HY-100 TRANSVERSE BUTT WELDS WITH INTENTIONAL POROSITY IN WELD

Specimen Number	Stress Cycle (ksi)	Life (cycles)	Percent Defect Area (Based on Radiography)	Radiographic Rating*	Description of Defects**
HY-54	0 to +50.0	134,700	0.12	F	one porosity cluster + single pore 0.02" dia.
HY-55	0 to +50.0	32,200	0.11	F	one porosity cluster + single pore 0.05" dia.

* Based on radiographic requirements of Navy Specifications[5]

** Fatigue failure initiated at single pore located away from porosity cluster

TABLE 3.10

RESULTS OF FATIGUE TESTS OF HY-100 PLATES WITH A FULL PENETRATION TRANSVERSE ATTACHMENT ON ONE SIDE

(Complete Reversal)

Specimen Number	Welding Procedure (see Fig. 2.6)	Stress Cycle (ksi)	Life (cycles)	Location of Fracture**	Computed Fatigue Strength, ksi*			
					$F_{20,000}$	$F_{50,000}$	$F_{100,000}$	$F_{200,000}$
HY-46	P100-11018-L	±40.0	63,800	e	83.2	46.6	30.1	19.4
HY-47	P100-11018-L	±40.0	38,900	e	61.0	34.1	22.0	14.2
HY-45	P100-11018-L	±20.0	175,000	d	----	44.2	28.5	18.4
HY-44	P100-11018-L	±20.0	121,800	d	----	34.1	22.7	14.6
				Average	72.1	40.0	25.8	16.7

* K = 0.632

** d: initiation at toe of weld on main member
e: initiation at mill scale surface on plain plate side

TABLE 3.11

RESULTS OF FATIGUE TESTS OF HY-100 PLATES WITH
FULL PENETRATION TRANSVERSE ATTACHMENTS ON TWO SIDES

(Complete Reversal)

Specimen Number	Welding Procedure (see Fig. 2.7)	Stress Cycle (ksi)	Life (cycles)	Location of Fracture**	Computed Fatigue Strength, ksi*			
					$F_{20,000}$	$F_{50,000}$	$F_{100,000}$	$F_{200,000}$
HY-37	P100-11018-K	±38.5	28,500	d	44.4	30.6	23.2	----
HY-38	P100-11018-K	±40.0	23,400	d	42.5	29.4	22.2	----
HY-32	P100-11018-K	±20.0	154,500	d	----	31.6	23.9	18.1
HY-36	P100-11018-K	±20.0	125,000	d	----	29.0	21.9	16.6
				Average	43.4	30.2	22.8	17.3

* K = 0.405

** d: initiation at toe of weld on main member

TABLE 3.12

RESULTS OF FATIGUE TESTS OF HY-100 PLATES WITH A FULL PENETRATION TEE JOINT

(Complete Reversal)

Specimen Number	Welding Procedure (see Fig. 2.8)	Stress Cycle (ksi)	Life (cycles)	Location of Fracture**	Computed Fatigue Strength, ksi*			
					$F_{20,000}$	$F_{50,000}$	$F_{100,000}$	$F_{200,000}$
HY-48	P100-11018-M	±40.0	25,200	d	43.7	30.8	23.6	----
HY-51	P100-11018-M	±40.0	19,600	d	40.0	27.9	----	----
HY-50	P100-11018-M	±20.0	157,500	d	----	31.0	23.8	18.3
HY-49	P100-11018-M	±20.0	118,200	d	----	28.0	21.3	16.4
				Average	41.9	29.4	22.9	17.3

* K = 0.383

** d: initiation at toe of weld on main member

TABLE 6.1

RESULTS OF FATIGUE TESTS OF HY-130/150 PLAIN PLATE SPECIMENS
(Zero-to-Tension)

Specimen Number	Stress Cycle (ksi)	Life* (cycles)	Location of Fracture***	Computed Fatigue Strength, ksi**				
				$F_{50,000}$	$F_{100,000}$	$F_{200,000}$	$F_{500,000}$	$F_{2,000,000}$
NA-8	0 to +100.0	26,800	g	87.3	74.8	----	----	----
NA-7	0 to +100.0	21,000	g	82.7	70.9	----	----	----
NA-1	0 to +80.0	64,200	a	84.5	72.6	62.2	----	----
NA-2	0 to +80.0	60,900	g	83.8	71.7	61.6	----	----
NA-5	0 to +80.0	51,100	h	80.6	69.0	59.4	----	----
NA-9	0 to +50.0	354,500	g	----	65.5	56.7	46.3	34.2
NA-3	0 to +50.0	280,900	a	----	62.8	53.8	44.1	----
NA-10	0 to +50.0	1,247,800+(1)	j	----	----	----	61.3	45.1
NA-6	0 to +50.0	712,000+(1)	j	----	77.0	66.1	54.0	39.8
NA-4	0 to +50.0	555,000±(2)	g	----	72.8	62.6	51.2	37.7
			Average	83.8	70.8	60.3	51.4	39.2

* (1) Specimen failed in pull-head
(2) Cycle counter on fatigue machine broke during test-failure occurred between 484,000 and 627,000 cycles

** K = 0.22

*** a: failure initiated at radius of test section
g: failure initiated at mill scale surface in specimen test section
h: failure initiated at polished edge of specimen test section
j: failure in pull-head

TABLE 6.2

SUMMARY OF FATIGUE TESTS OF HY-100 AND HY-130/150 MATERIAL

Specimen Type	Surface Condition	K	Computed Fatigue Strength, ksi				
			$F_{20,000}$	$F_{50,000}$	$F_{100,000}$	$F_{200,000}$	$F_{500,000}$
(a) 1/2 In. Thick HY-130/150 Material (Zero-to-Tension)							
Plain Plate	As-Received	0.22	102.3	83.8	70.8	60.3	51.4
(b) 3/4 In. Thick HY-100 Material (Zero-to-Tension)*							
Plain Plate	As-Received	0.301	----	84.5	68.6	55.7	42.9
Transverse Butt Weld	As-Welded	0.394	77.8	54.2	41.4	31.5	----
(c) 3/4 In. Thick HY-100 Material (Complete Reversal)							
Plain Plate	As-Received	0.187	----	56.2	49.4	43.4	37.0
Transverse Butt Weld	As-Welded	0.346	56.3	40.8	32.1	25.1	----
Transverse Attachment (one side)	As-Welded	0.632	(72.1)**	40.0	25.8	16.7	----
Transverse Attachment (two sides)	As-Welded	0.405	43.4	30.2	22.8	17.3	----
Tee Joint	As-Welded	0.383	41.9	29.4	22.9	17.3	----

* Results reported in Ref. 4

** Questionable

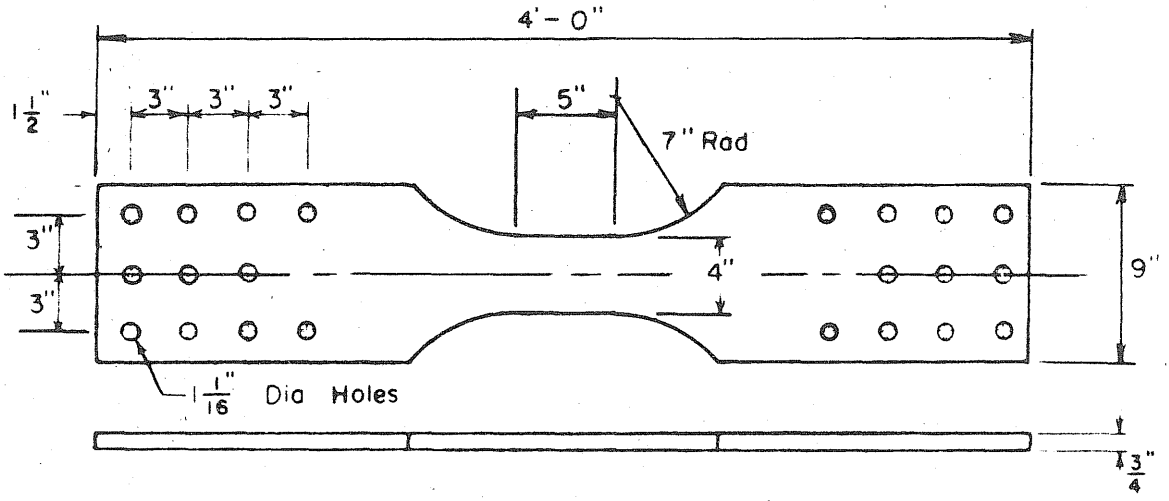

(a) Plain Plate (HY-100 Material)

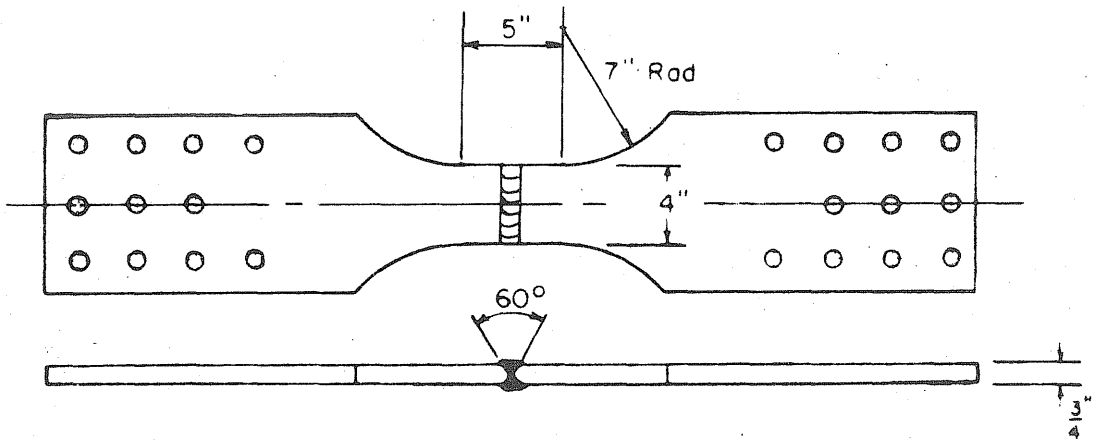

(b) Transverse Butt Weld (HY-100 Material)

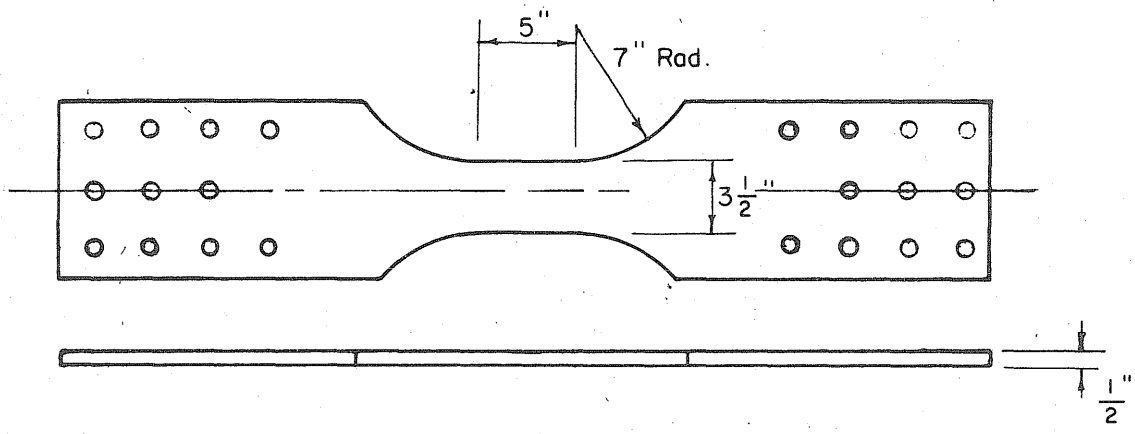

(c) Plain Plate (HY-130/150 Material)

FIG. 2.1 DETAILS OF TEST SPECIMENS.

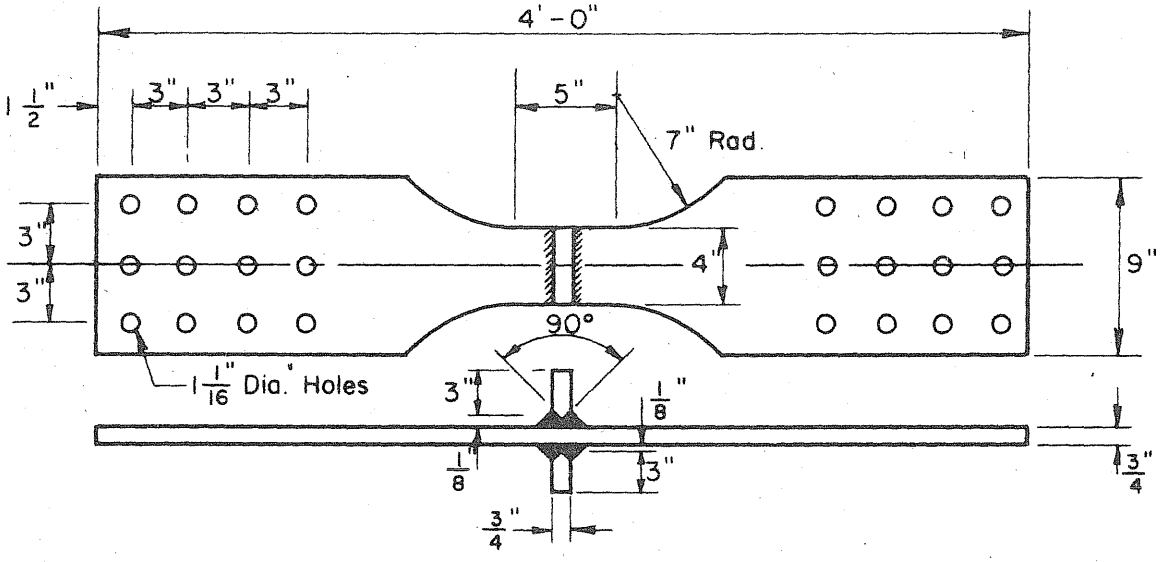

(a) Full Penetration Transverse Attachments

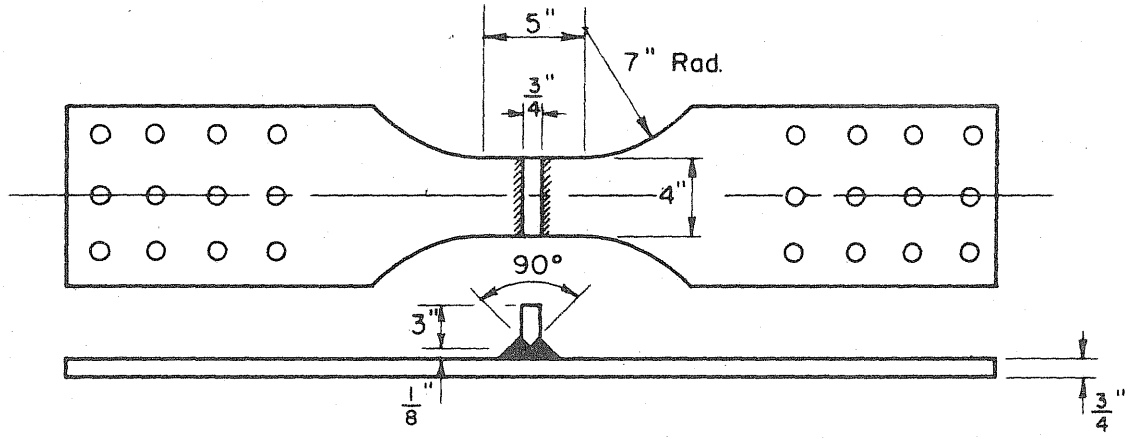

(b) Full Penetration Transverse Attachment

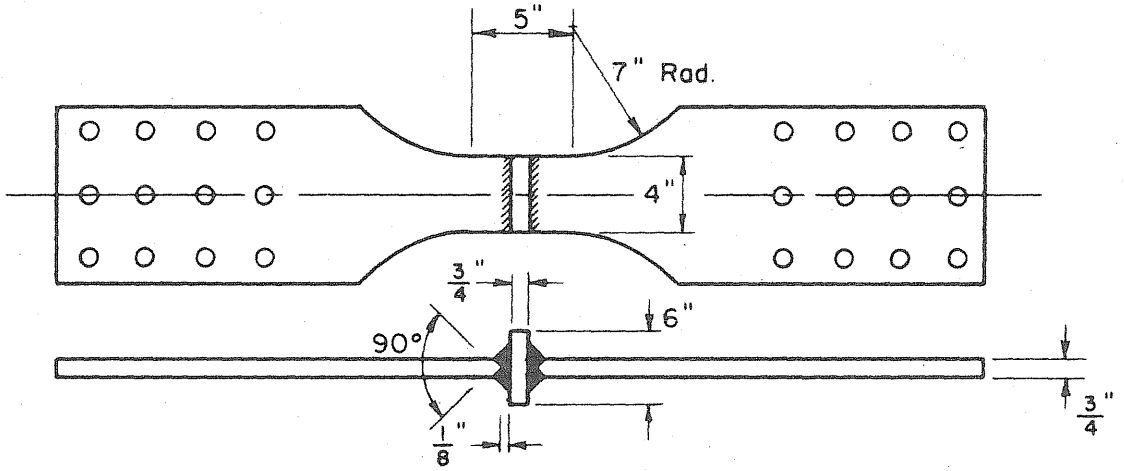

(c) Full Penetration Tee Joint

FIG. 2.2 DETAILS OF TEST SPECIMENS.

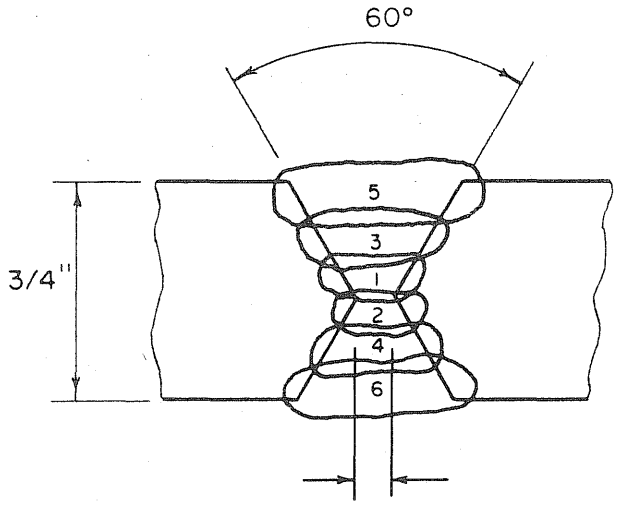

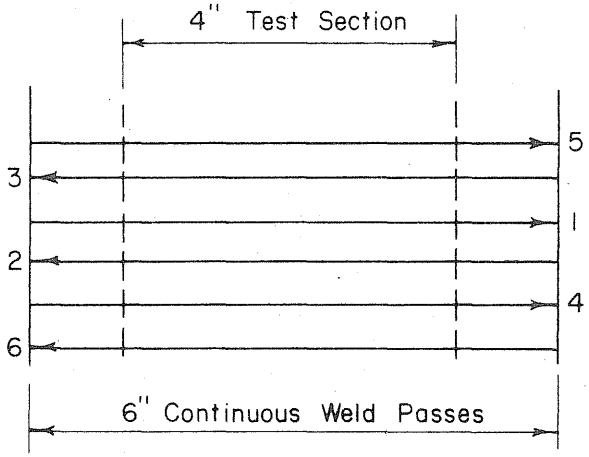

Arrows indicate direction of welding.

Surface of plate adjacent to weld cleaned by grinding before welding.

Pass	Electrode size, in.	Current, amps.	Rate of travel, in./min.
1	5/32	130	5
2	5/32	140	5
3	3/16	230	8
4	3/16	220	7
5	3/16	210	7
6	3/16	210	7

Voltage: 21 Volts
Polarity: DC Reversed
Preheat: 150°F
Electrode: MIL 11018
Interpass Temperature: 200°F (Maximum)
Heat Input: 40,000 Joules/in. (Maximum)
All welding in flat position
Underside of pass 1 ground before placing pass 2

FIG. 2.3 WELDING PROCEDURE P100-11018-J
(Transverse Butt Welds in HY-100)

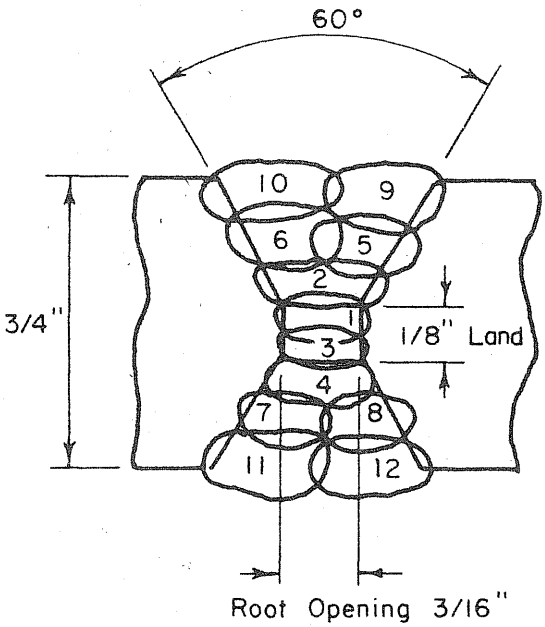

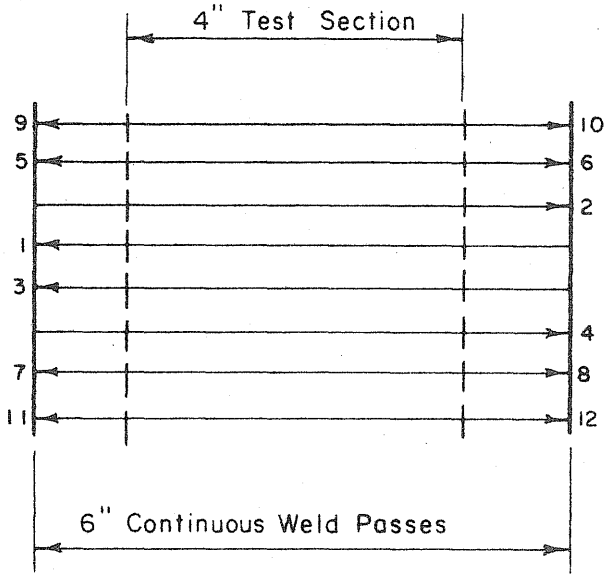

Arrows indicate direction of welding.

Surface of plate adjacent to weld cleaned by grinding before welding.

Pass	Electrode Size, in.	Current, amps	Rate of Travel, in./min.
1	1/8	110	4
2 – 12	5/32	175	8

Voltage : 21 volts
Polarity : D.C. Reversed
Preheat : 150 ° F
Electrode : MIL 11018
Interpass Temperature : 100° F (Maximum)

Heat Input : 30,000 Joules/in. (Maximum)
All welding in flat position.
Underside of pass 1 ground before placing pass 2.

FIG.2.4 WELDING PROCEDURE P100-11018-J30
(Transverse Butt Welds in HY-100)

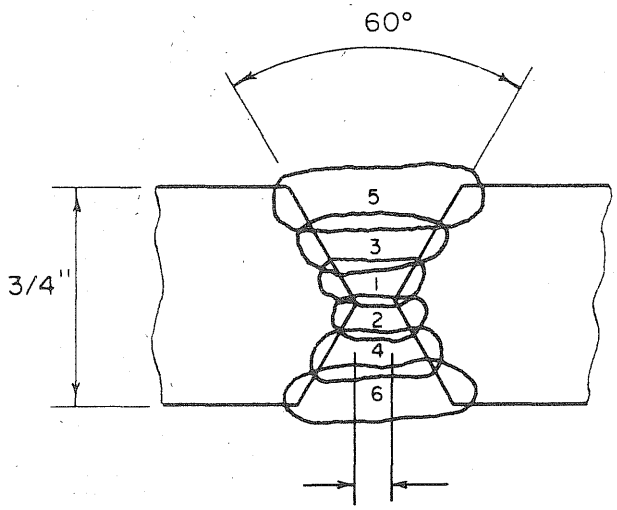

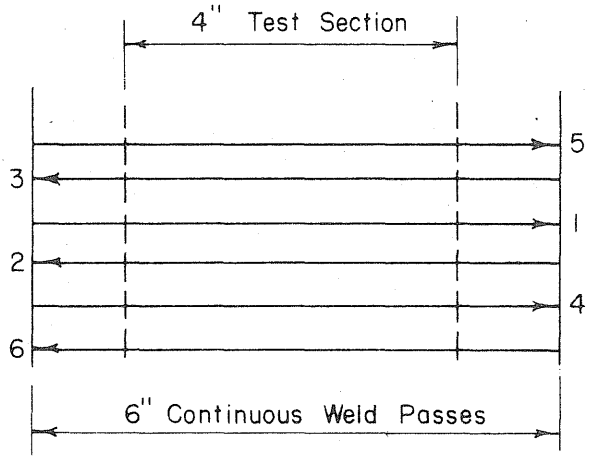

Arrows indicate direction of welding.

Surface of plate adjacent to weld cleaned by grinding before welding.

Pass	Electrode size, in.	Current, amps.	Rate of travel, in./min.
1	5/32	150	5
2	5/32	150	5
3	3/16	220	6
4	3/16	220	6
5	3/16	220	6
6	3/16	220	6

Voltage: 21 Volts
Polarity: D C Reversed
Preheat: 150°F
Electrode: MIL 11018
Interpass Temperature: 200°F (Maximum)
Heat Input: 50,000 Joules/in. (Maximum)
All welding in flat position
Underside of pass 1 ground before placing pass 2

FIG. 2.5 WELDING PROCEDURE P100-11018-J50
(Transverse Butt Welds in HY-100)

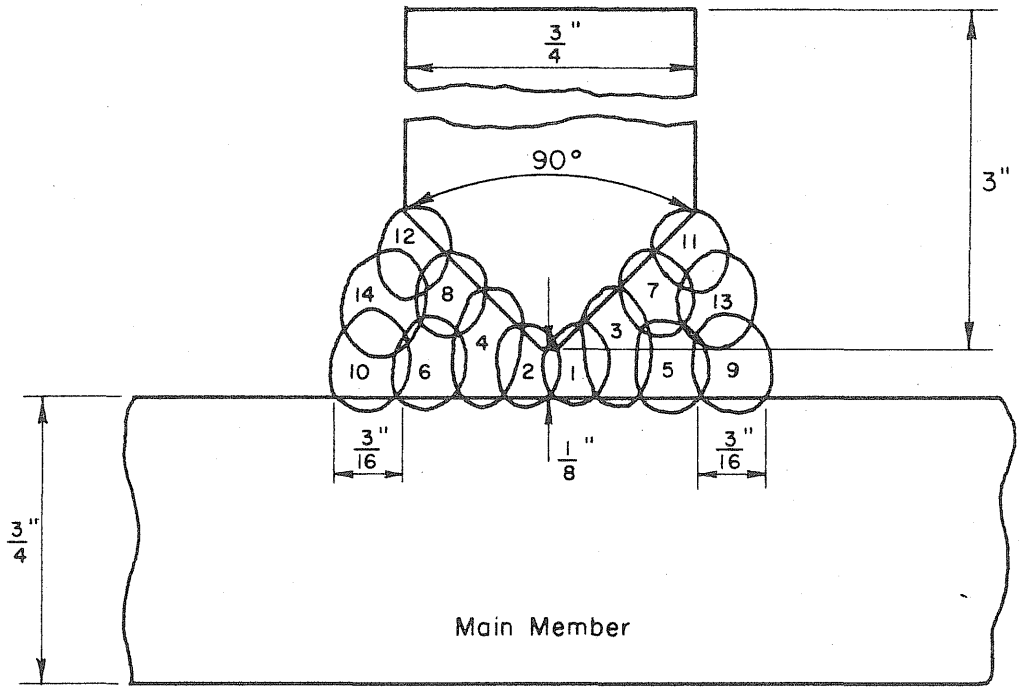

Pass	Electrode size, in.	Current, amps.	Rate of travel, in./min.
1	5/32	140	4.5
2–14	5/32	175	5.5

Voltage: 21 Volts
Polarity: D. C. Reversed
Interpass Temp: 200° F (Max.)
Preheat: 200° F
Electrode: MIL 11018
Heat Imput: 40,000 Joules/in. (Max.)

Surfaces cleaned by grinding before welding.
All welding in flat position
Underside of pass 1 ground before placing pass 2, 4.

FIG. 2.6 WELDING PROCEDURE P100-11018-L (Full Penetration Transverse Attachments)

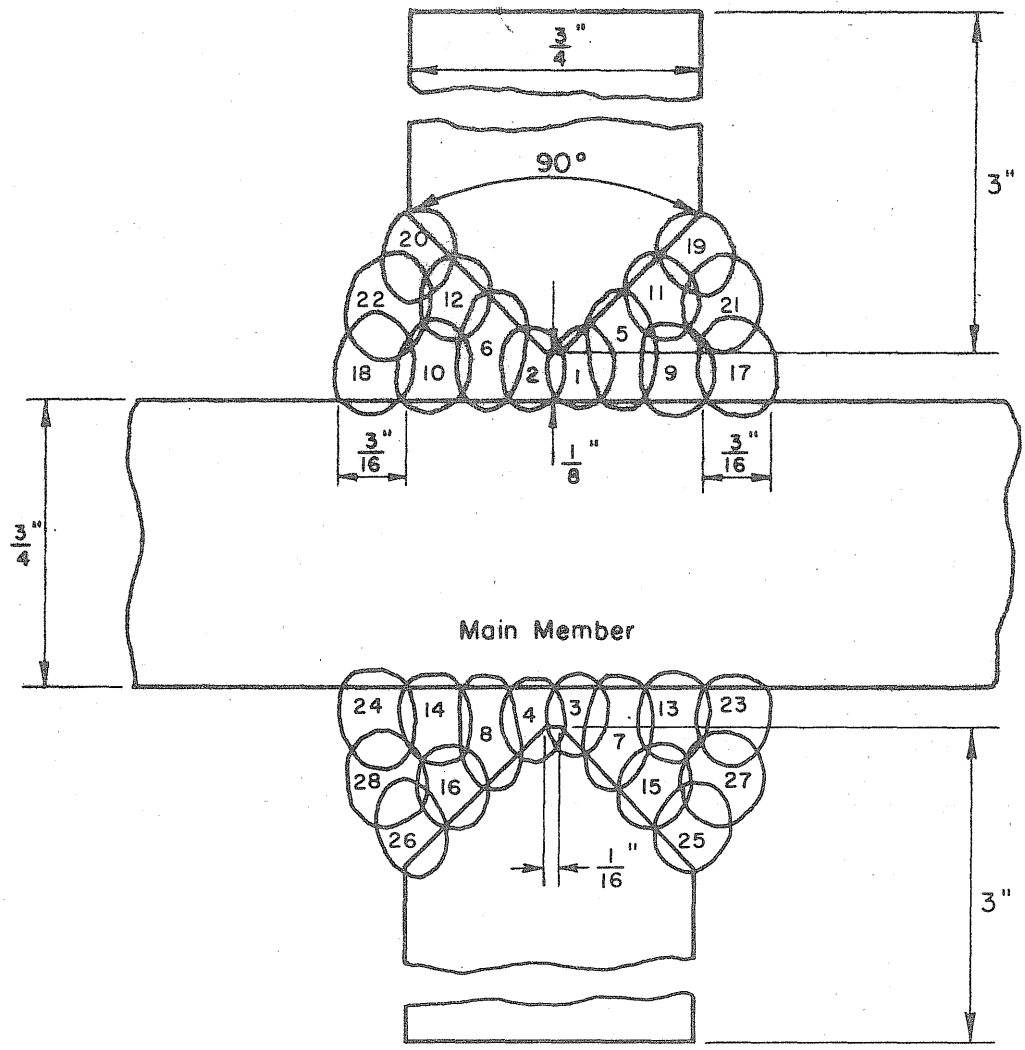

Pass	Electrode size, in.	Current, amps.	Rate of travel, in./min.
1, 3	$\frac{5}{32}$	140	4.5
2, 4-28	$\frac{5}{32}$	175	5.5

Voltage: 21 Volts
Polarity: D. C. Reversed
Interpass Temp: 200° F (Max.)
Preheat: 200° F
Electrode: MIL 11018
Heat Imput: 40,000 Joules/in. (Max.)

Surfaces cleaned by grinding before welding.
All welding in flat position
Underside of pass 1, 3 ground before placing pass 2, 4.

FIG.2.7 WELDING PROCEDURE P100-11018-K
(Full Penetration Transverse Attachments)

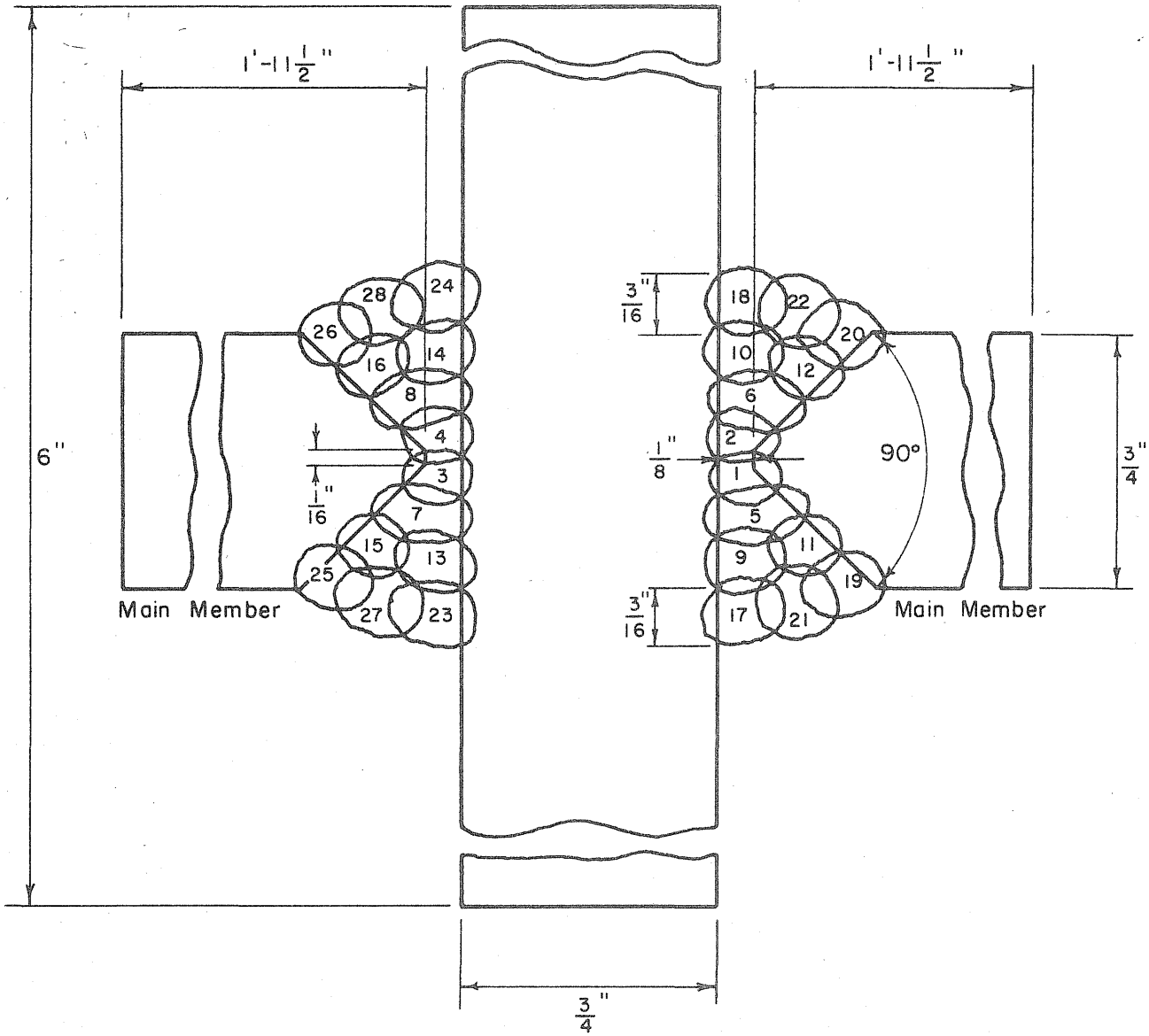

Pass	Electrode Size, in.	Current, amps.	Rate of Travel, in./min.
1, 3	5/32	140	4.5
2, 4 - 28	5/32	175	5.5

Voltage : 21 Volts

Polarity : D.C. Reversed

Interpass Temp : 200° F (Max.)

Preheat : 200° F

Electrode : MIL 11018

Heat Input : 40,000 Joules / in. (Max.)

Surfaces cleaned by grinding before welding.
All welding in flat position.
Underside of pass 1, 3 ground before placing pass 2, 4.

FIG. 2.8 WELDING PROCEDURE P100-11018-M (Full Penetration Tee Joint)

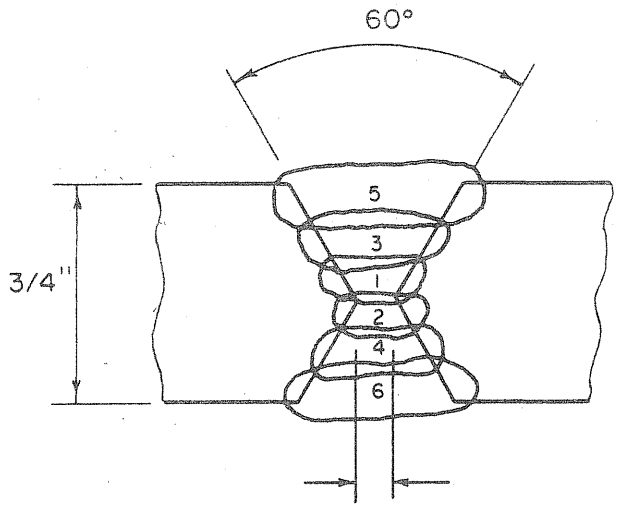

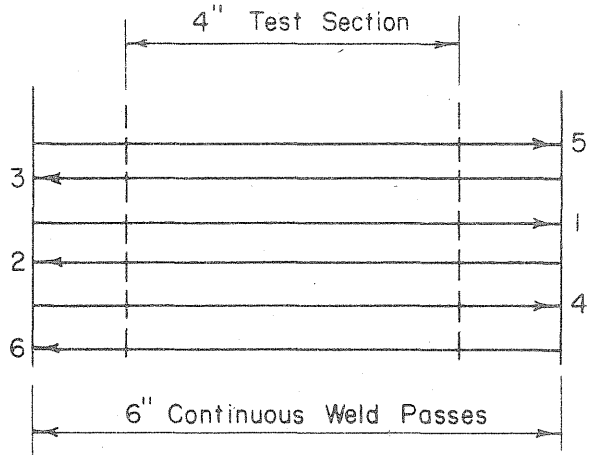

Arrows indicate direction of welding.

Surface of plate adjacent to weld cleaned by grinding before welding.

Pass	Electrode size, in.	Current, amps.	Rate of travel, in./min.
1	5/32	130	5
2	5/32	140	5
3	3/16	230	8
4	3/16	220	7
5	3/16	210	7
6	3/16	210	7

Voltage: 21 Volts
Polarity: D C Reversed
Preheat: 150°F
Electrode: MIL 12018
Interpass Temperature: 200°F (Maximum)
Heat Input: 40,000 Joules/in. (Maximum)
All welding in flat position
Underside of pass 1 ground before placing pass 2

FIG. 2.9 WELDING PROCEDURE P100-12018-A
(Transverse Butt Welds in HY-100)

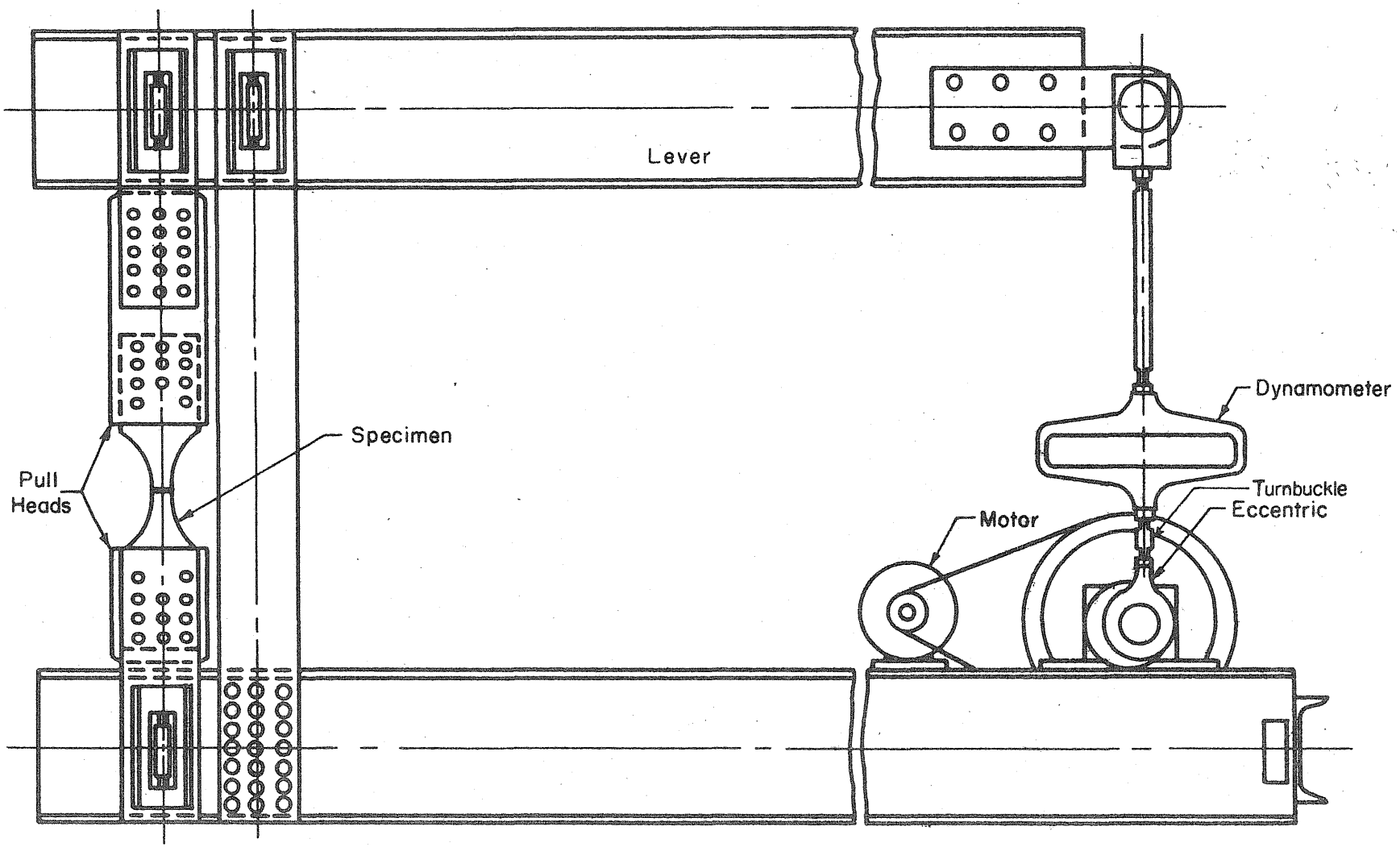

FIG. 2.10 ILLINOIS' FATIGUE TESTING MACHINE AS USED FOR AXIAL LOADING OF WELDED JOINTS.

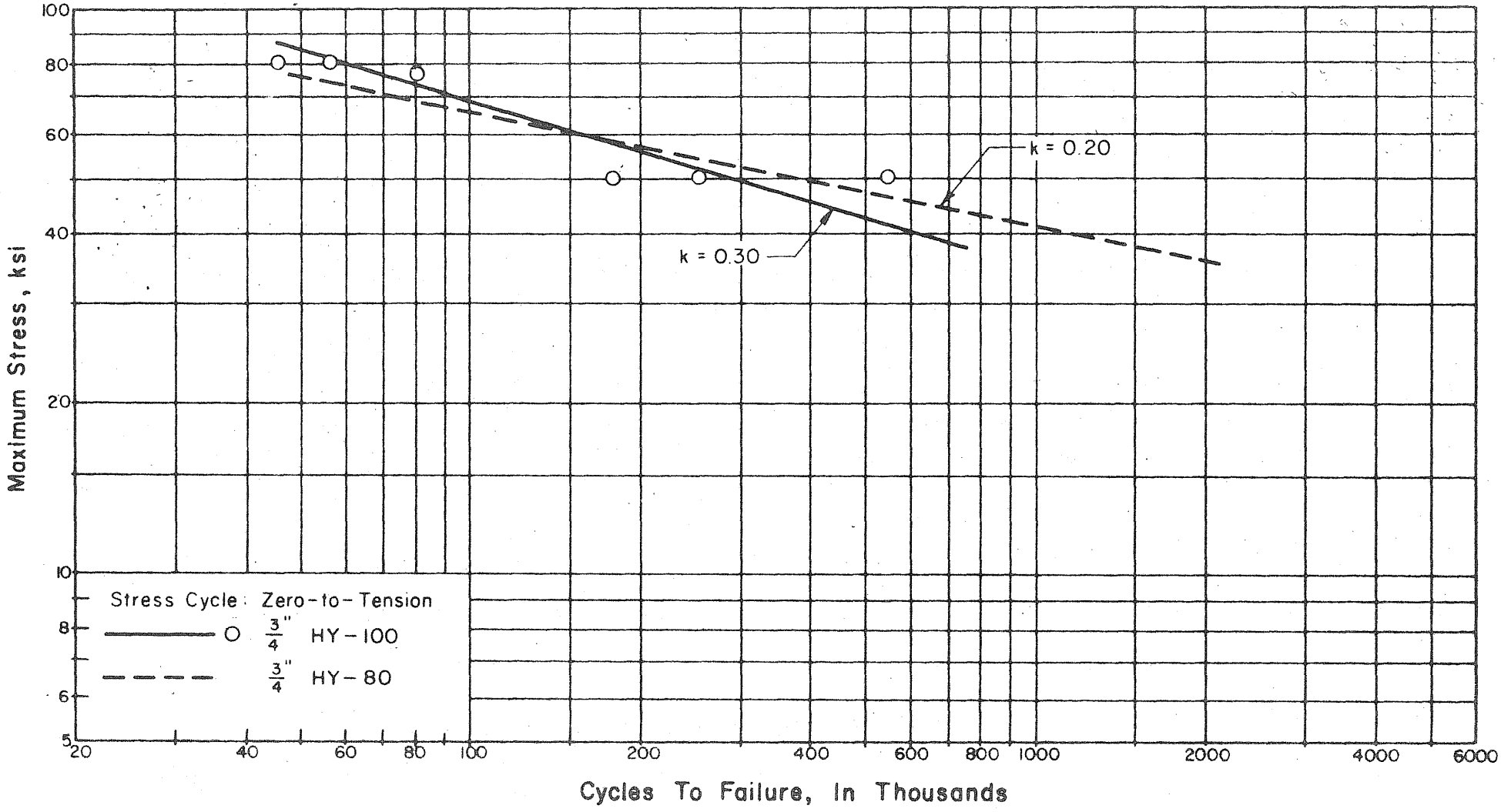

FIG.3.1 RESULTS OF FATIGUE TESTS OF AS-RECEIVED HY-100 PLAIN PLATE SPECIMENS (ZERO-TO-TENSION).

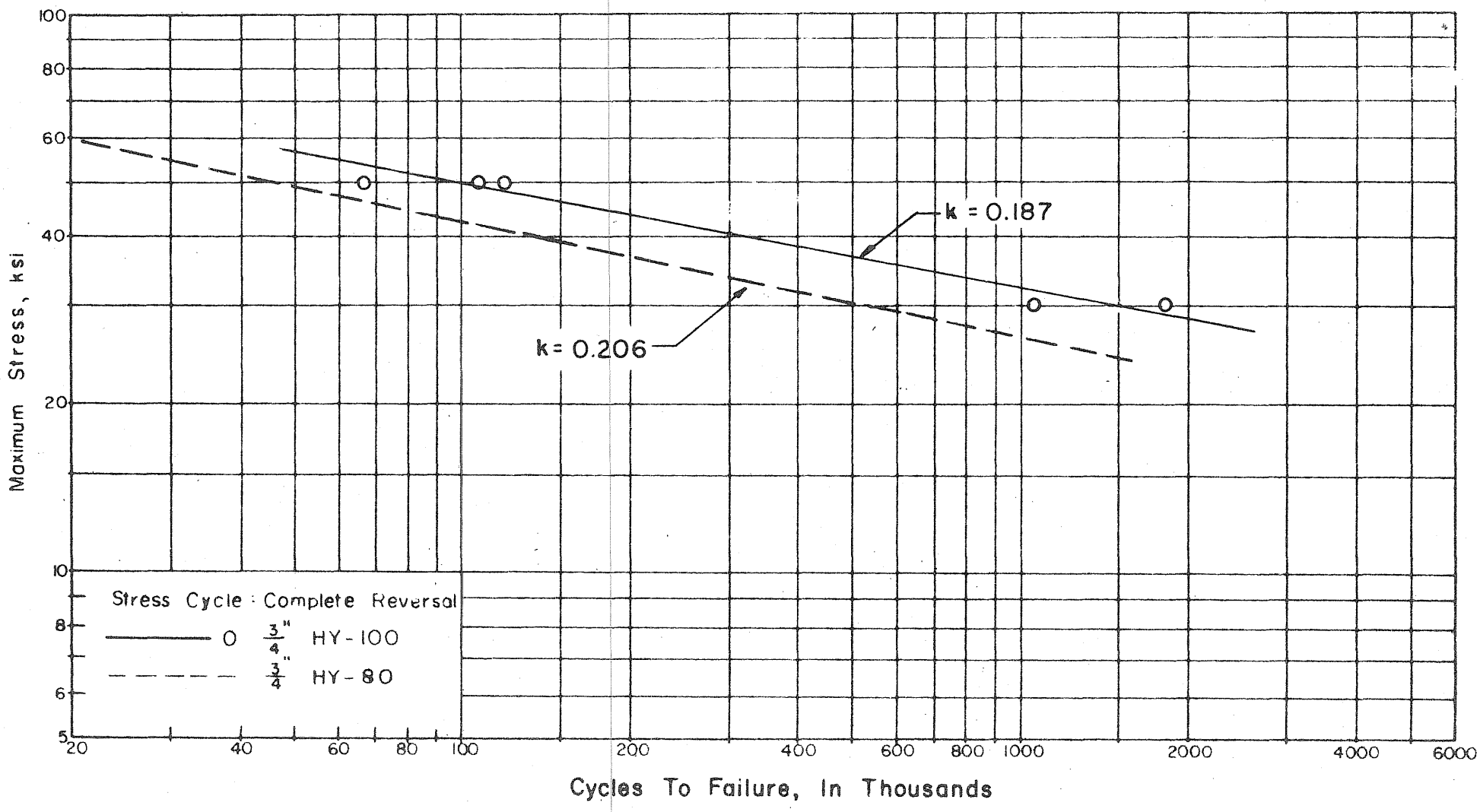

FIG. 3.2 RESULTS OF FATIGUE TESTS OF AS-RECEIVED HY-100 PLAIN PLATE SPECIMENS (COMPLETE REVERSAL).

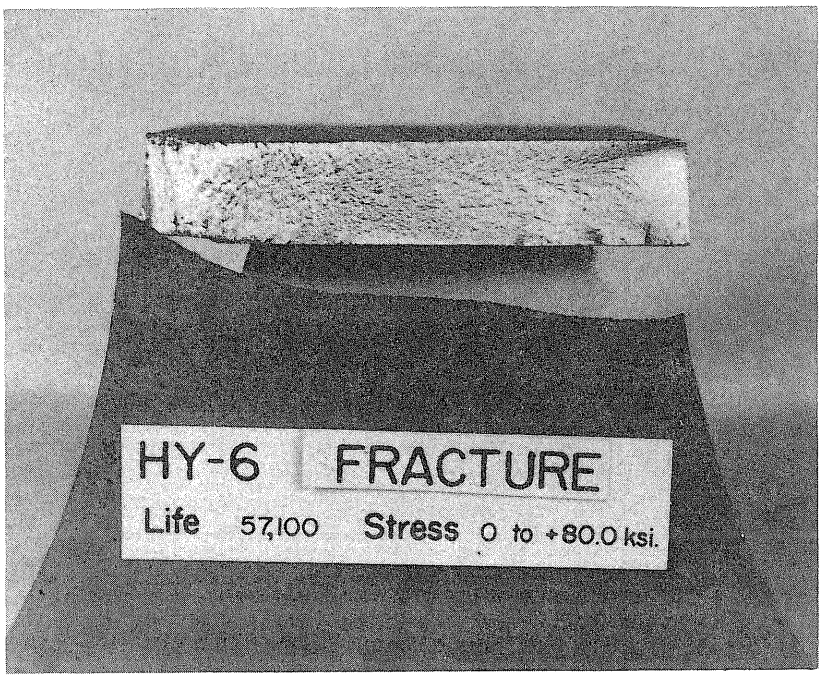

NOTE: FAILURE INITIATED AT MILL SCALE SURFACE.

FIG. 3.3 FRACTURE SURFACE OF AS-RECEIVED HY-100 PLAIN PLATE SPECIMEN.

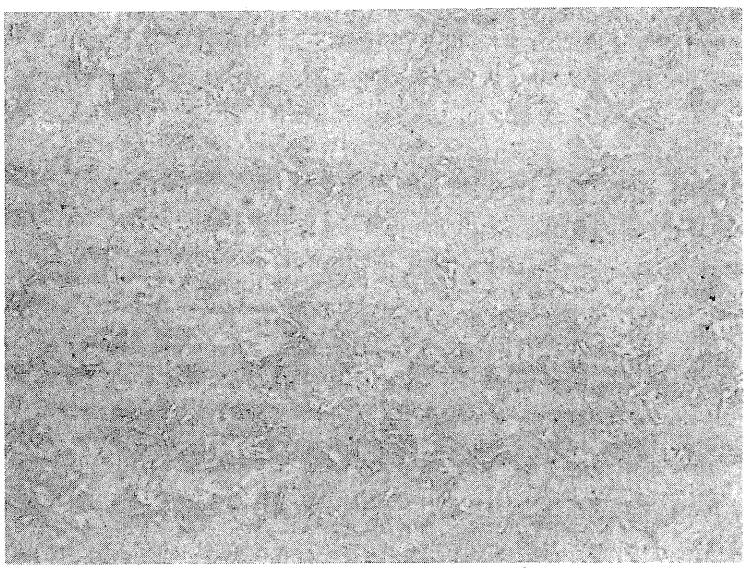

a) Base Metal (200X)

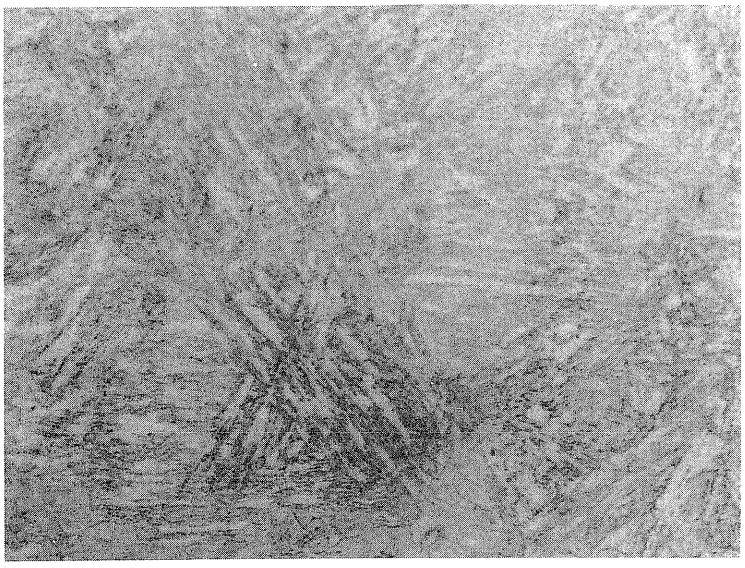

b) Heat Affected Zone (750X)

FIG. 3.4 TYPICAL PHOTOMICROGRAPHS OF TRANSVERSE BUTT WELD IN 3/4 IN. HY-100 MATERIAL.

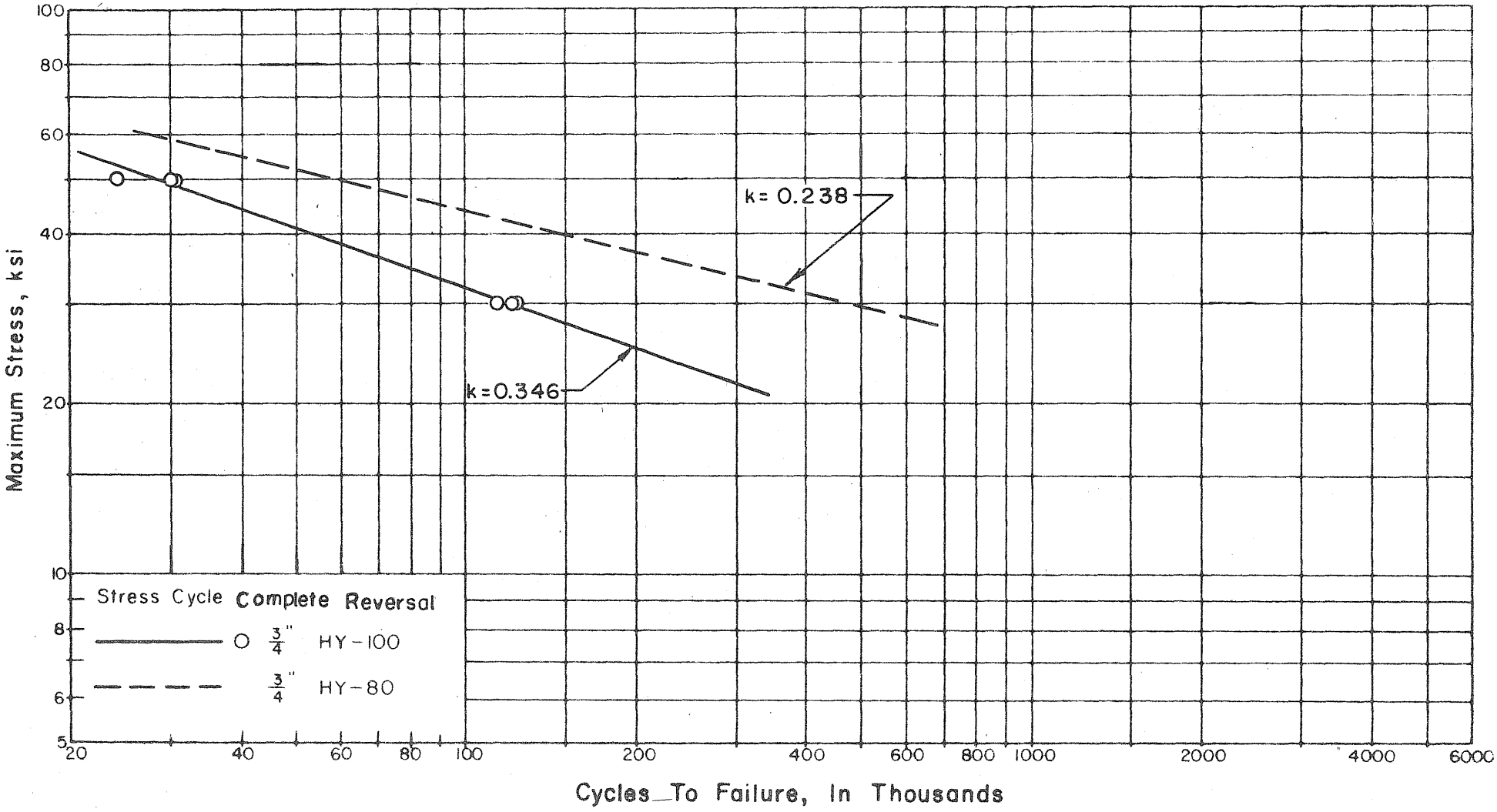

FIG.3.5 RESULTS OF FATIGUE TESTS OF HY-100 TRANSVERSE BUTT WELDS IN THE AS-WELDED CONDITION (COMPLETE REVERSAL).

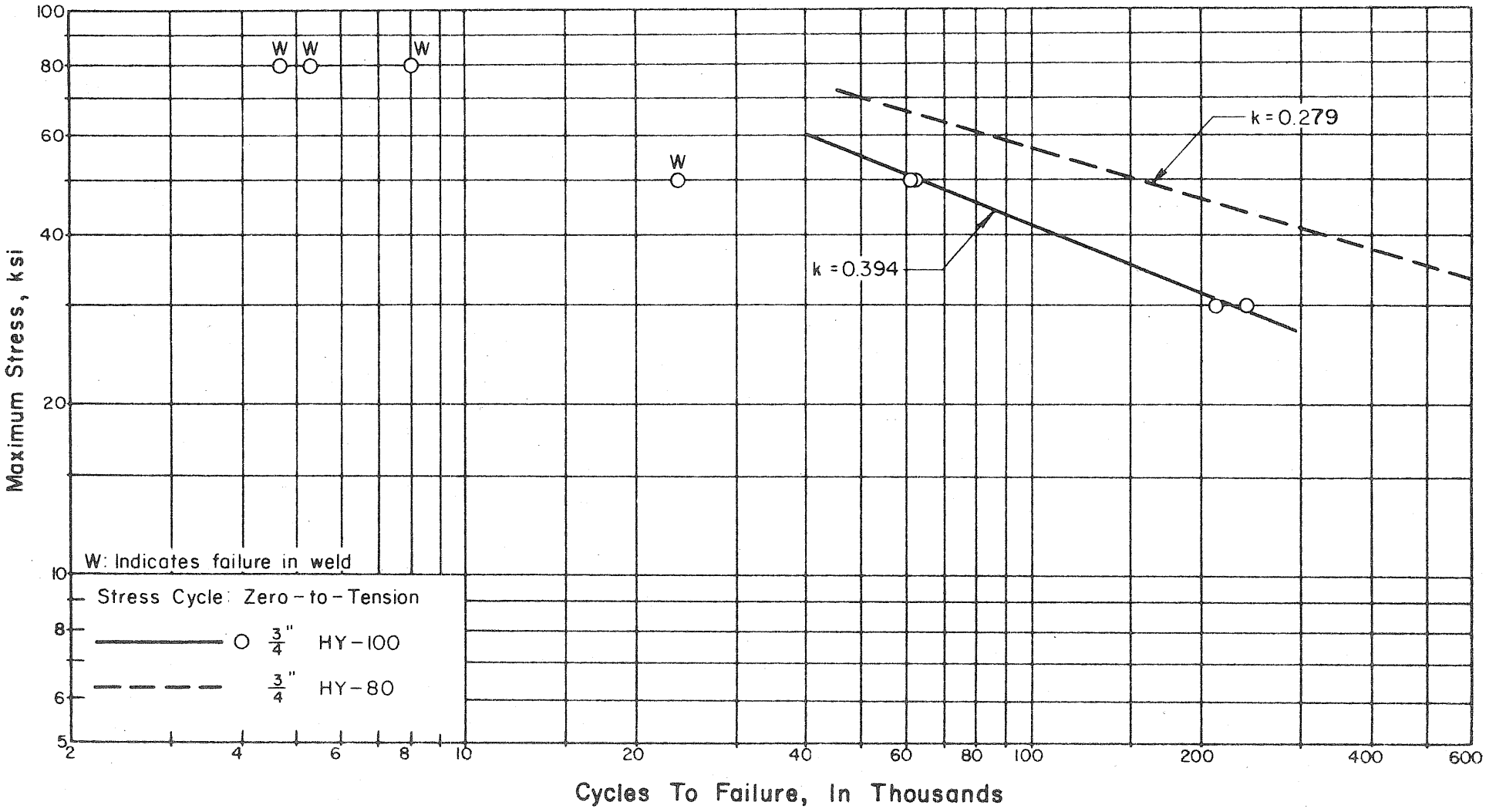

FIG. 3.6 RESULTS OF FATIGUE TESTS OF HY-100 TRANSVERSE BUTT WELDS IN THE AS-WELDED CONDITION (ZERO - TO - TENSION).

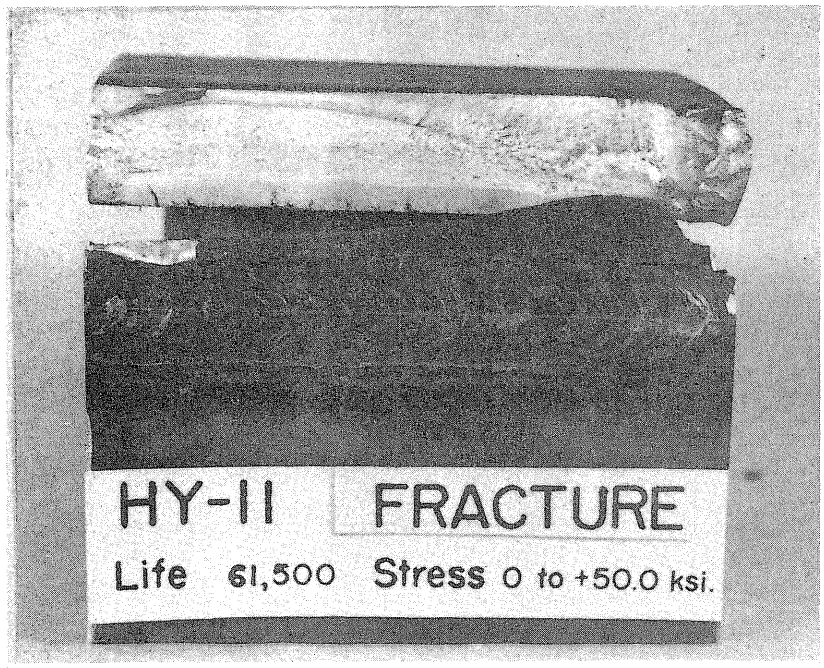

a) FAILURE INITIATED AT EDGE OF WELD REINFORCEMENT.

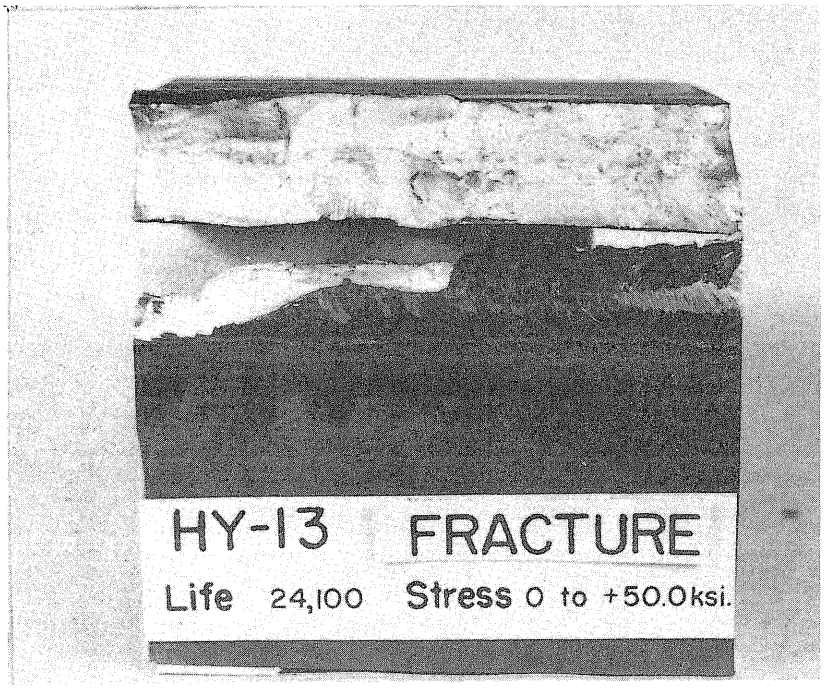

b) FAILURE INITIATED IN WELD.

FIG.3.7 TYPICAL FRACTURES OF TRANSVERSE BUTT WELDS IN 3/4 IN. HY-100 MATERIAL.

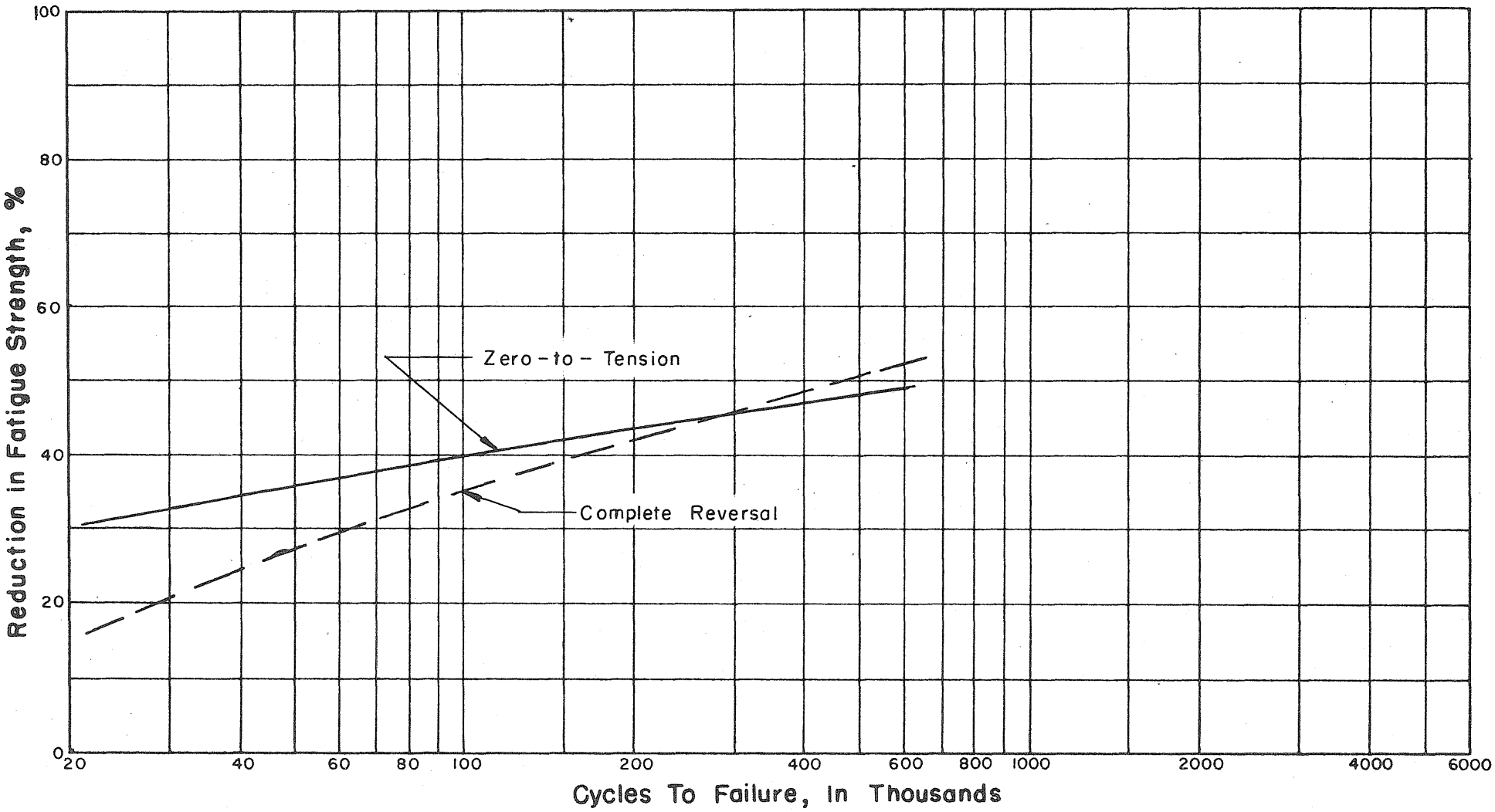

FIG. 3.8 REDUCTION IN FATIGUE STRENGTH FROM AS-RECEIVED PLAIN PLATES DUE TO A TRANSVERSE BUTT WELD IN THE AS-WELDED CONDITION.

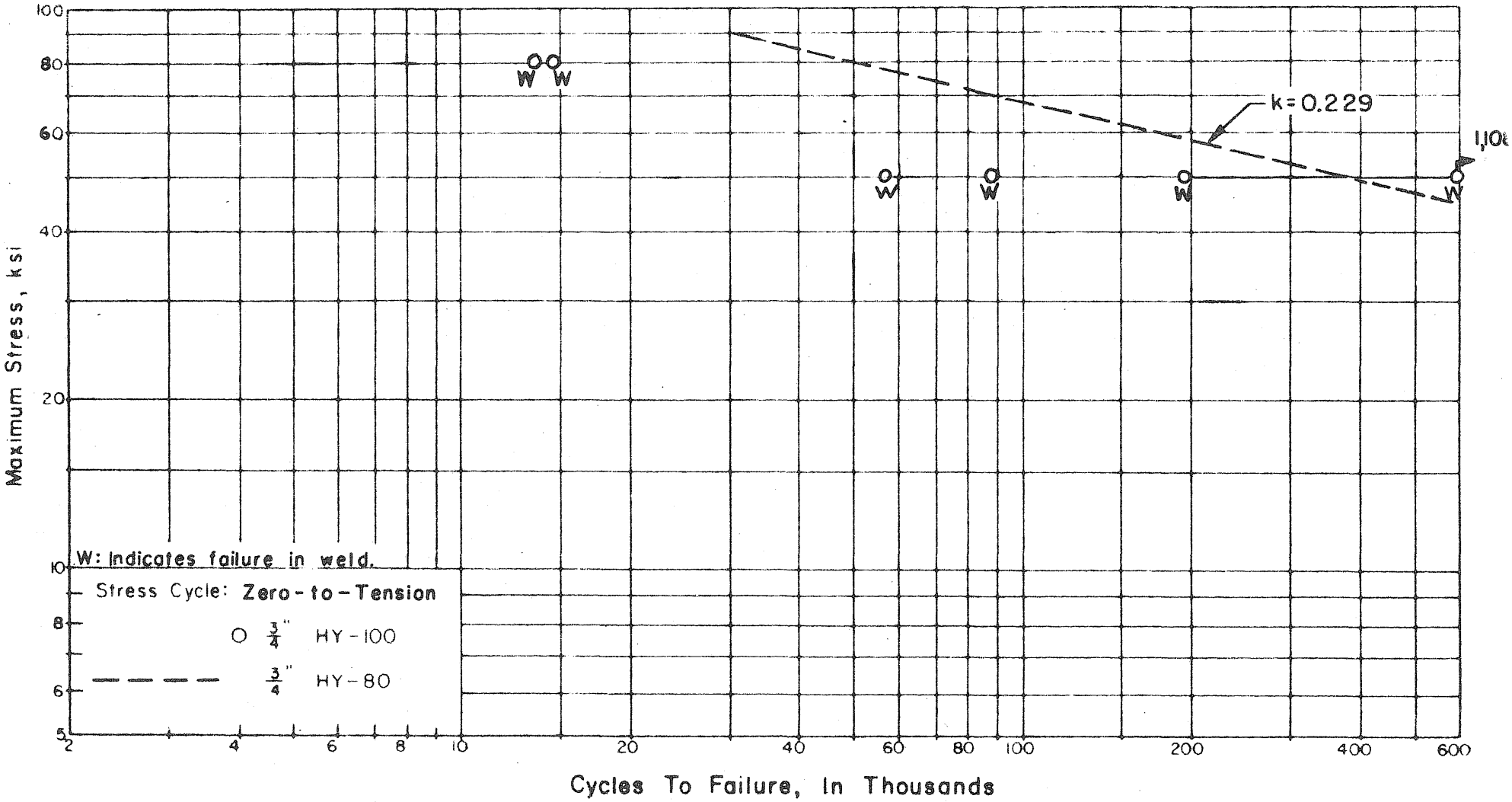

FIG.3.9 RESULTS OF FATIGUE TESTS OF HY-100 TRANSVERSE BUTT WELDS WITH REINFORCEMENT REMOVED. (ZERO-TO-TENSION)

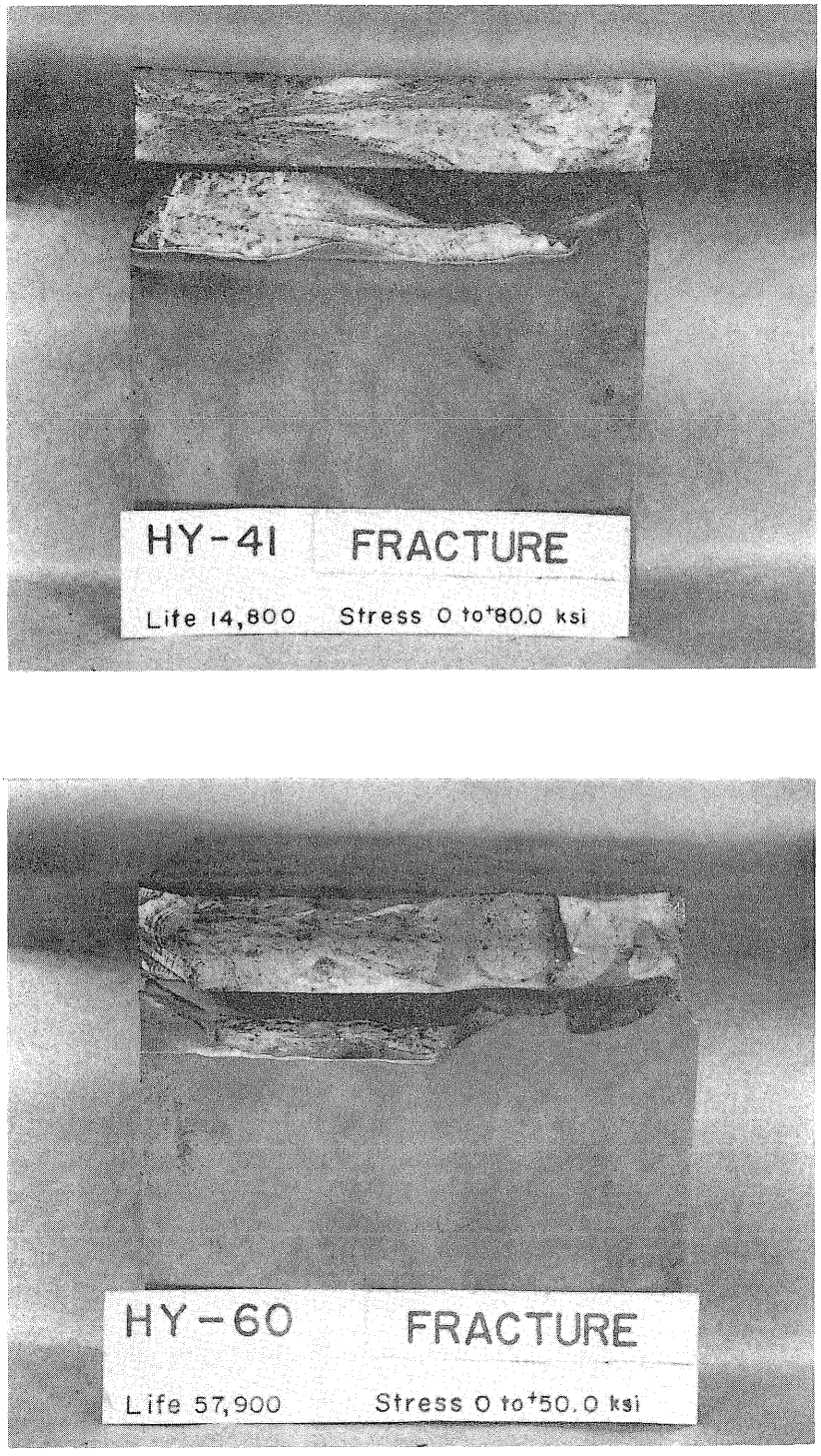

FIG. 3.10 TYPICAL FRACTURES OF TRANSVERSE BUTT WELDS WITH REINFORCEMENT REMOVED. (3/4 IN. HY-100 MATERIAL)

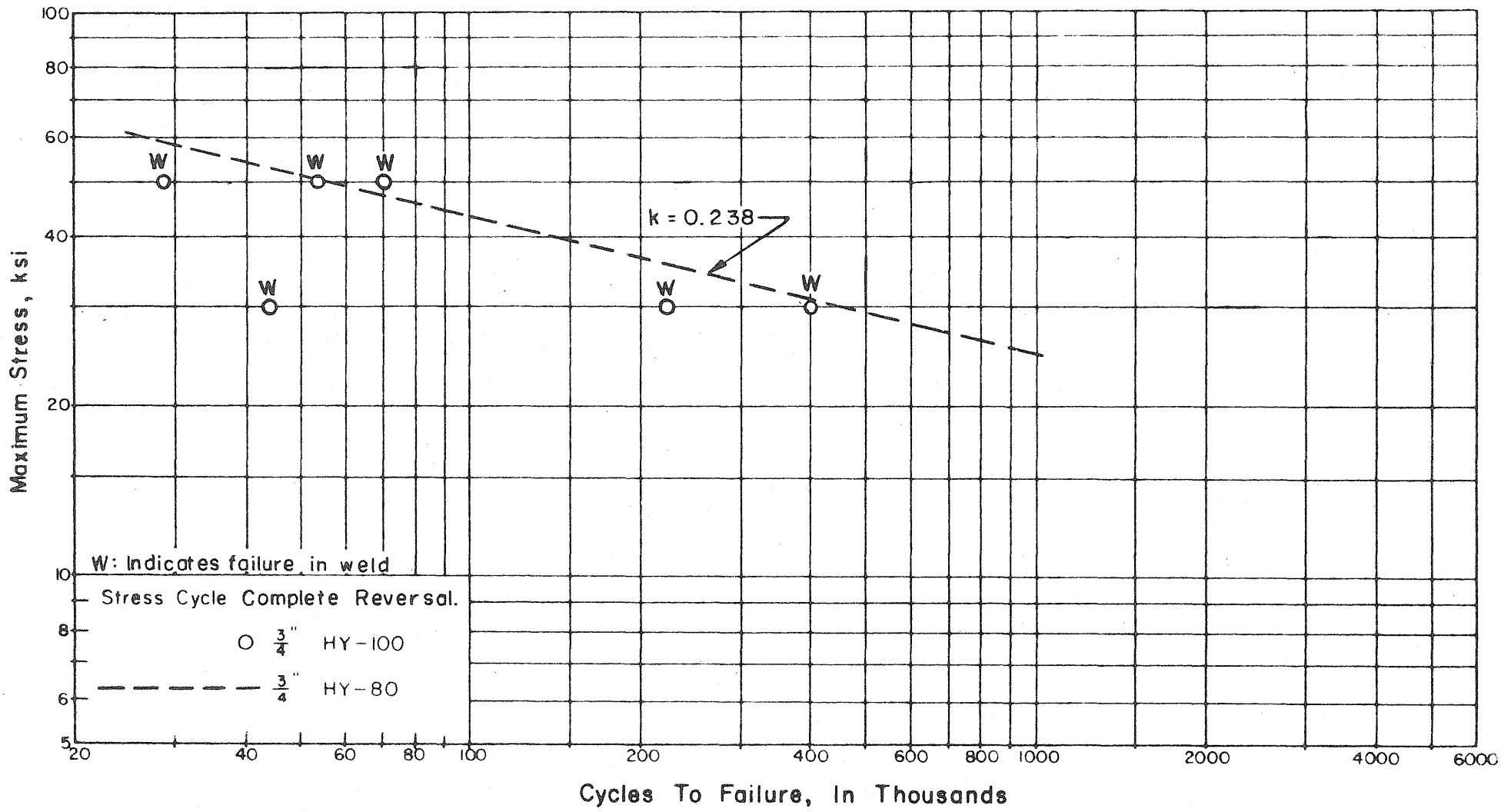

FIG. 3.11 RESULTS OF FATIGUE TESTS OF HY-100 TRANSVERSE BUTT WELDS WITH REINFORCEMENT REMOVED (COMPLETE REVERSAL).

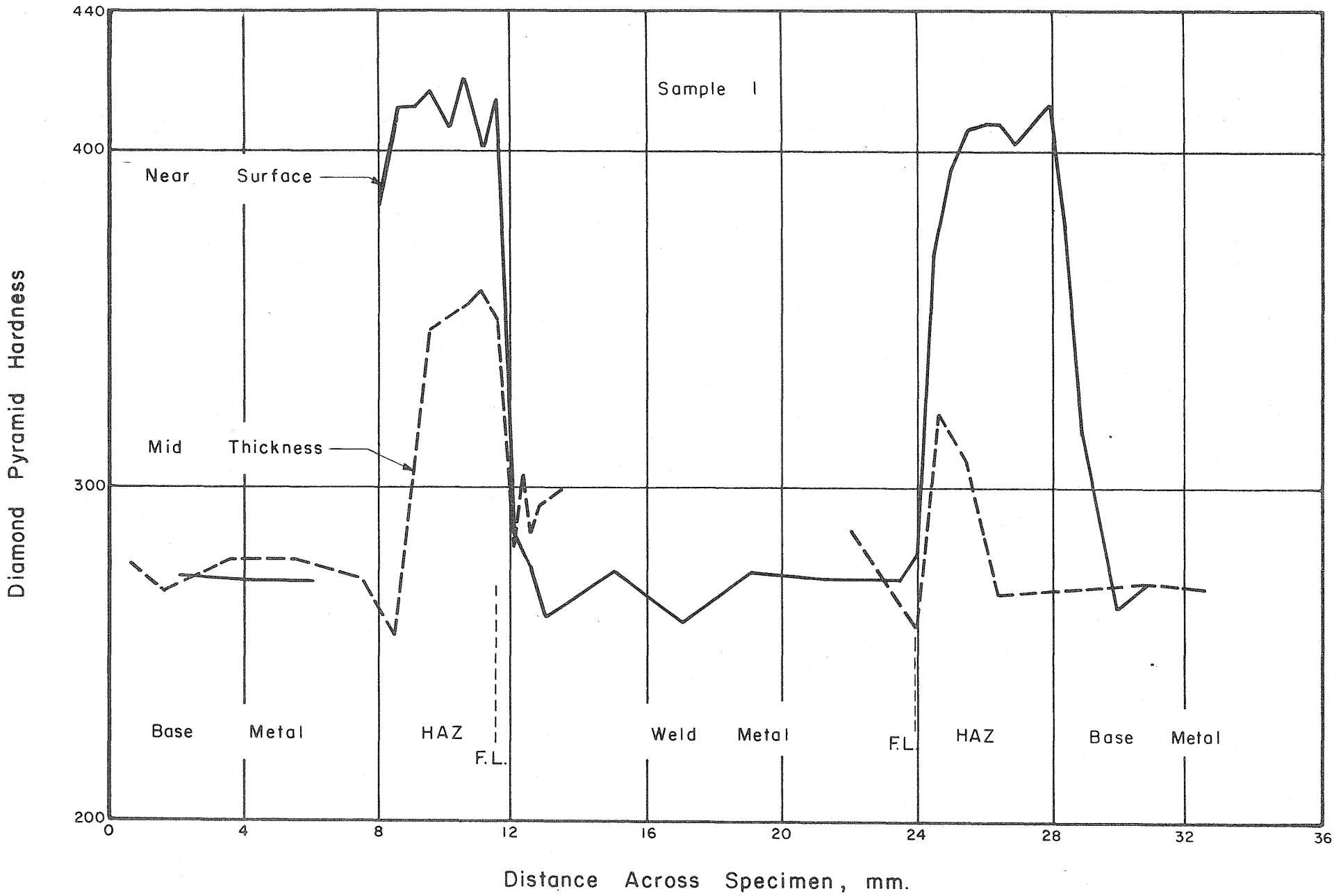

FIG. 3.12 MICRO-HARDNESS SURVEY OF 3/4 IN. THICK HY-100 STEEL WELDMENT USING PROCEDURE P100-11018-J.

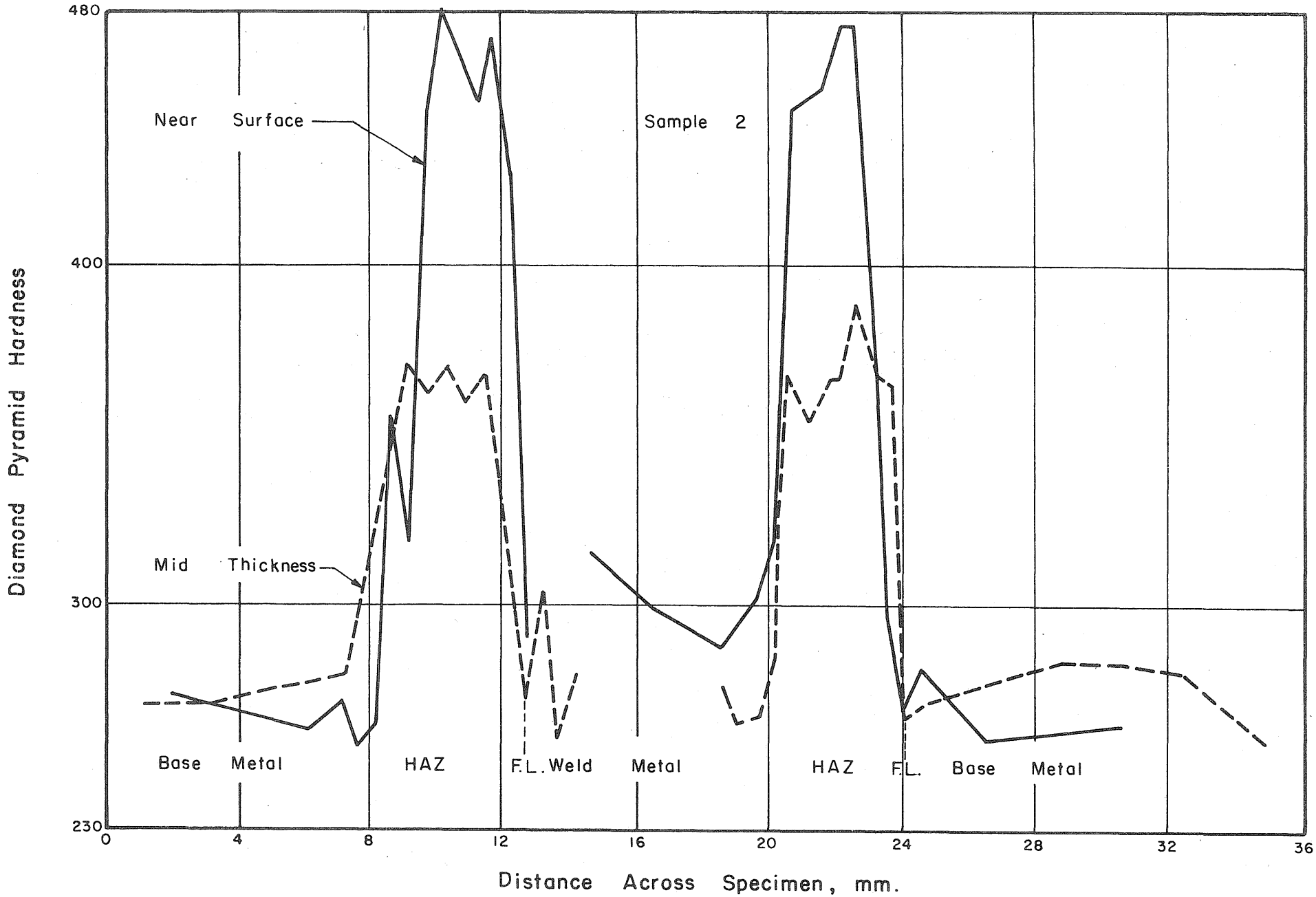

FIG. 3.13 MICRO-HARDNESS SURVEY OF 3/4 IN. THICK HY-100 STEEL WELDMENT USING PROCEDURE P100-11018-J50.

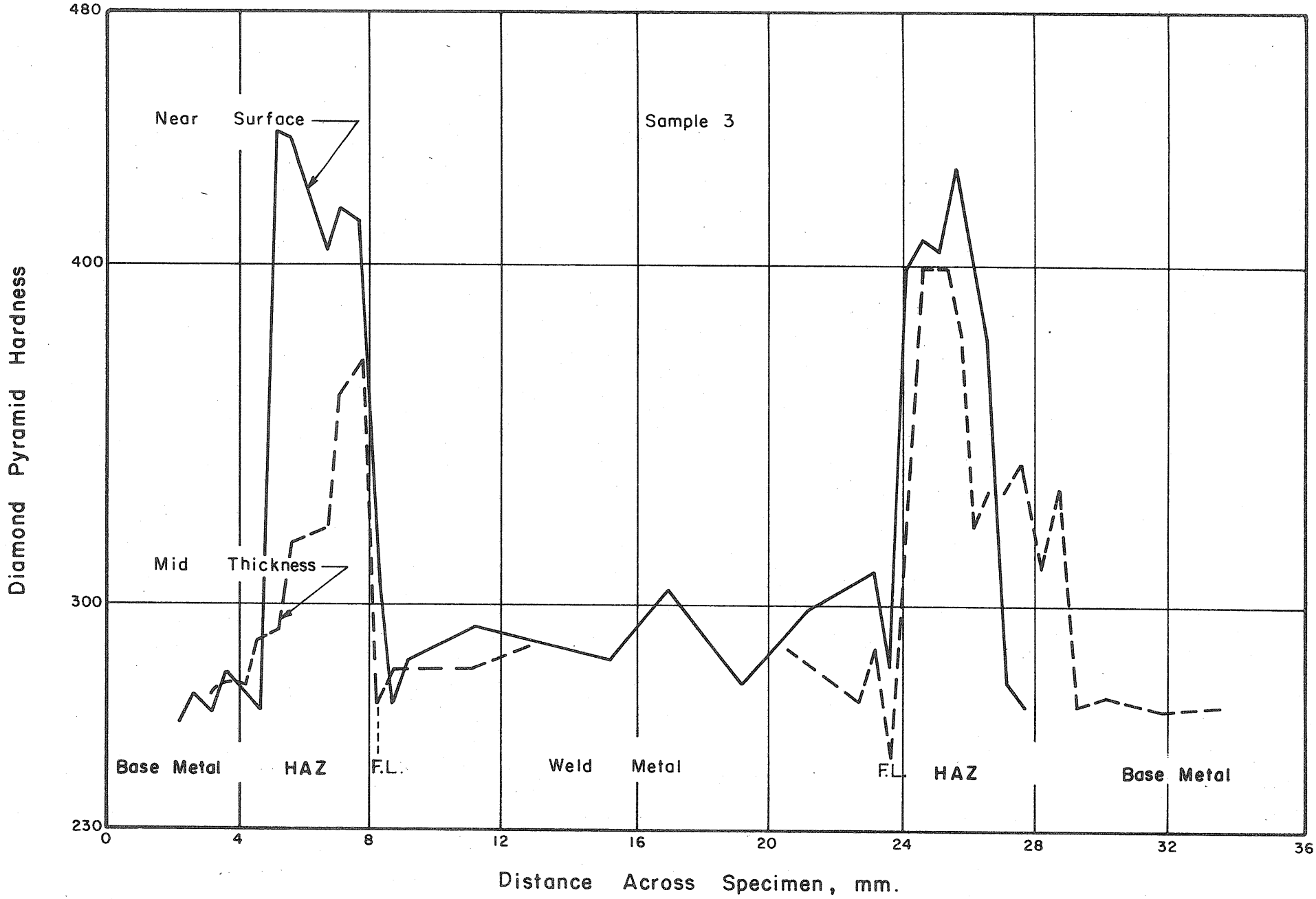

FIG. 3.14 MICRO-HARDNESS SURVEY OF 3/4 IN. THICK HY-100 STEEL WELDMENT USING PROCEDURE P100-11018-J30.

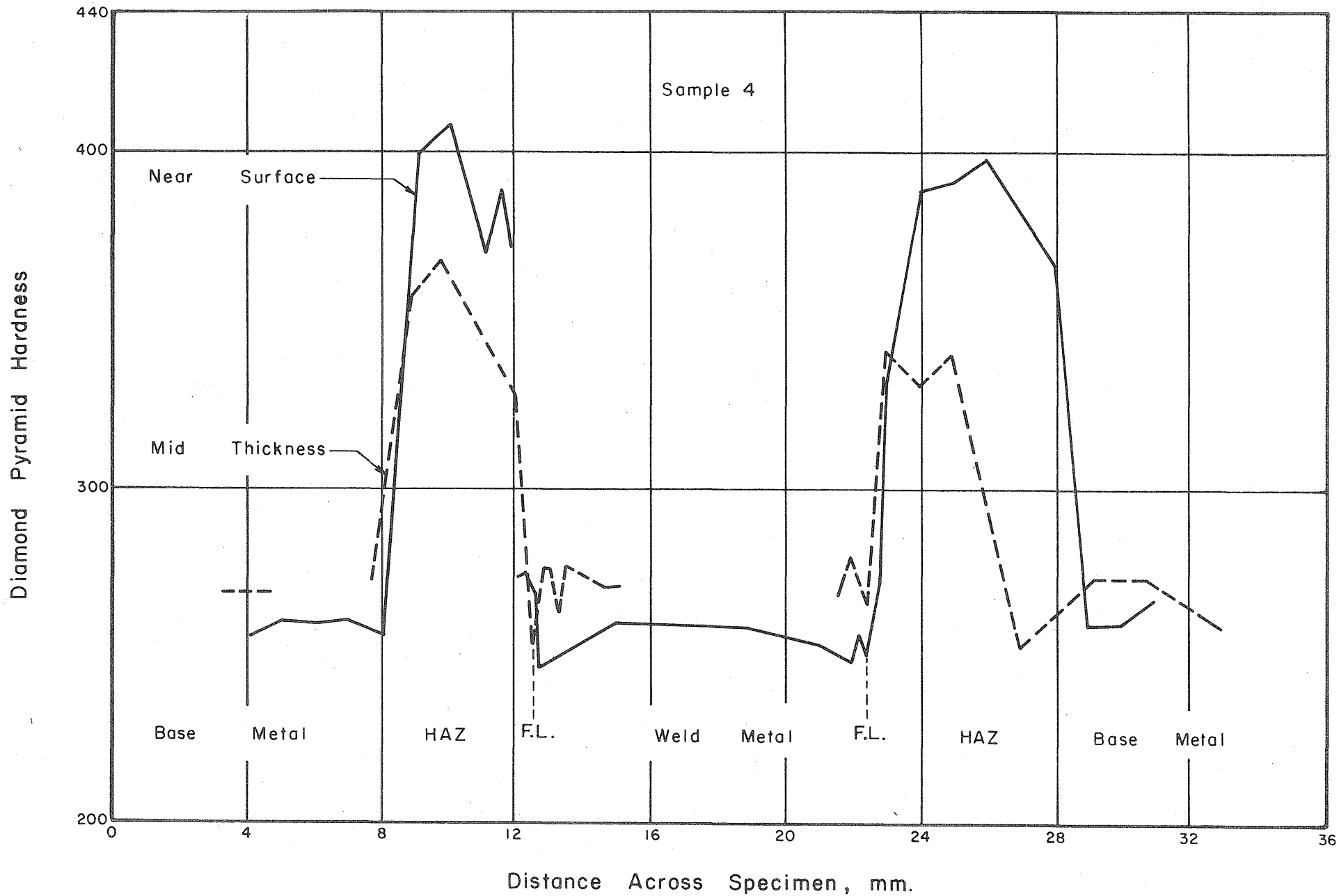

FIG. 3.15 MICRO-HARDNESS SURVEY OF 3/4 IN. THICK HY-100 STEEL WELDMENT USING PROCEDURE P100-11018-JH

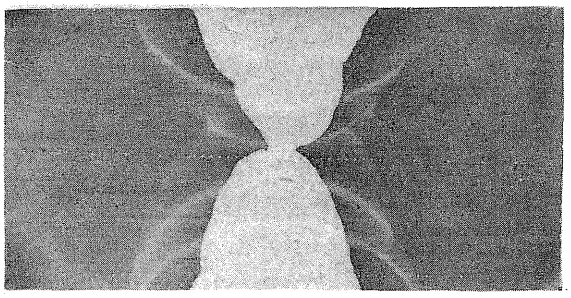

a) Normal Weldment (Sample 1)

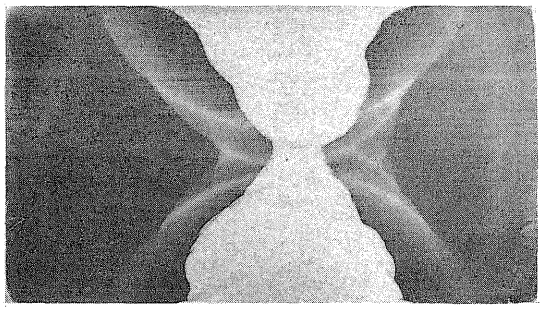

b) High Energy, 6 Pass Weldment (Sample 2)

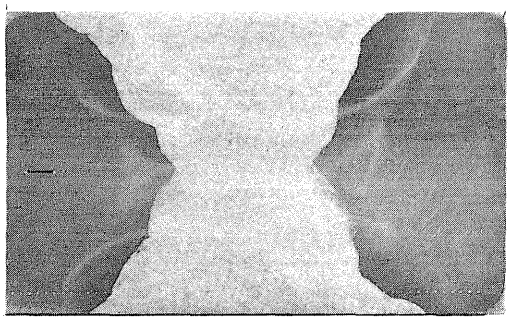

c) Low Energy, 12 Pass Weldment (Sample 3)

FIG. 3.16 MACROSTRUCTURE OF HY-100 WELDMENTS. 2X.

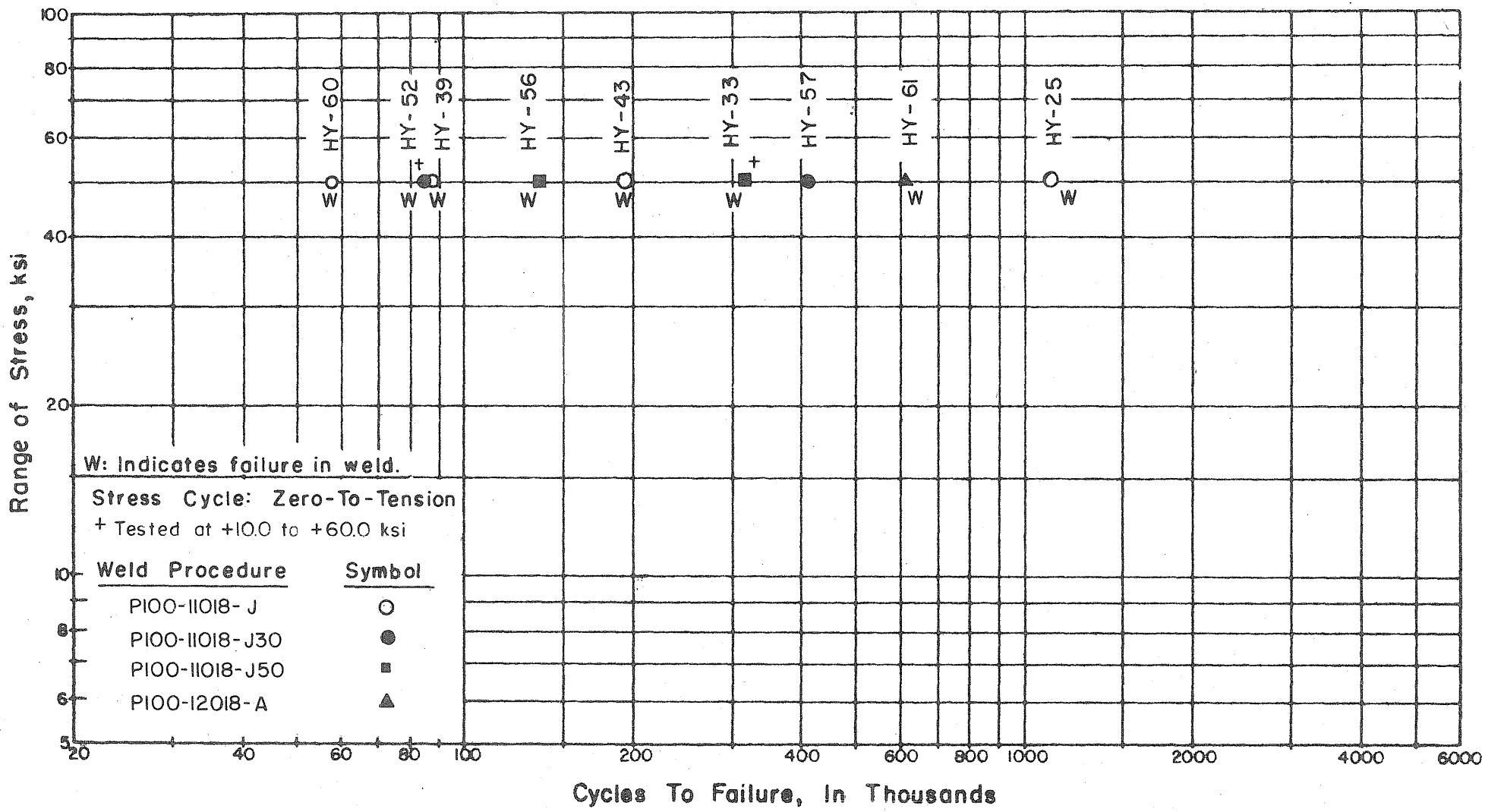

FIG. 3.17 RESULTS OF FATIGUE TESTS OF EXPERIMENTAL HY-100 TRANSVERSE BUTT WELDS WITH REINFORCEMENT REMOVED (ZERO-TO-TENSION).

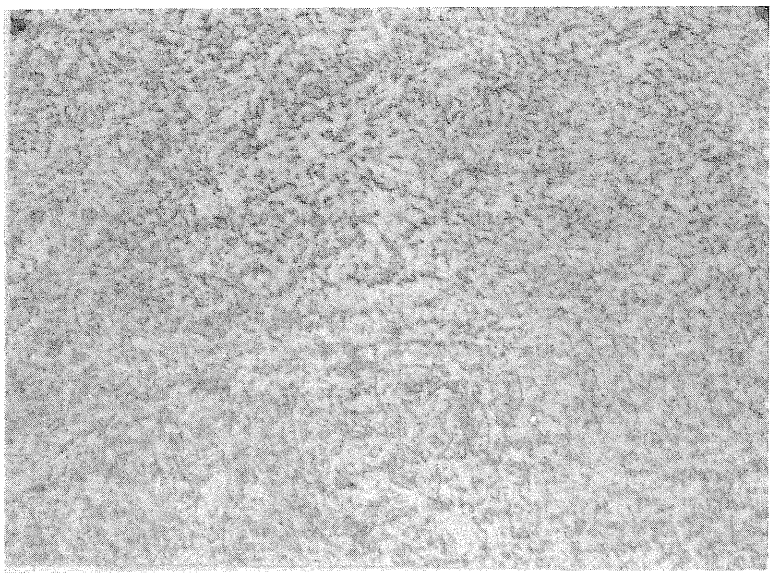

a) MIL-11018 Electrode

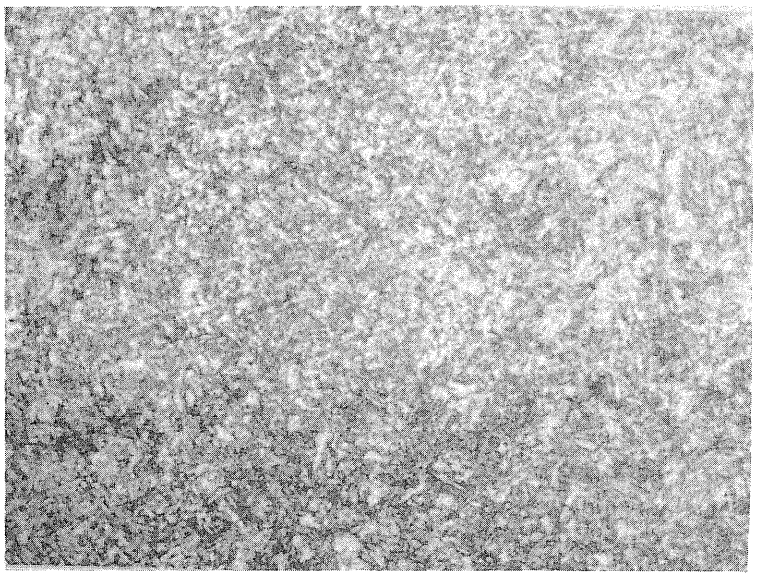

b) MIL-12018 Electrode

FIG. 3.18 TYPICAL PHOTOMICROGRAPHS OF WELD METAL FOR TRANSVERSE BUTT WELDS IN 3/4 IN. THICK HY-100 MATERIAL. 750X

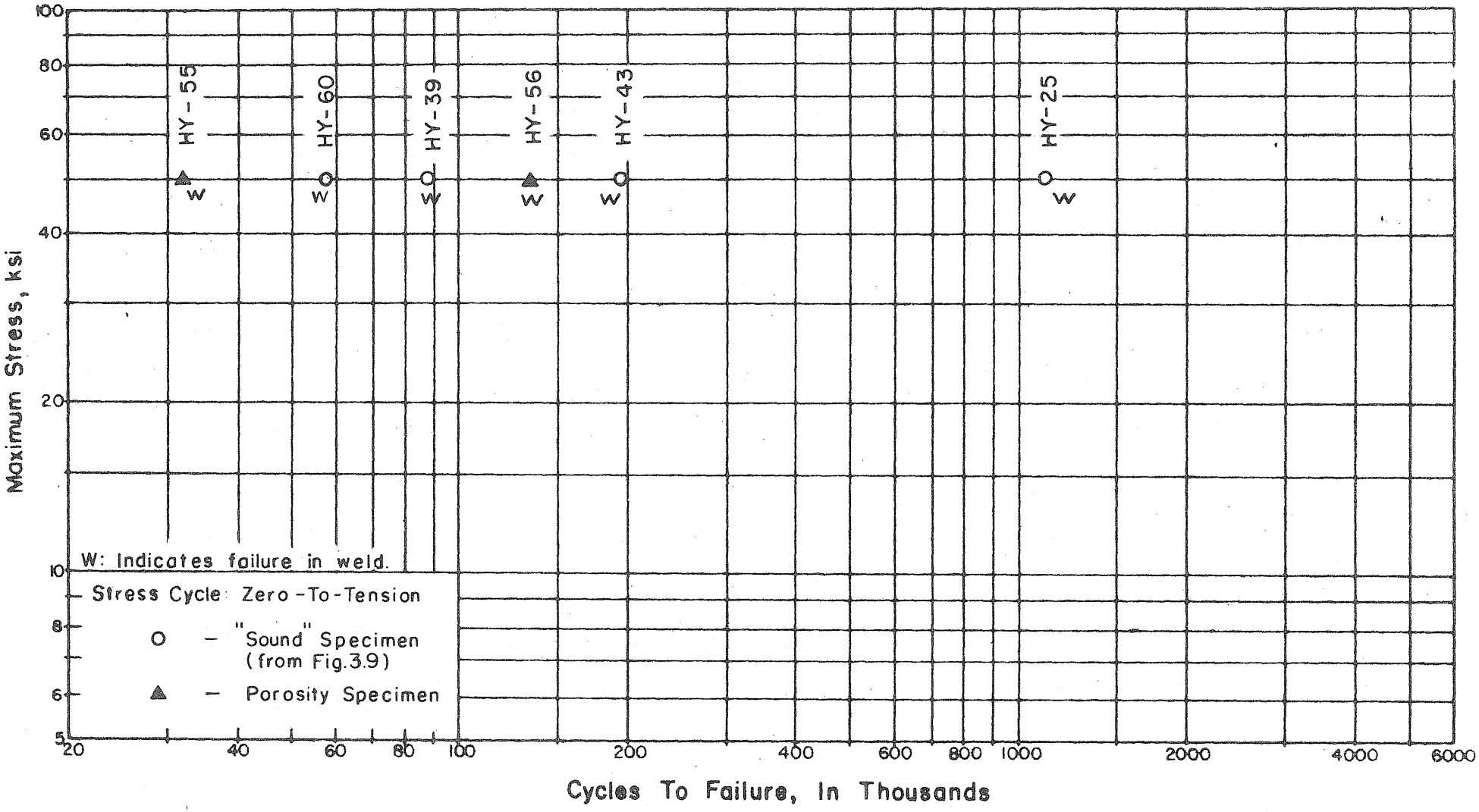

FIG. 3.19 RESULTS OF FATIGUE TESTS OF HY-100 TRANSVERSE BUTT WELDS WITH INTENTIONAL POROSITY. (ZERO-TO-TENSION)

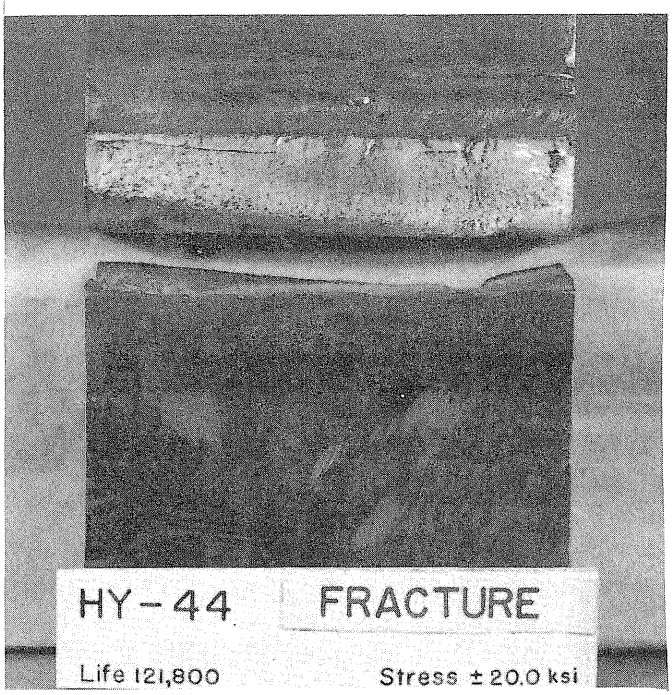

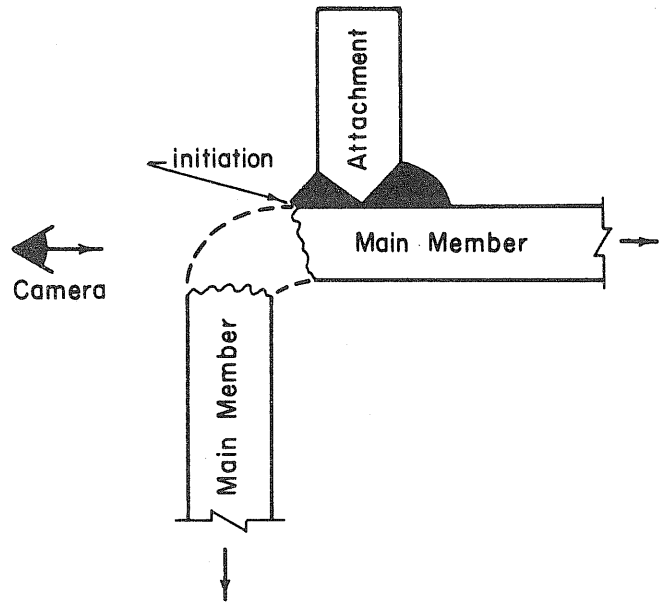

a) FAILURE INITIATED AT TOE OF WELD.

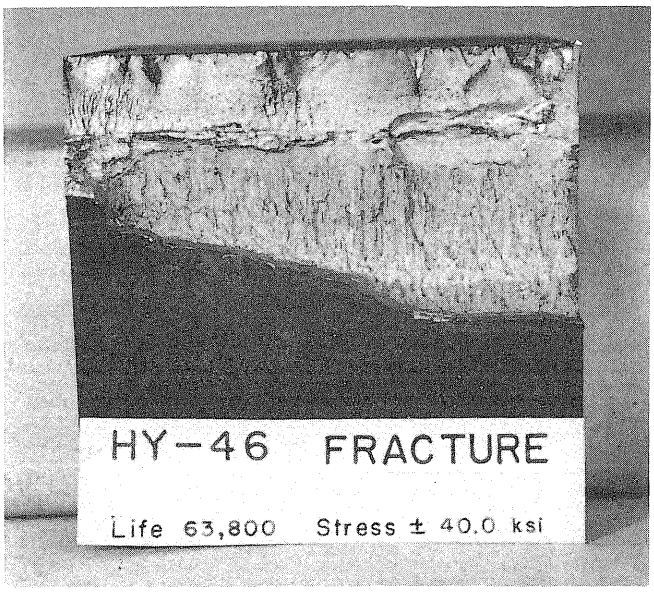

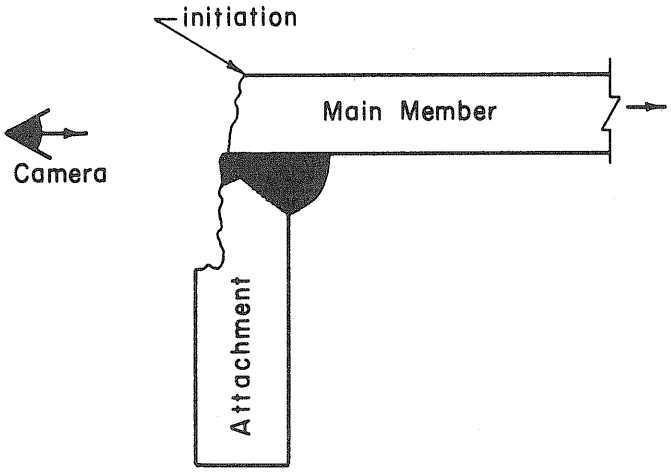

b) FAILURE INITIATED ON MILL SCALE SURFACE.

FIG. 3.20 FRACTURE SURFACES OF HY-100 PLATES WITH A FULL PENETRATION TRANSVERSE ATTACHMENT ON ONE SIDE.

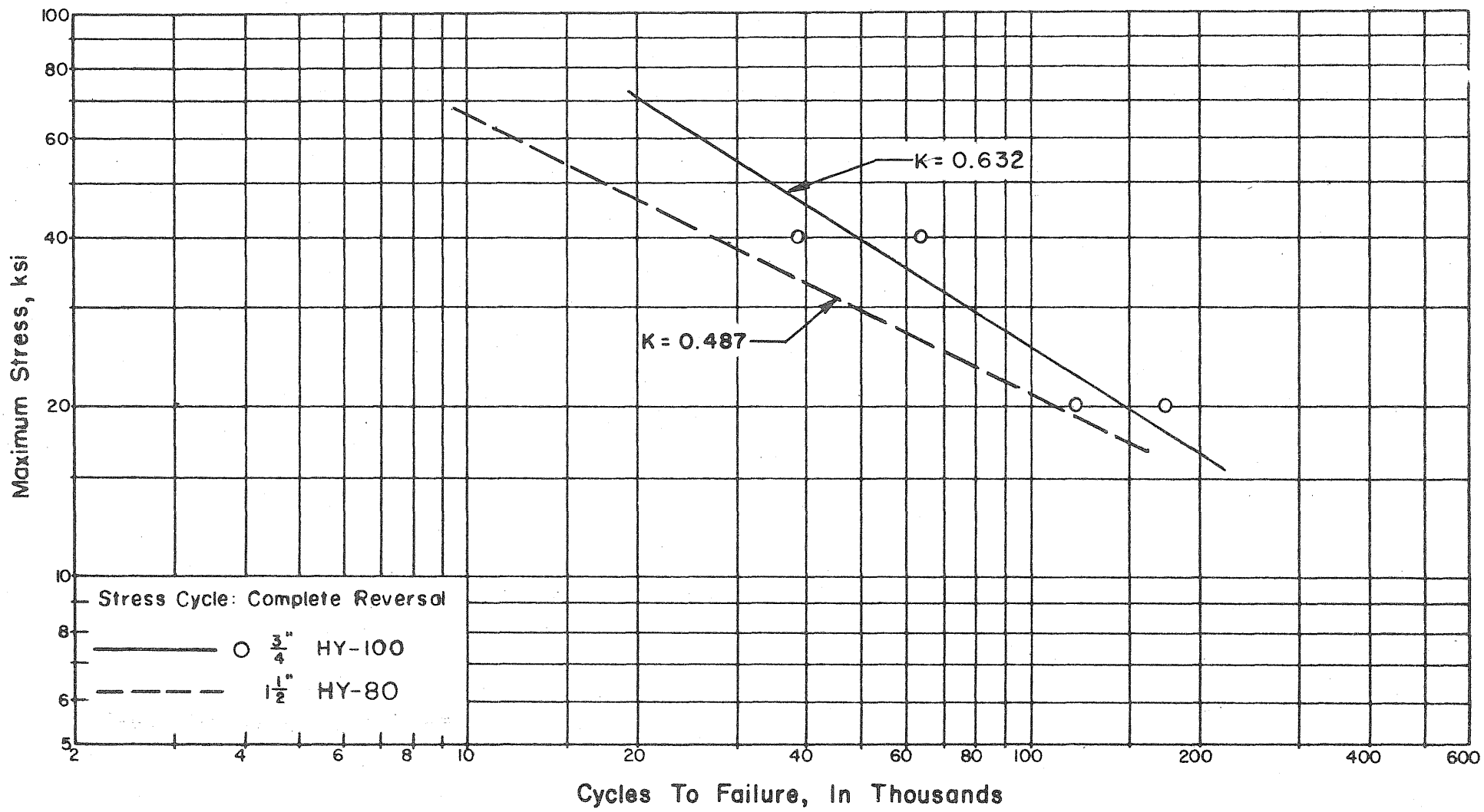

FIG. 3.21 RESULTS OF FATIGUE TESTS OF HY-100 PLATES WITH FULL PENETRATION TRANSVERSE ATTACHMENT ON ONE SIDE (COMPLETE REVERSAL).

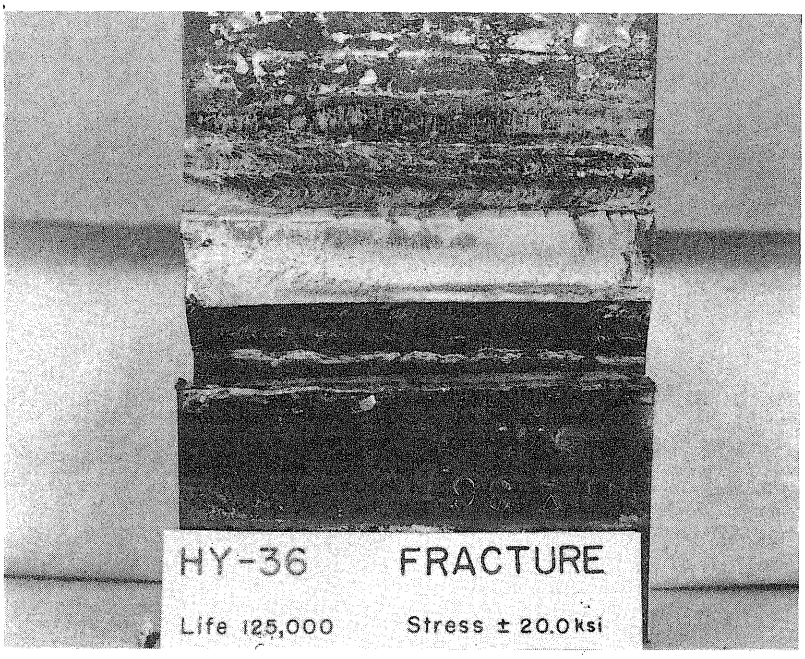

FAILURE INITIATED AT TOE OF WELD.

FIG.3.22 FRACTURE SURFACE OF HY-100 PLATE WITH FULL PENETRATION TRANSVERSE ATTACHMENTS ON TWO SIDES.

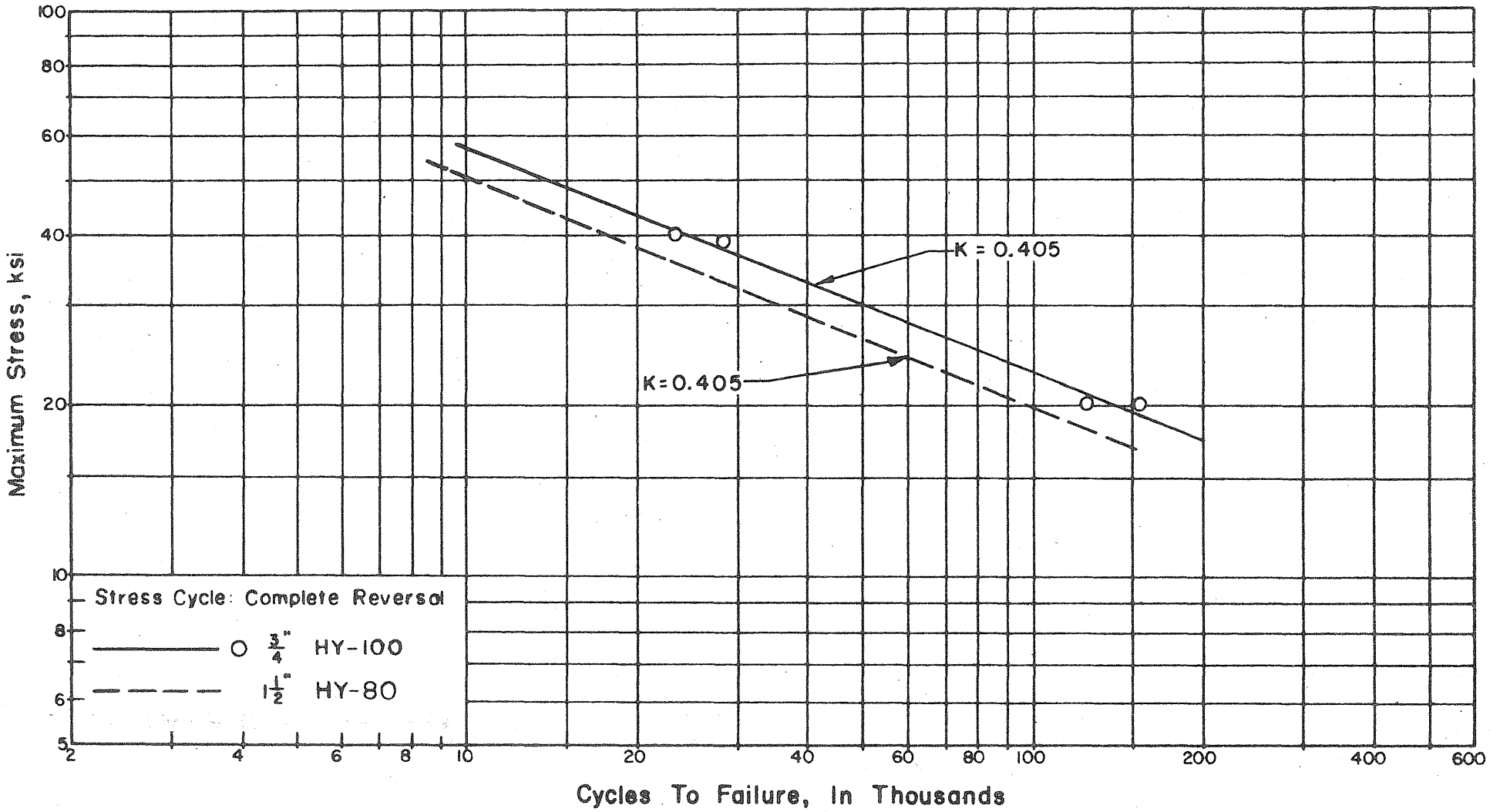

FIG.3.23 RESULTS OF FATIGUE TESTS OF HY-100 PLATES WITH FULL PENETRATION TRANSVERSE ATTACHMENTS ON TWO SIDES. (COMPLETE REVERSAL).

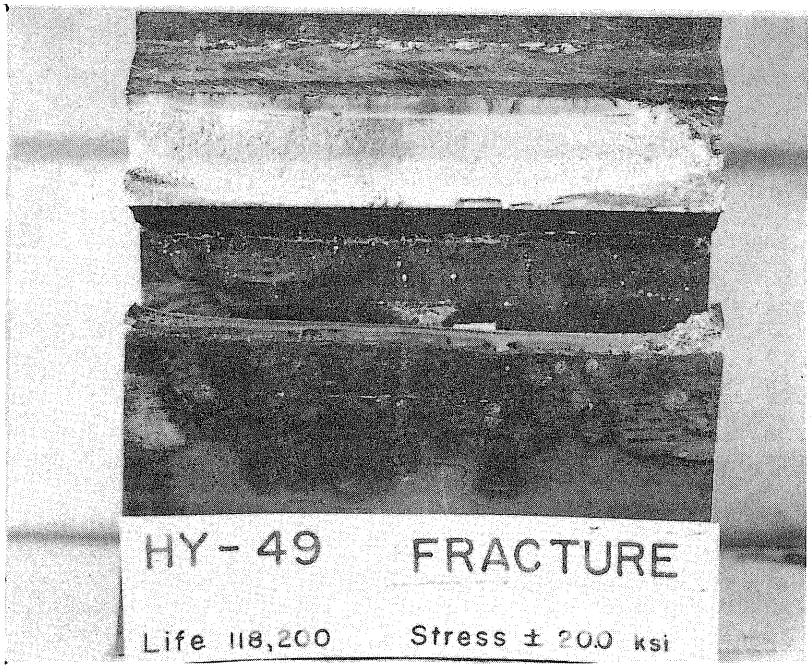

FAILURE INITIATED AT TOE OF WELD.

FIG.3.24 FRACTURE SURFACE OF HY-100 PLATE WITH FULL PENETRATION TRANSVERSE TEE JOINT.

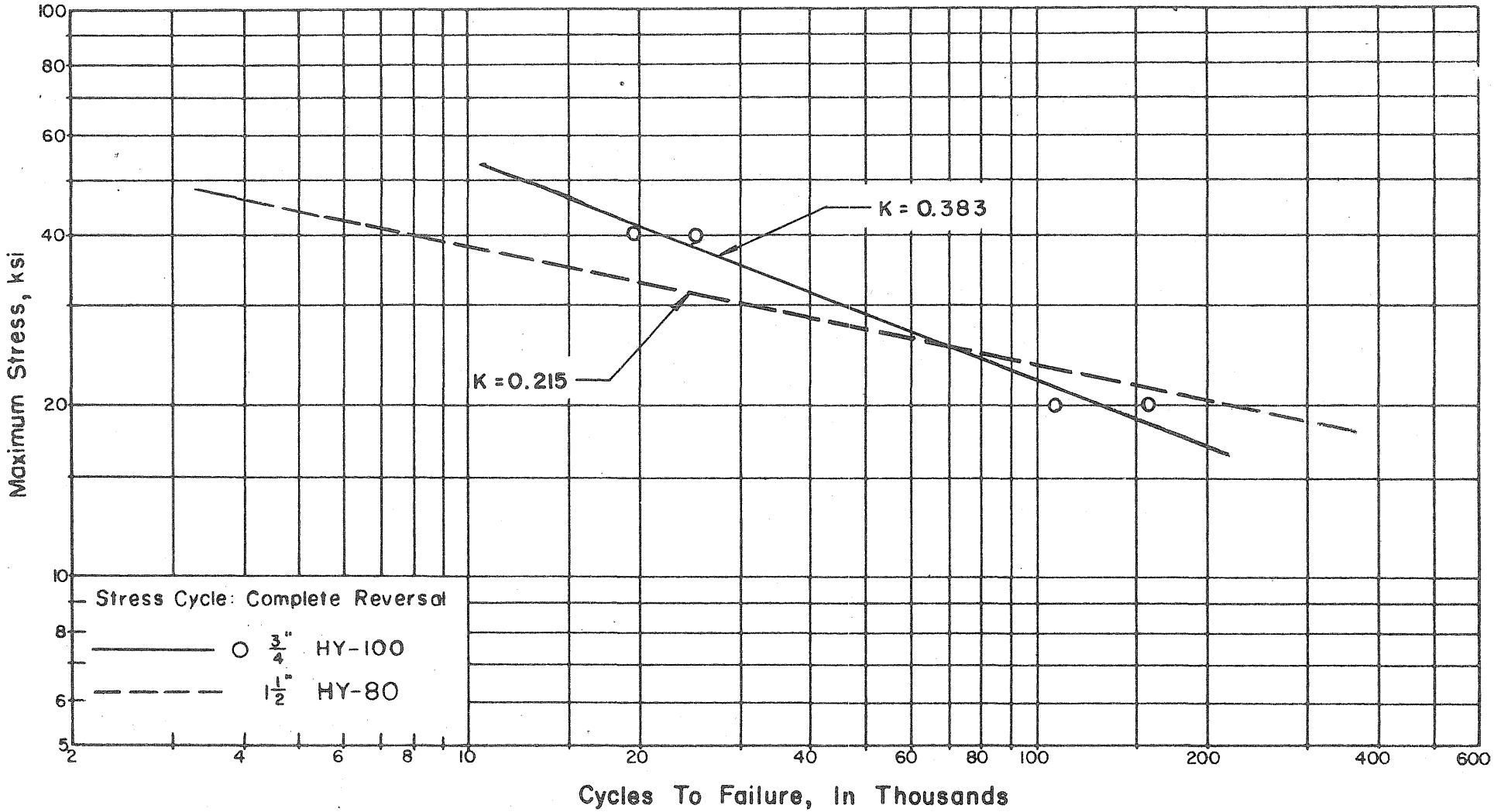

FIG. 3.25 RESULTS OF FATIGUE TESTS OF HY-100 PLATES WITH FULL PENETRATION TRANSVERSE TEE JOINTS. (COMPLETE REVERSAL).

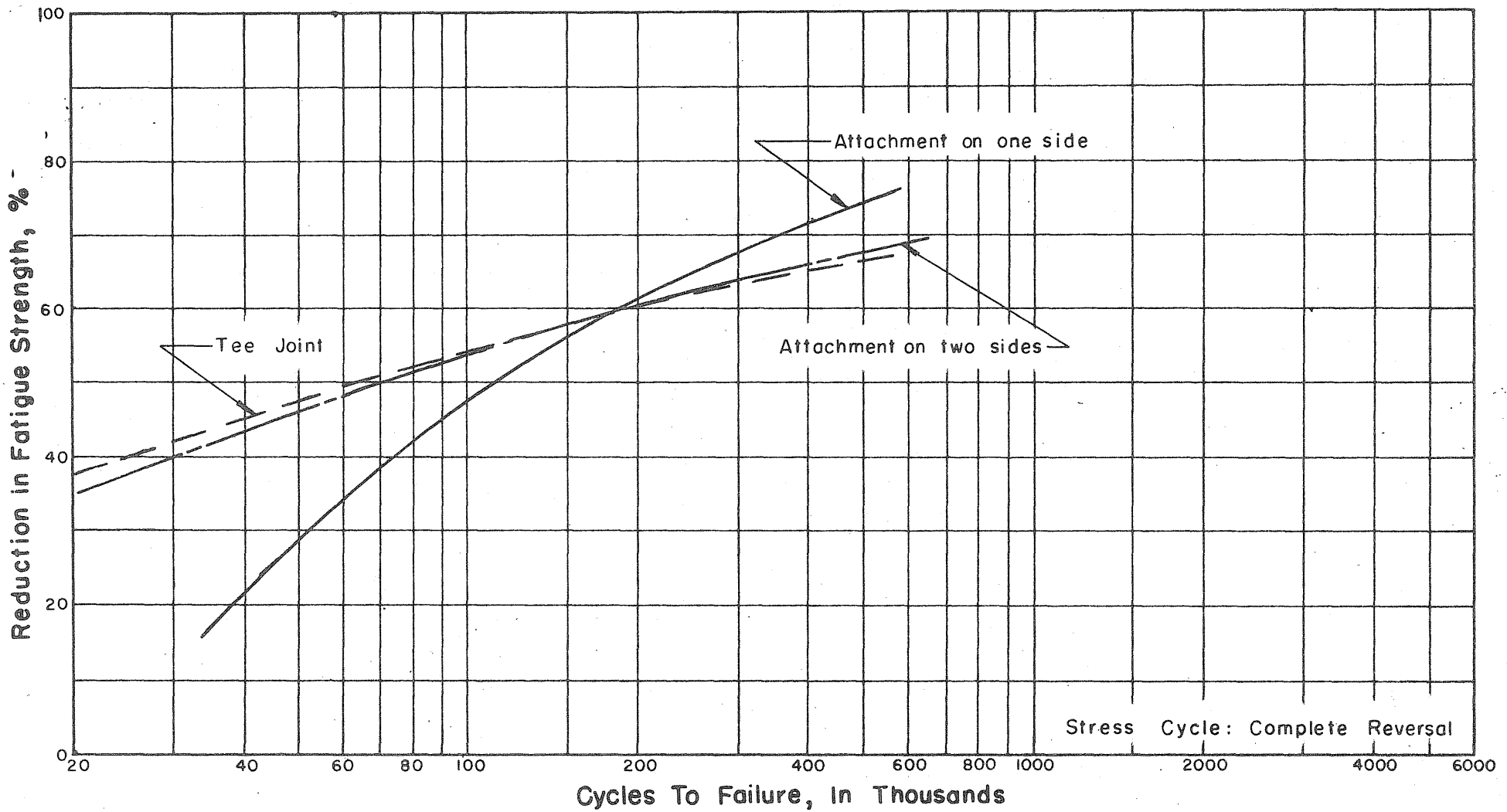

FIG.3.26 REDUCTION IN FATIGUE STRENGTH FROM AS-RECEIVED PLAIN PLATES DUE TO TRANSVERSE ATTACHMENTS.

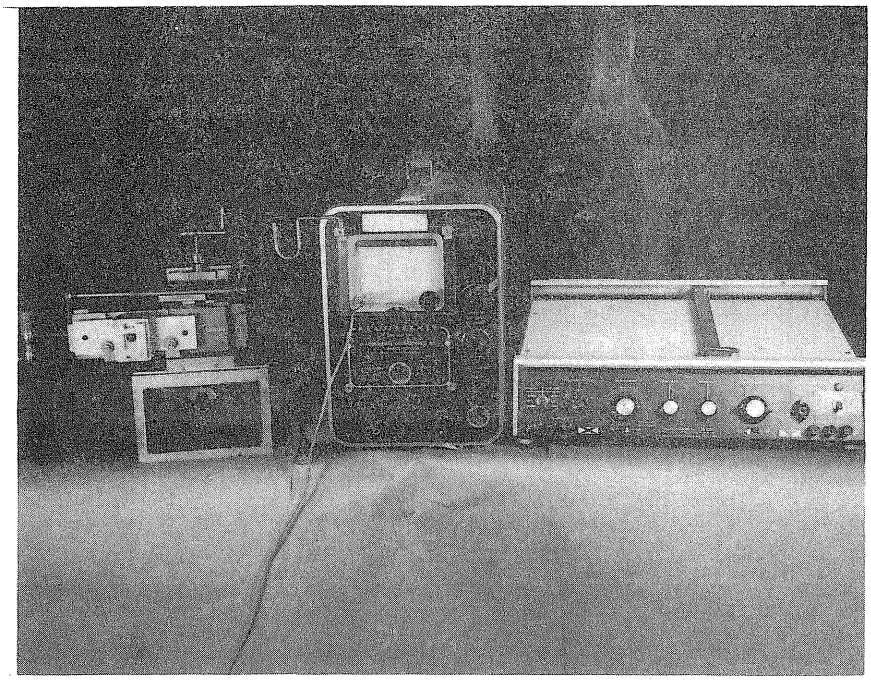

a) Probe Support, Detector And X-Y Recorder

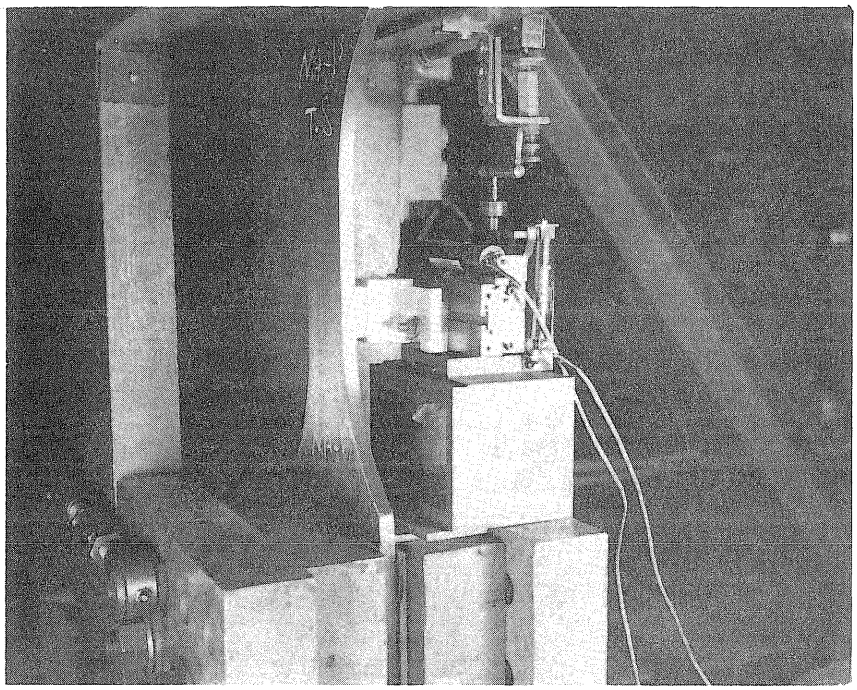

b) Unit In Position For Testing

FIG. 4.1 ULTRASONIC TESTING EQUIPMENT.

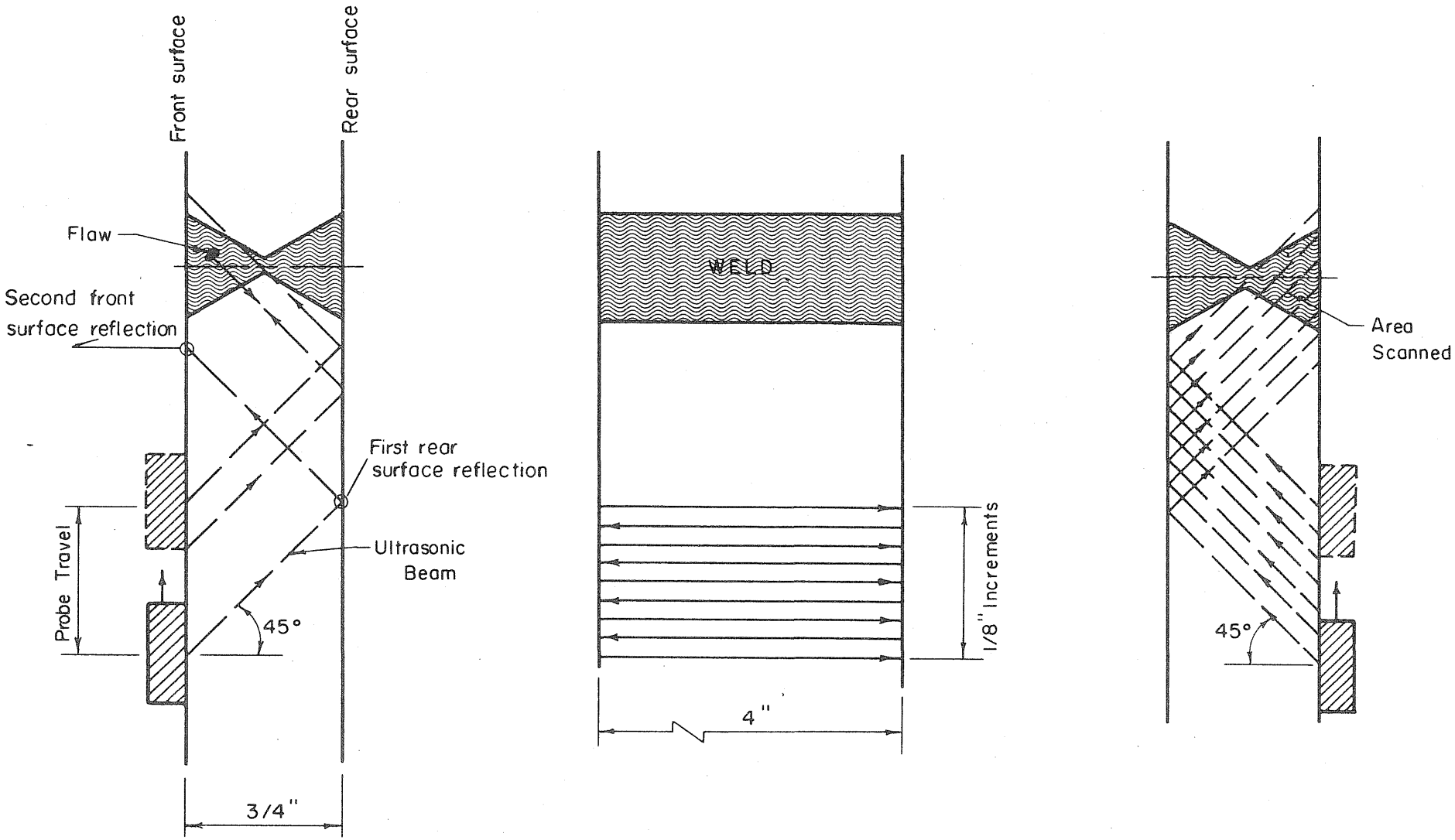

FIG. 4.2 SCANNING PROCEDURE FOR ULTRASONIC EXAMINATION.

SPECIMEN HY-33

Stress Cycle ± 30.0ksi Life 43,900

KEY:

FRACTURE SURFACE

1) Internal weld flaws visible on fracture surface . . . . . .

2) Extent of fatigue crack propagation at intersection with surface. . . . . .

ULTRASONIC READINGS

1) Location and extent of responses as indicated on detector scope . . . . . .

2) a. Number designation corresponds to magnitude of peak response as indicated on detector scope.

b. Letter designation corresponds to location along the length of the specimen and with respect to the weld. (Section A and E are at the toes of the weld). . . . . .

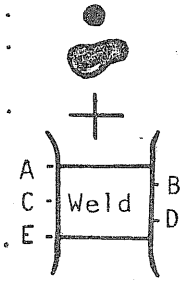

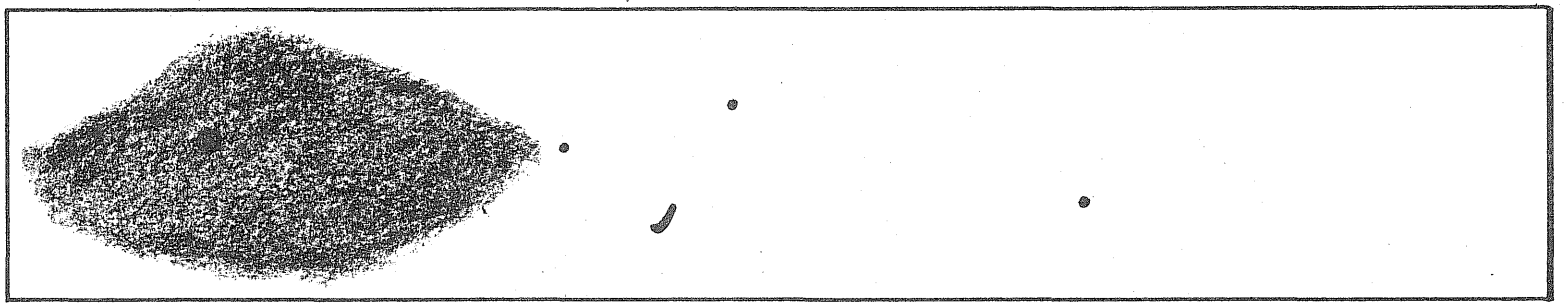

FRACTURE SURFACE

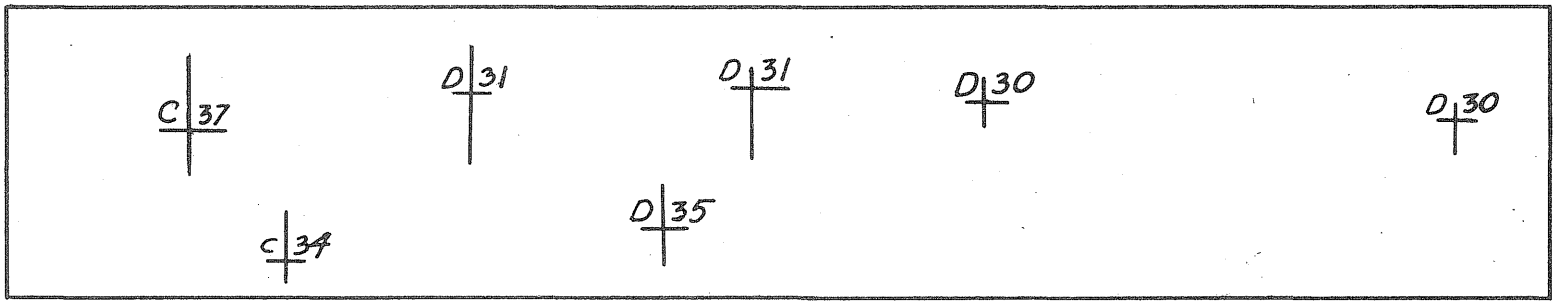

ULTRASONIC READINGS (Projection on a plane perpendicular to longitudinal axis of specimen)

0 Cycles

FIG. 4.3 SKETCH OF FRACTURE SURFACE AND ULTRASONIC READINGS FOR FLAWS IN WELD OF SPECIMEN HY-33.

SPECIMEN HY-43

Stress Cycle 0 to +50.0ksi Life 198,100

KEY:

FRACTURE SURFACE

1) Internal weld flaws visible on fracture surface . . . . . .
2) Extent of fatigue crack propagation at intersection with surface. . . . . .

ULTRASONIC READINGS

1) Location and extent of responses as indicated on detector scope . . . . . .
2) a. Number designation corresponds to magnitude of peak response as indicated on detector scope.
   b. Letter designation corresponds to location along the length of the specimen and with respect to the weld. (Section A and E are at the toes of the weld) . . . . . .

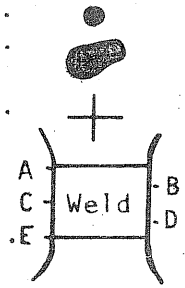

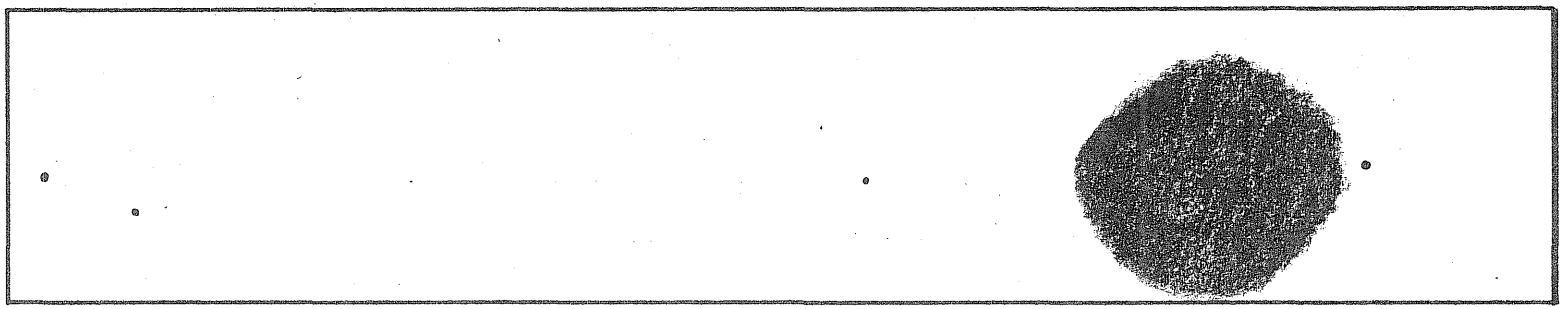

FRACTURE SURFACE
(See Fig. 5.1)

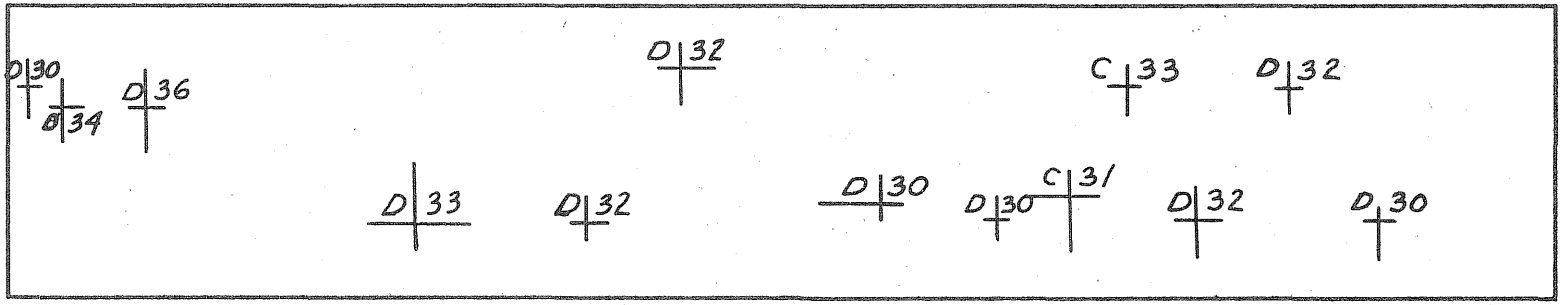

ULTRASONIC READINGS
(Projection on a plane perpendicular to longitudinal axis of specimen)
0 Cycles

FIG. 4.4 SKETCH OF FRACTURE SURFACE AND ULTRASONIC READINGS FOR FLAWS IN WELD OF SPECIMEN HY-43.

SPECIMEN HY-52
Stress Cycle +10.0 to +60.0 ksi Life 85,400

KEY:

FRACTURE SURFACE

1) Internal weld flaws visible on fracture surface . . . . . +

2) Extent of fatigue crack propagation at intersection with surface. . . . . .

ULTRASONIC READINGS

1) Location and extent of responses as indicated on detector scope . . . . . +

2) a. Number designation corresponds to magnitude of peak response as indicated on detector scope.

   b. Letter designation corresponds to location along the length of the specimen and with respect to the weld. (Section A and E are at the toes of the weld) . . . . . .

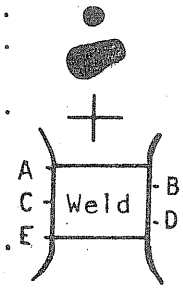

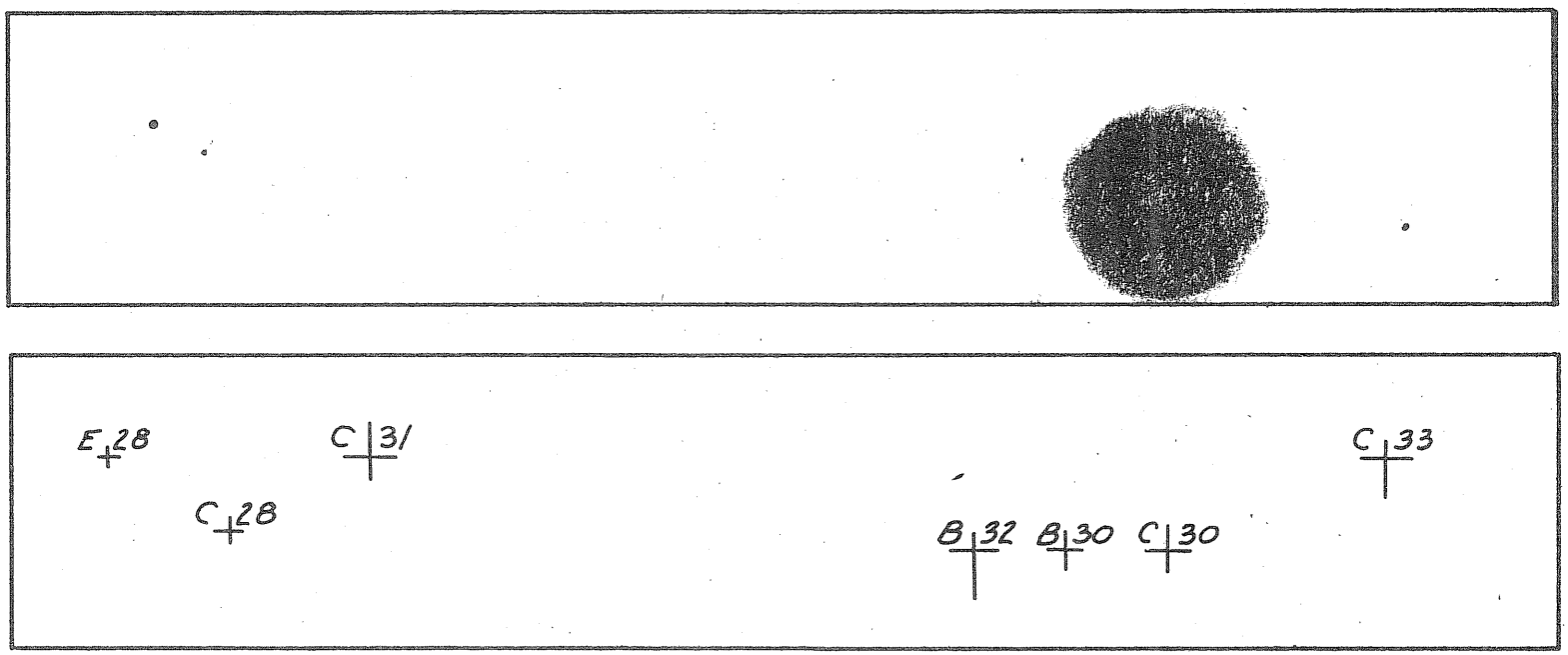

FRACTURE SURFACE

ULTRASONIC READINGS (Projection on a plane perpendicular to longitudinal axis of specimen)

0 Cycles

FIG. 4.5 SKETCH OF FRACTURE SURFACE AND ULTRASONIC READINGS FOR FLAWS IN WELD OF SPECIMEN HY-52.

SPECIMEN HY-53

Stress Cycle +10.0 to +60.0 ksi Life 318,600

KEY:

FRACTURE SURFACE

1) Internal weld flaws visible on fracture surface . . . . . .

2) Extent of fatigue crack propagation at intersection with surface. . . . . .

ULTRASONIC READINGS

1) Location and extent of responses as indicated on detector scope . . . . . .

2) a. Number designation corresponds to magnitude of peak response as indicated on detector scope.

b. Letter designation corresponds to location along the length of the specimen and with respect to the weld. (Section A and E are at the toes of the weld). . . . . .

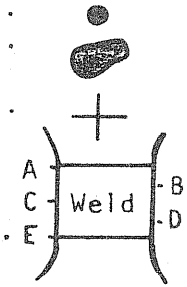

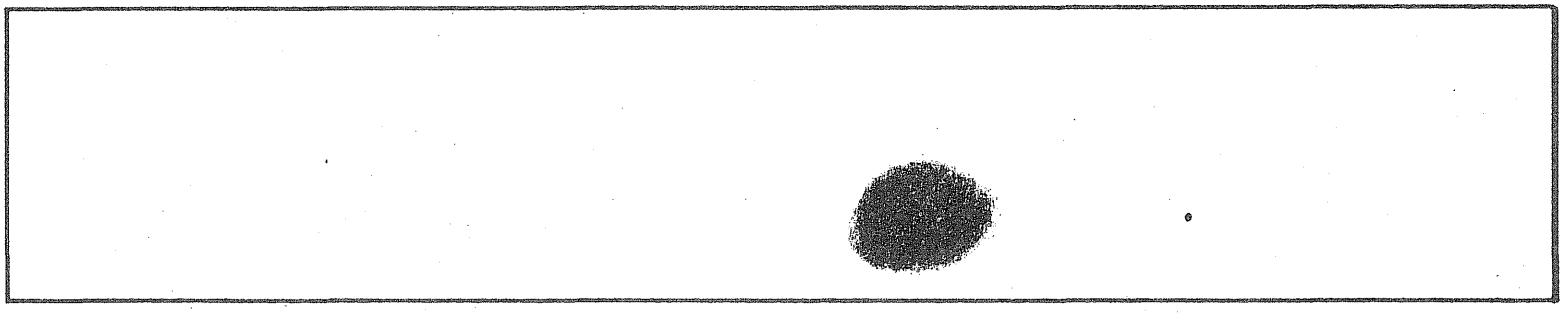

FRACTURE SURFACE

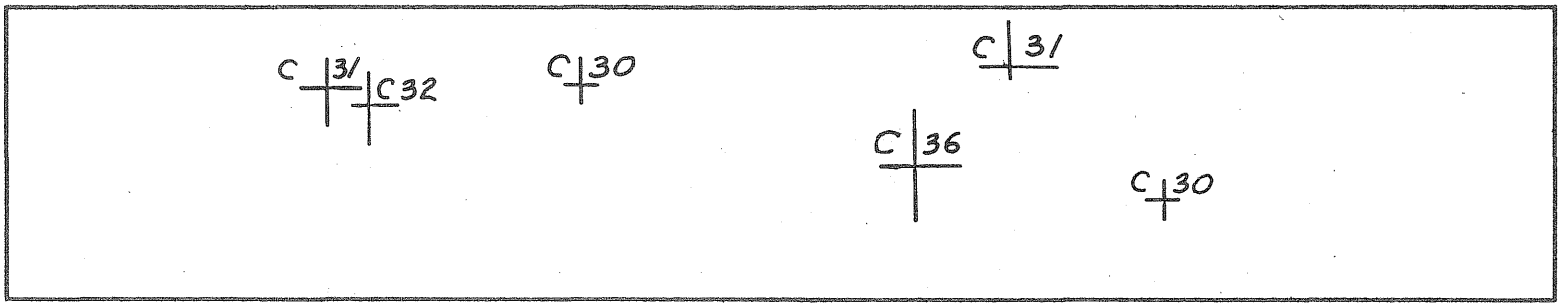

ULTRASONIC READINGS (Projection on a plane perpendicular to longitudinal axis of specimen)

0 Cycles

FIG.4.6 SKETCH OF FRACTURE SURFACE AND ULTRASONIC READINGS FOR FLAWS IN WELD OF SPECIMEN HY-53.

SPECIMEN HY-55
Stress Cycle 0 to 50.0 ksi Life 32,200

KEY:

FRACTURE SURFACE

1) Internal weld flaws visible on fracture surface . . . . . 

2) Extent of fatigue crack propagation at intersection with surface. . . . .

ULTRASONIC READINGS

1) Location and extent of responses as indicated on detector scope . . . . .

2) a. Number designation corresponds to magnitude of peak response as indicated on detector scope.

b. Letter designation corresponds to location along the length of the specimen and with respect to the weld. (Section A and E are at the toes of the weld) . . . . .

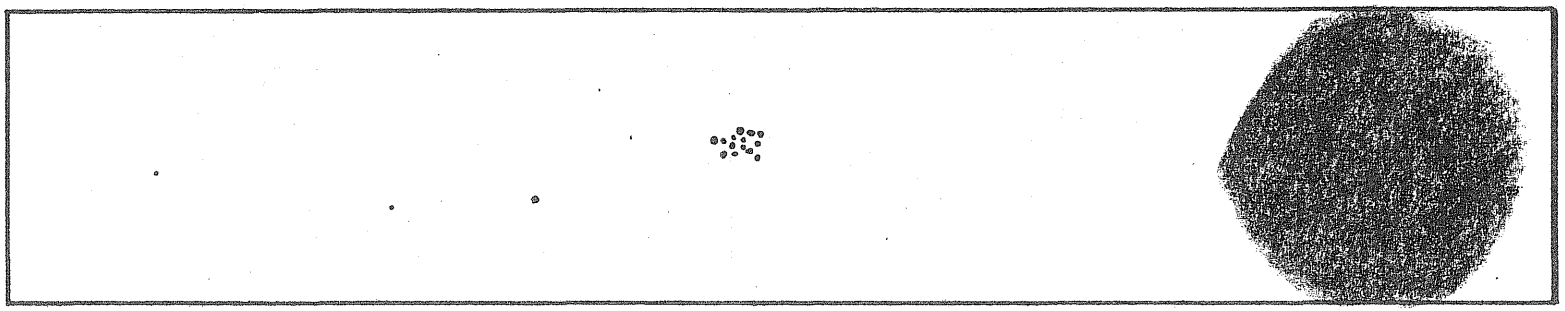

FRACTURE SURFACE

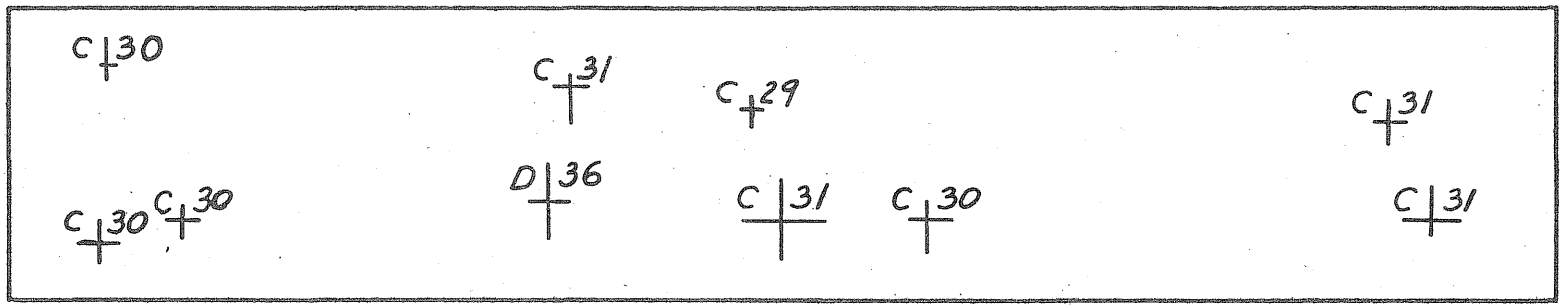

ULTRASONIC READINGS
(Projection on a plane perpendicular to longitudinal axis of specimen)

0 Cycles

FIG. 4.7 SKETCH OF FRACTURE SURFACE AND ULTRASONIC READINGS FOR FLAWS IN WELD OF SPECIMEN HY-55.

SPECIMEN HY-35

Stress Cycle ± 30.0ksi Life 403,100

KEY:

FRACTURE SURFACE

1) Internal weld flaws visible on fracture surface . . . . . 

2) Extent of fatigue crack propagation at intersection with surface. . . . .

ULTRASONIC READINGS

1) Location and extent of responses as indicated on detector scope . . . . .

2) a. Number designation corresponds to magnitude of peak response as indicated on detector scope.

b. Letter designation corresponds to location along the lendth of the specimen and with respect to the weld. (Section A and E are at the toes of the weld). . . . .

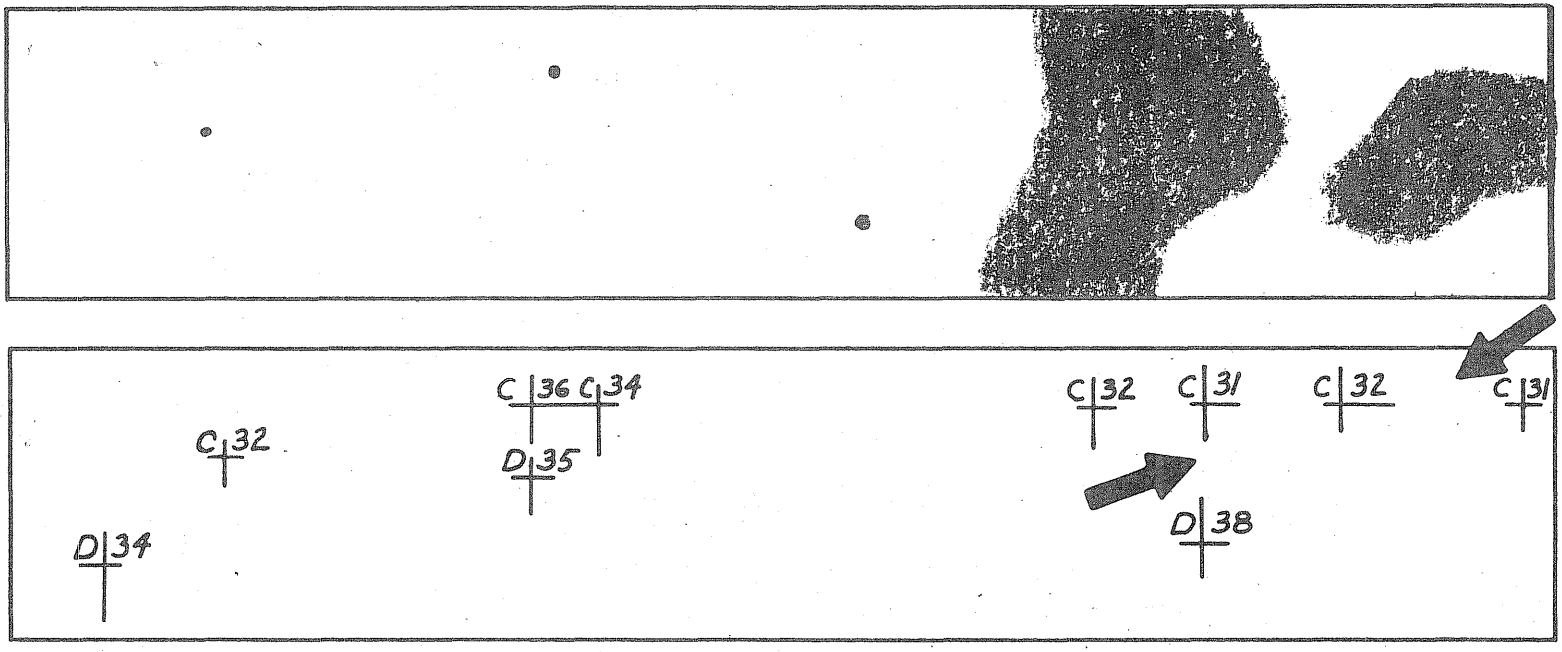

FRACTURE SURFACE

ULTRASONIC READINGS (Projection on a plane perpendicular to longitudinal axis of specimen)

0 Cycles

FIG. 4.8 SKETCH OF FRACTURE SURFACE AND ULTRASONIC READINGS FOR FLAWS IN WELD OF SPECIMEN HY-35.

SPECIMEN HY-35 (CONT.)

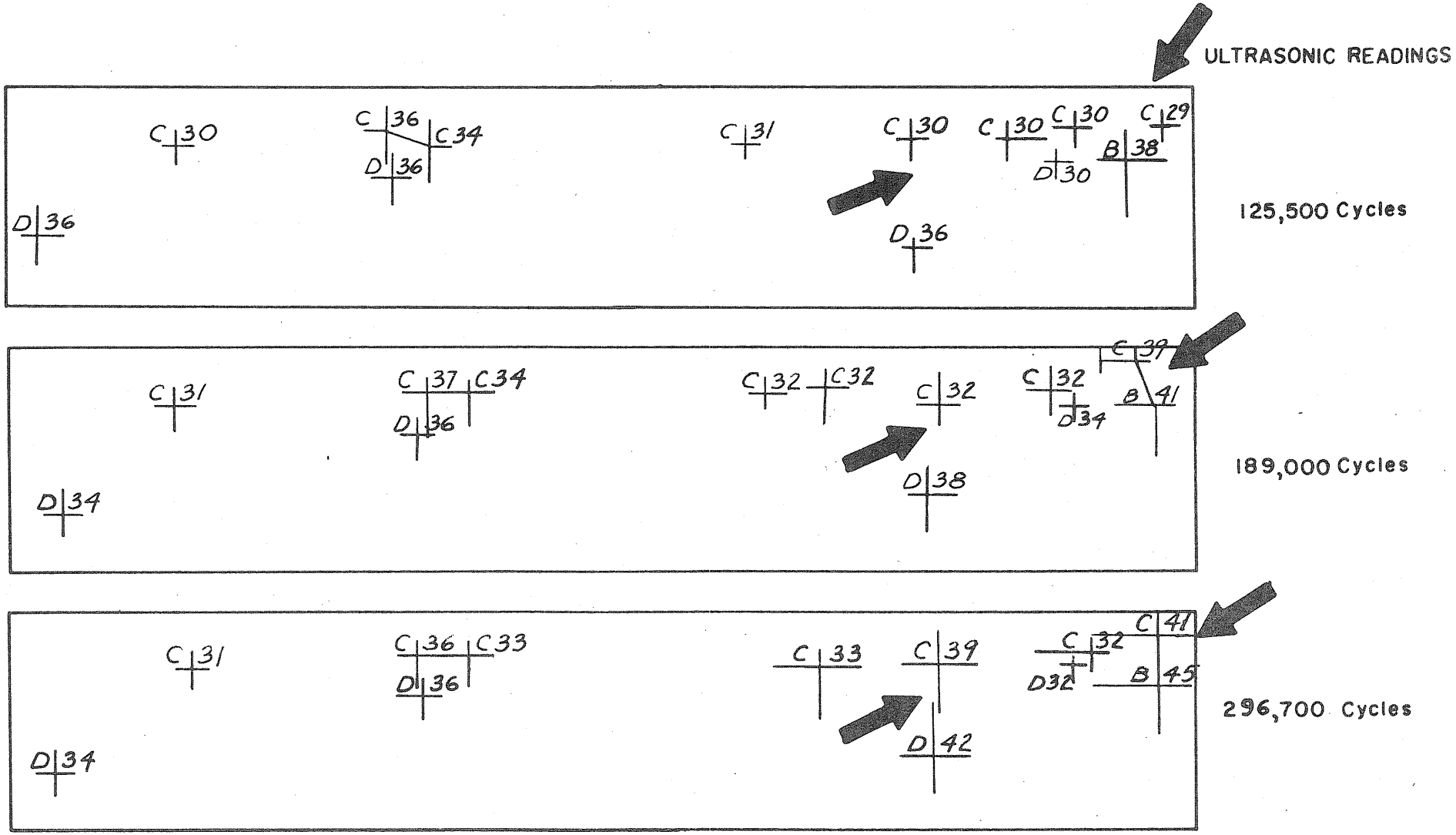

FIG. 4.8 (CONT.) SKETCH OF FRACTURE SURFACE AND ULTRASONIC READINGS FOR FLAWS IN WELD OF SPECIMEN HY-35.

SPECIMEN HY-34
STRESS CYCLE +10.0 to +60.0ksi, 263,400 Cycles

KEY:

ULTRASONIC READINGS

1) Location and extent of response as indicated on detector scope . . . . . +

2) a. Number designation corresponds to magnitude of peak response as indicated on detector scope.

b. Letter designation corresponds to the location through the thickness of the specimen . . . . . North Face g e k p South Face, 3/4"

c. Cross hatched area gives estimated location of the porosity observed on the radiograph . . . . . ▨

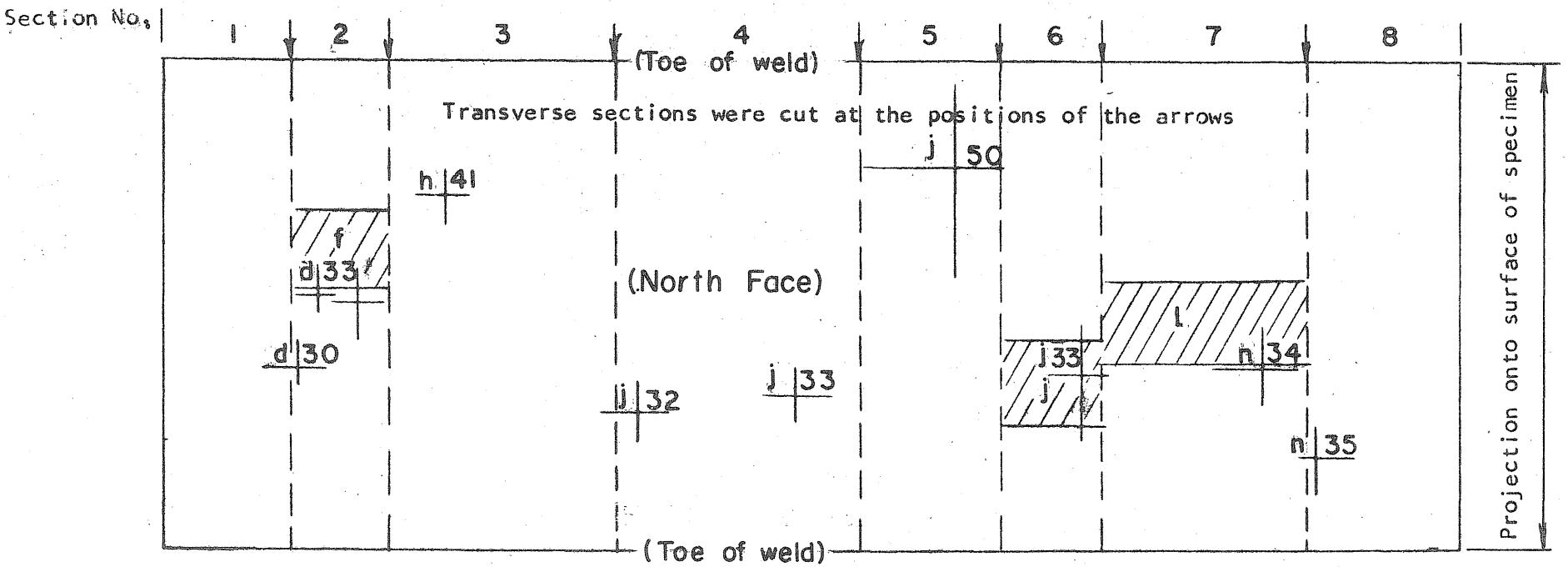

FIG.4.9 METALLOGRAPHIC SURFACES AND ULTRASONIC READINGS OF SPECIMEN HY-34.

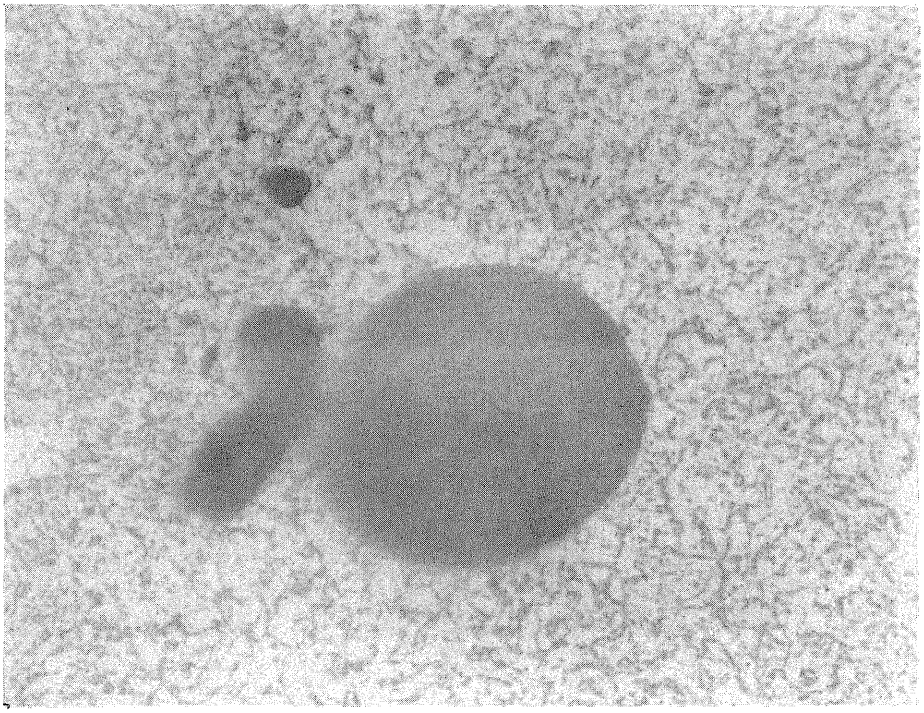

FIG. 4.10 PHOTOMICROGRAPH OF A PORE IN THE WELD METAL OF SPECIMEN HY-34. 900X

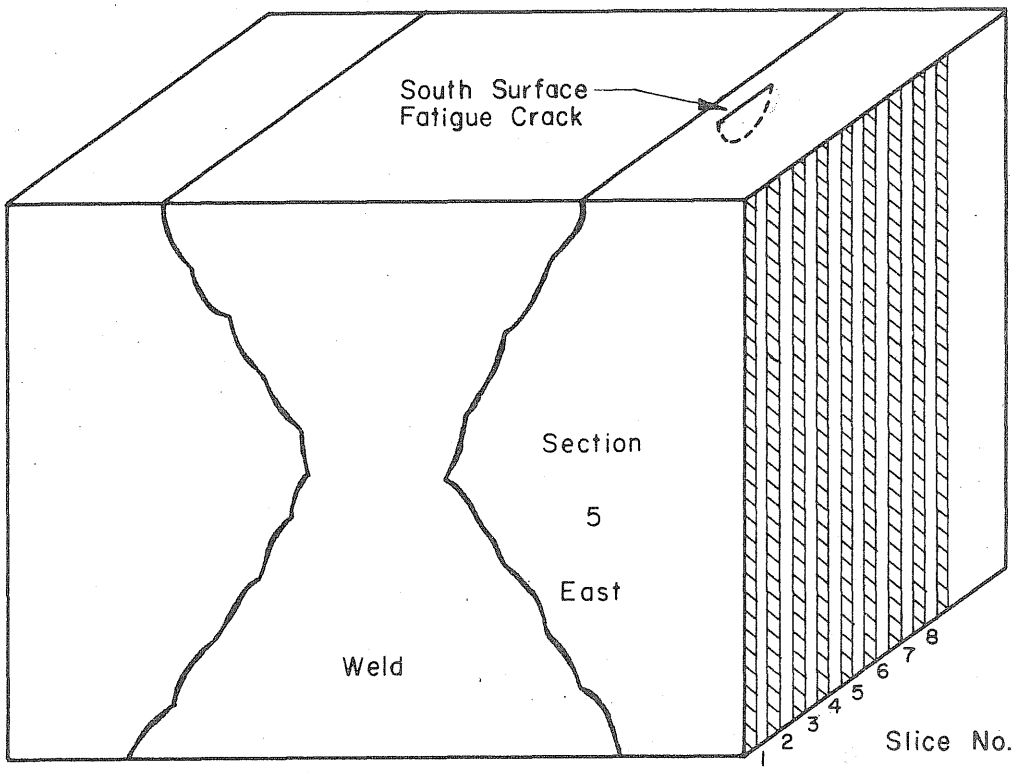

FIG. 4.11 CUTTING DIAGRAM FOR THIN SLICES CUT FROM SECTION 5 OF SPECIMEN HY-34.

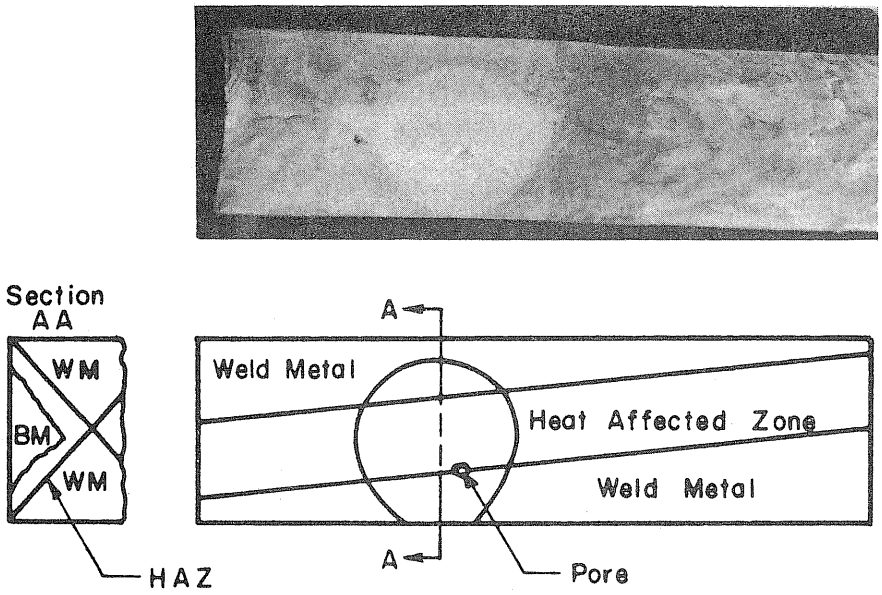

FIG.5.1 FRACTURE SURFACE OF SPECIMEN HY-43.

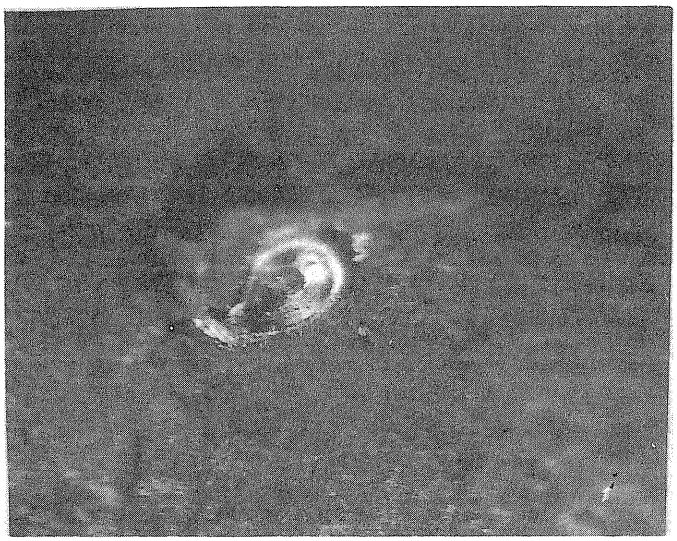

FIG.5.2 PORE AT THE CENTER OF THE FRACTURE SURFACE OF SPECIMEN HY-43. 15X.

FIG. 5.3 ELECTRON MICROGRAPH SHOWING FRACTURE SURFACE OF THE WELD METAL OF SPECIMEN HY-43. 6,400X

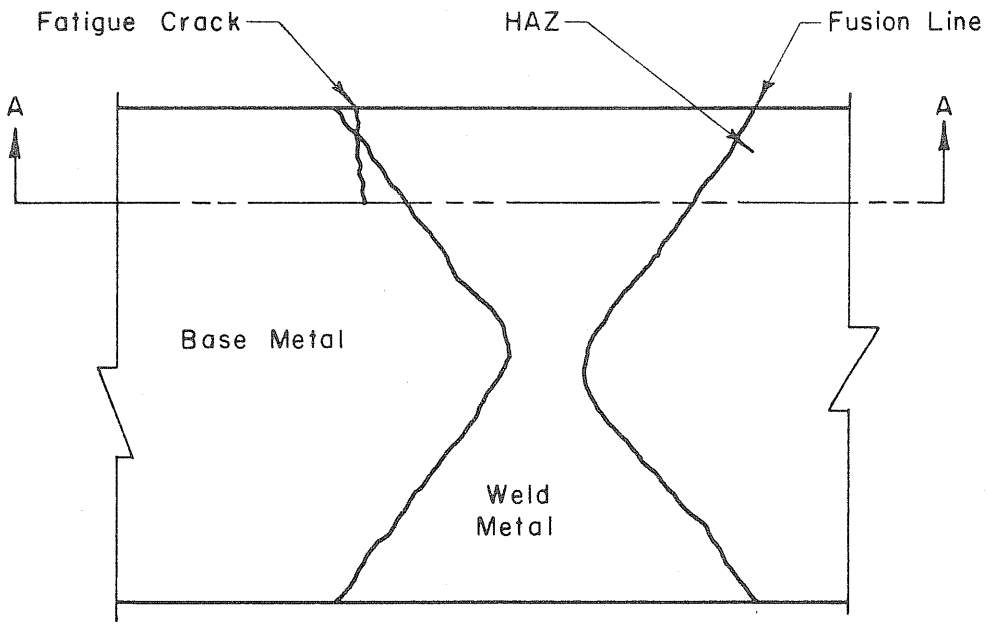

Cross Section of Weld.

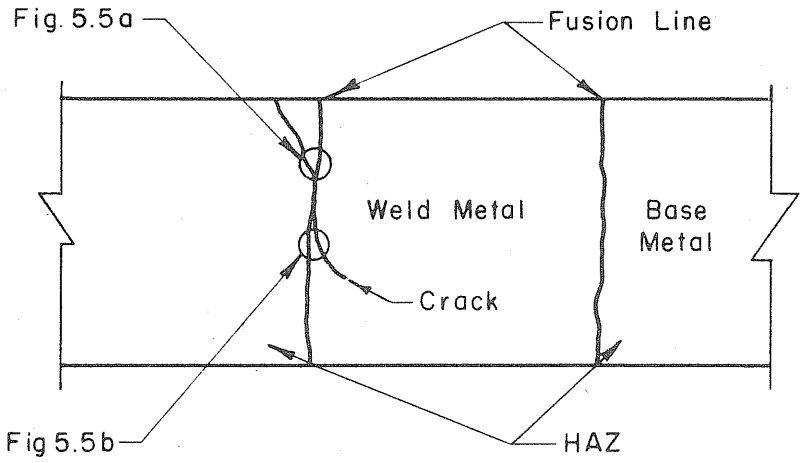

Section A-A.

FIG. 5.4 SKETCH OF CROSS SECTION OF SPECIMEN HY-25 WELD SHOWING POSITION OF FATIGUE CRACK.

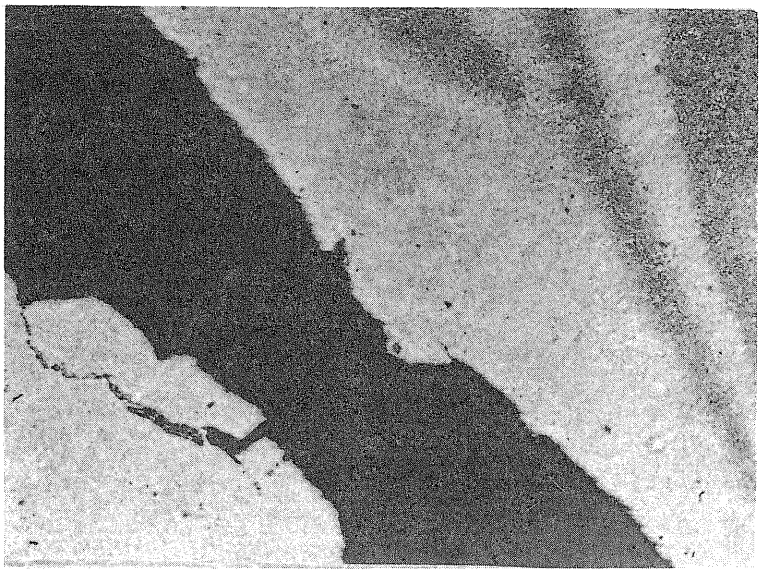

FIG. 5.5a TRANSVERSE SECTION OF FRACTURE SURFACE CUT FROM SPECIMEN HY-25 SHOWING H. A. Z. 100X

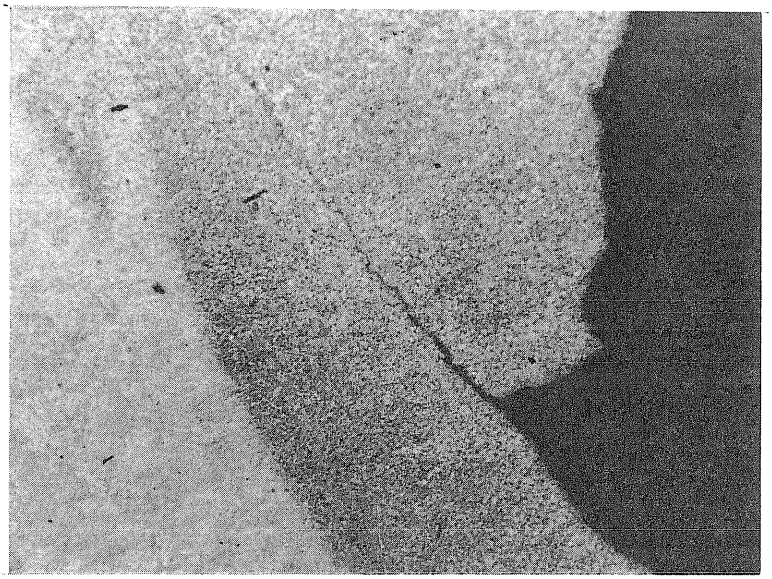

FIG. 5.5b TRANSVERSE SECTION OF FRACTURE SURFACE OF SPECIMEN HY-25 SHOWING WELD METAL. 100X

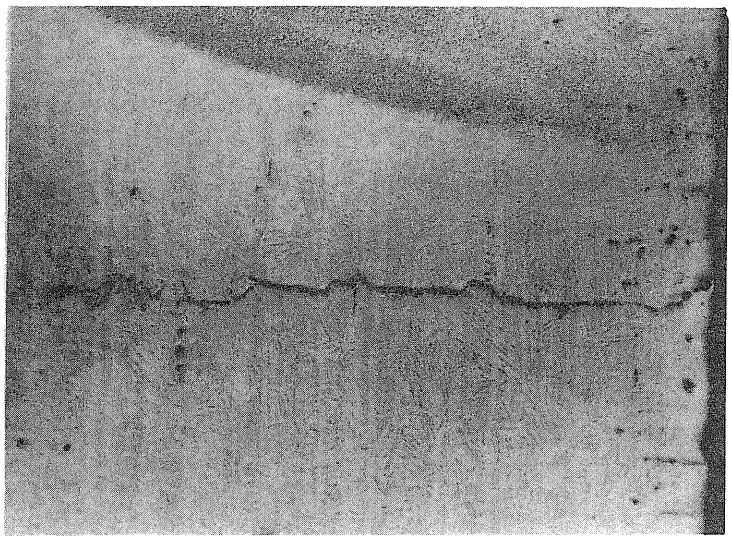

FIG. 5.6 TRANSVERSE SECTION OF SLICE 6 WEST (FIG.4.11) SHOWING THE FATIGUE CRACK IN SPECIMEN HY-34. 100X

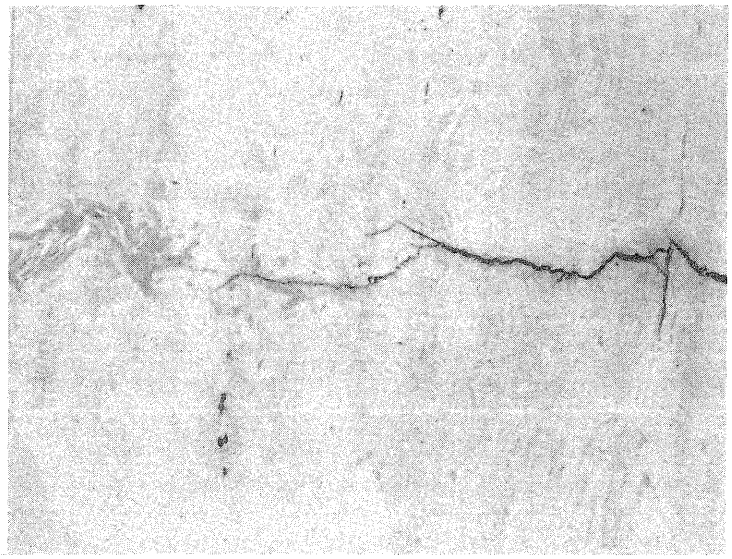

FIG. 5.7 HIGHER MAGNIFICATION OF FATIGUE CRACK SHOWN IN FIG. 5.6. 200X

a) Base Metal

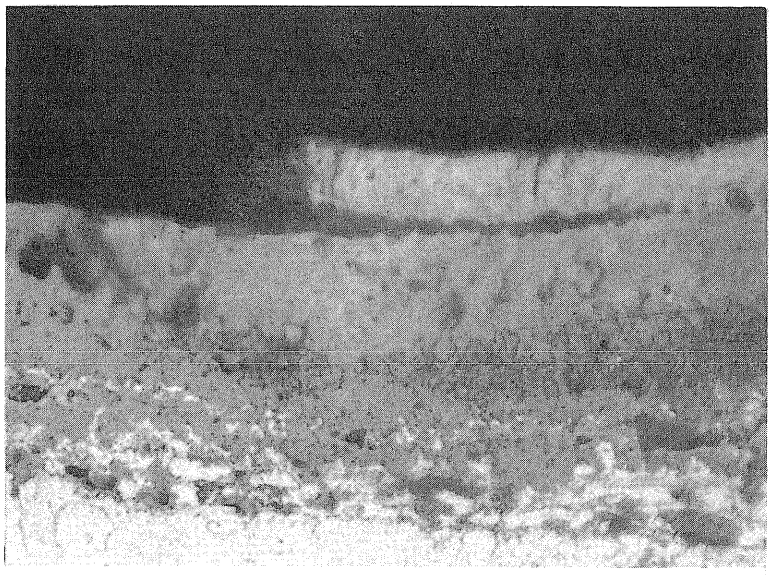

b) Mill Scale

FIG. 6.1 PHOTOMICROGRAPHS OF 1/2 IN. HY-130/150 MATERIAL. 750X.

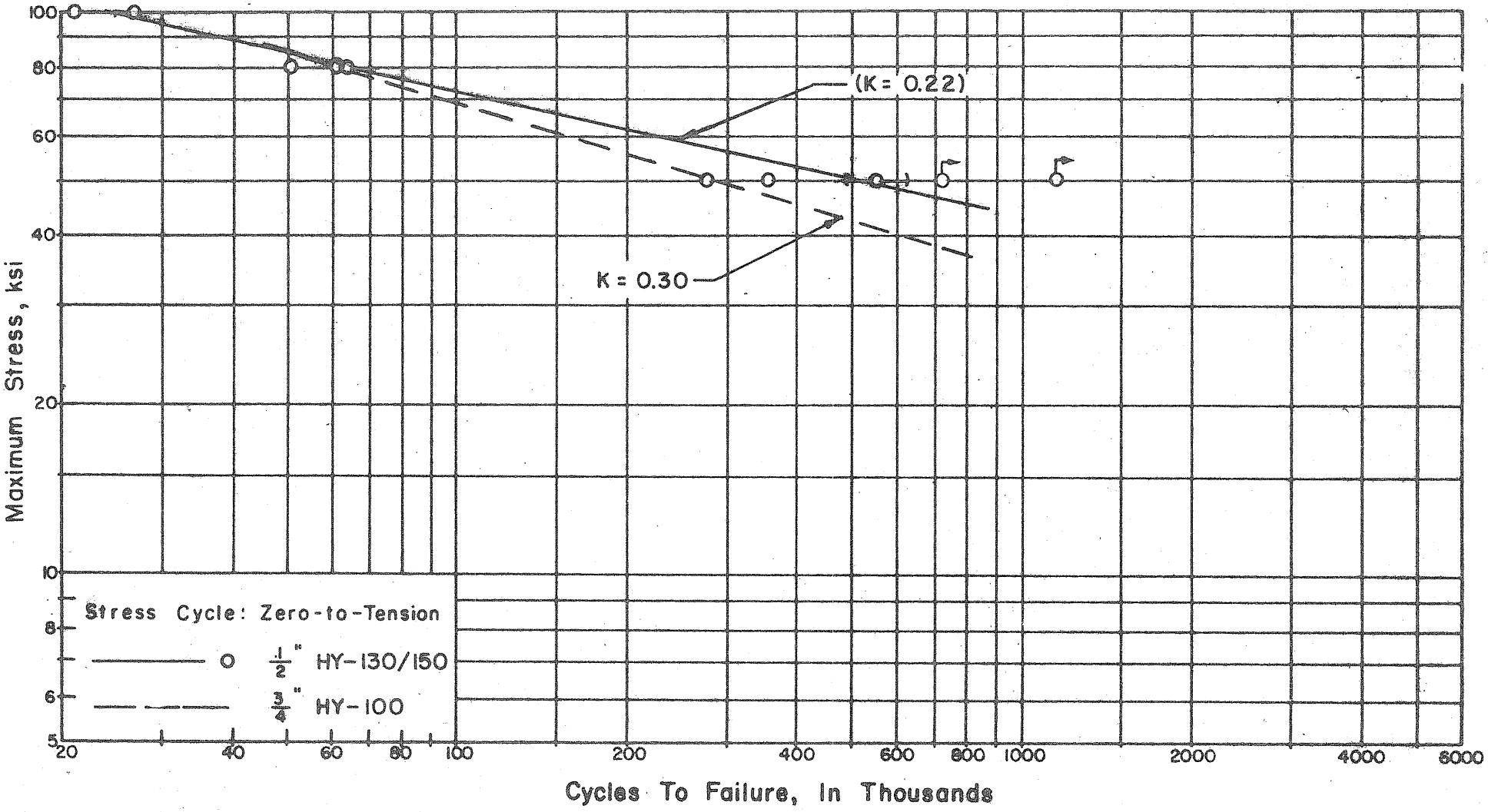

FIG. 6.2 RESULTS OF FATIGUE TESTS OF AS-RECEIVED HY-130/150 PLAIN PLATE SPECIMENS. (ZERO-TO-TENSION)

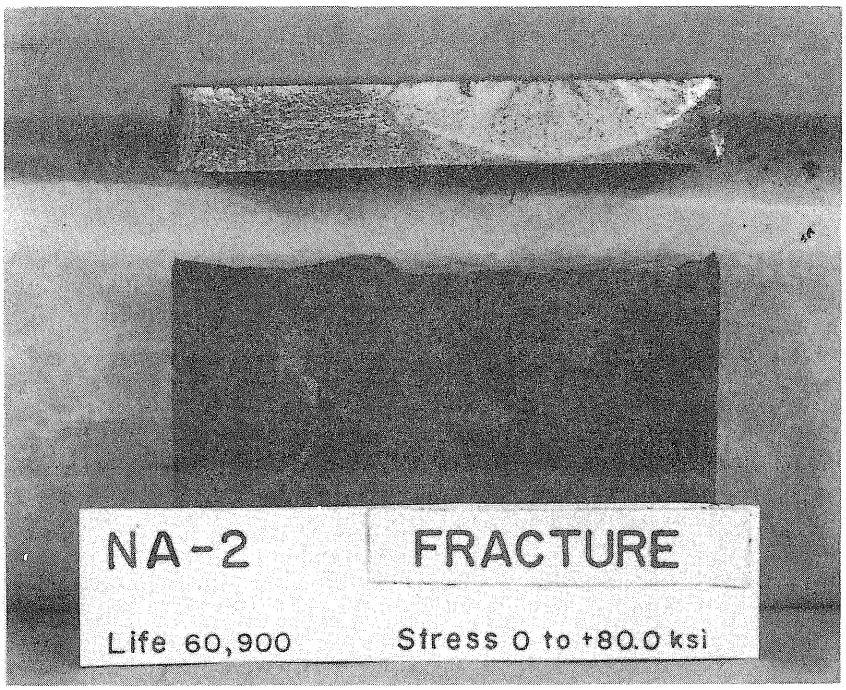

a) Failure Initiated At Mill Scale Surface

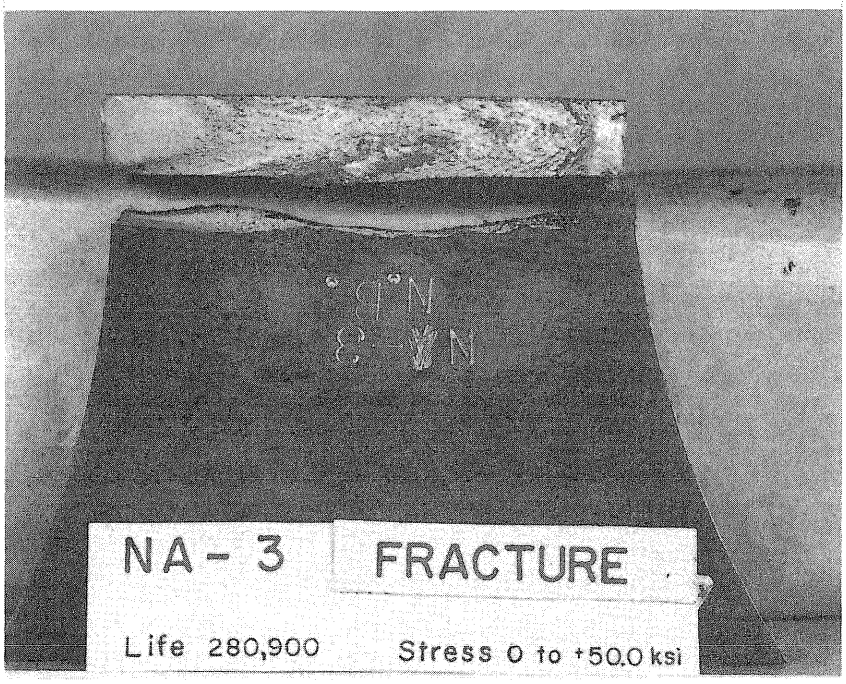

b) Failure Initiated At Radius

FIG. 6.3 TYPICAL FRACTURES OF 1/2 IN. PLAIN PLATES OF HY-130/150 MATERIAL.